MATH5004M: Knot Theory

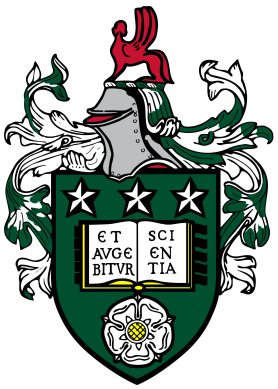

Bradley Ryan

University of Leeds

School of Mathematics

Submitted in accordance with the requirements for the degree of

Master of Mathematics

May 2020

Abstract

Knots are closed curves in $\mathbb{R}^3$ that do not self-intersect. It is not uncommon to work almost exclusively with so-called knot diagrams, that is the projection of a knot onto the plane. This paper will begin with the definition of a knot from a differential geometric foundation before considering such projections, the purpose of which is to give a rigorous groundwork to build the theory upon in a simpler way. This will be followed by in-depth discussion of a number of knot invariants, namely tri-colourability, the knot determinant (with reference to general p-colourability) and skein relations generating a number of polynomials. We will then consider the so-called knot group, from a combinatorial group-theoretic perspective, and use the theory of surfaces from topology to determine the characteristics of manifolds with a given knot as its boundary. The following section will focus on braid theory, in which we will see that knots and braids are closely related. The paper then concludes with the relevant set-up and proof of the Fáry-Milnor Theorem.

Acknowledgements

My thanks goes to Martin Speight for supervising me during this project. It is only due to the many meetings with him that I stood a chance at understanding this interesting topic. I am also grateful to João Faria Martins for a useful conversation on some technical linear algebra.

Contents

1 Elementary Topology

We begin with an introduction to a mathematical knot, via concepts seen in differential calculus. This will pave the way towards a beautiful result by [Mil50] which will provide us with a sufficient condition to test if a knot can be unknotted to a circle. In practice, this section will not be referred to all that often and theory will instead be established for so-called knot projections as mentioned in the abstract. However, it is important to understand the calculus and topological angle now in preparation for Sections 4 and 7. We first follow the framework of [GP94].

1.1 Parametrised Curves

Definition 1.1 A parametrised curve in $\mathbb{R}^n$ is a smooth map $\gamma : I \to \mathbb{R}^n$, where $I \subseteq \mathbb{R}$ is some interval. It is called regular if $\gamma'(t) \neq 0$, $\forall t \in I$.

Example 1.2 Consider the curve $\gamma : \mathbb{R} \to \mathbb{R}^2$, given by $\gamma(t) = (t^2, t^5)$. This is a parametrised curve because the functions t^2 and t^5 are polynomial and hence smooth. However, it is clear that $\gamma'(t) = (2t, 5t^4) = 0$ if and only if $t = 0$, and so it is **not** a regularly parametrised curve.

Definition 1.3 Let $\gamma : I \to \mathbb{R}^n$ be a parametrised curve. Then, the velocity of the curve is γ', the speed of the curve is $||\gamma'||$ and the acceleration of the curve is γ''.

Example 1.4 Consider the curve $\gamma : [0, 1] \to \mathbb{R}^2$, given by $\gamma(t) = (t^3 - 3t, t^3 + t)$. This is a regularly parametrised curve. Indeed, the velocity is $\gamma'(t) = (3t^2 - 3, 3t^2 + 1)$, which is zero if and only if both co-ordinates are zero, but $3t^2 - 3 = 0$ only if $t = \pm 1$; in this case, the second coordinate is non-zero. Note that velocity is also a parametrised curve and that the acceleration is $\gamma''(t) = (6t, 6t)$, which is zero when $t = 0$.

It is clear by Example 1.4 that the condition of regularity is **not** necessarily preserved under taking derivatives. Furthermore, it is clear that a curve is regular if and only if its velocity, and thus speed, is everywhere non-vanishing.

Definition 1.5 Let $\gamma : I \to \mathbb{R}^n$ be a parametrised curve. The arc length along $[a, b] \subseteq I$ is

$$L(\gamma|_{[a,b]}) = \int_a^b ||\gamma'(t)|| \, dt.$$

Example 1.6 Consider the curve $\gamma : [0, \pi] \to \mathbb{R}^2$, given by $\gamma(t) = (\cos t, \sin t)$. Its velocity is $\gamma'(t) = (-\sin t, \cos t)$, so it has speed $||\gamma'(t)|| = 1$. Thus, the arc-length along the curve is

$$L(\gamma|_{[0,\pi]}) := L(\gamma) = \int_0^\pi 1 \, dt = \pi.$$

Note that parametrised curves live up to their name: they are parametrised by some variable. It is

now possible to make precise the idea of reparametrising a curve, which has some soon-to-be-seen useful applications.

Definition 1.7 A reparametrisation of a parametrised curve $\gamma : I \to \mathbb{R}^n$ is a parametrised curve $\tilde{\gamma} : J \to \mathbb{R}^n$ such that $\tilde{\gamma} = \gamma \circ \varphi$, where $\varphi : J \to I$ is a smooth surjection with $\varphi'(s) > 0$, $\forall s \in J$.

It is important to have both the surjection and positive derivative assumptions in Definition 1.7 so as to exclude the possibility of taking a regular curve and reparametrising it to one that is non-regular. This result will be proven after we first study an example of a reparametrisation.

Example 1.8 Consider the curve $\gamma : [0,1] \to \mathbb{R}^2$, given by $\gamma(t) = (t^2, t)$. An example of a reparametrisation is the curve $\tilde{\gamma} : [0,2] \to \mathbb{R}^2$, given by $\tilde{\gamma}(s) = (s^2/4, s/2)$. Indeed, it is clear that $\tilde{\gamma} = \gamma \circ \varphi$, where $\varphi(s) = s/2$ is the so-called parameter transformation. This does satisfy the hypotheses of Definition 1.7 because φ is surjective and $\varphi'(s) = 1/2 > 0$.

Lemma 1.9 *Suppose $\gamma : I \to \mathbb{R}^n$ is a regularly parametrised curve. Every reparametrisation of γ is also regular.*

Proof: Suppose $\tilde{\gamma} : J \to \mathbb{R}^n$ is such a reparametrisation. By definition, $\tilde{\gamma}(s) = \gamma(\varphi(s))$, where φ is the parameter transformation. Consequently, $\tilde{\gamma}'(s) = \gamma'(\varphi(s))\varphi'(s) \neq 0$ for every $s \in J$ because $\gamma'(\varphi(s)) \neq 0$ by regularity and $\varphi'(s) > 0$ by assumption. □

Lemma 1.10 *Suppose $\gamma : I \to \mathbb{R}^n$ is a regularly parametrised curve. The arc length along γ is invariant under reparametrisation.*

Proof: Suppose $\tilde{\gamma} : J \to \mathbb{R}^n$ is such a reparametrisation with parameter transformation φ. Then, for every $s_0, s_1 \in J$, it is clear that

$$\begin{aligned}
L(\tilde{\gamma}|_{[s_0,s_1]}) &= \int_{s_0}^{s_1} ||\tilde{\gamma}'(s)||\, ds \\
&= \int_{s_0}^{s_1} ||\gamma'(\varphi(s))||\varphi'(s)\, ds, \text{ by the Chain Rule and using that } \varphi'(s) > 0, \\
&= \int_{\varphi^{-1}(t_0)}^{\varphi^{-1}(t_1)} ||\gamma'(\varphi(s))||\varphi'(s)\, ds \\
&= \int_{t_0}^{t_1} ||\gamma'(t)||\, dt, \text{ by changing variables to } t = \varphi(s), \\
&= L(\gamma|_{[t_0,t_1]}),
\end{aligned}$$

where we define $t_0 = \varphi(s_0)$ and $t_1 = \varphi(s_1)$. □

Definition 1.11 Let $\gamma : I \to \mathbb{R}^n$ be a regularly parametrised curve. The curvature vector is the image of the function $k : I \to \mathbb{R}^n$ defined as

$$k(t) = \frac{1}{||\gamma'(t)||^2}\Big(\gamma''(t) - \frac{\gamma'(t)\cdot\gamma''(t)}{||\gamma'(t)||^2}\gamma'(t)\Big).$$

By construction, the curvature vector is orthogonal to velocity. Indeed, this is clear since

$$k(t)\cdot\gamma'(t) \;=\; \frac{\gamma'(t)\cdot\gamma''(t)}{||\gamma'(t)||^2} - \frac{\gamma'(t)\cdot\gamma''(t)}{||\gamma'(t)||^4}||\gamma'(t)||^2 \;=\; 0.$$

Example 1.12 Let $\gamma : [0, 2\pi] \to \mathbb{R}^2$ be given by $\gamma(t) = (e^t\cos t, e^t\sin t)$; this is a parametrised curve. Then, we can compute the following:

$$\begin{aligned}
\gamma'(t) &= (e^t\cos t - e^t\sin t, e^t\cos t + e^t\sin t).\\
\gamma''(t) &= (-2e^t\sin t, 2e^t\cos t).\\
\gamma'(t)\cdot\gamma''(t) &= 2e^{2t}.\\
||\gamma'(t)||^2 &= 2e^{2t}.
\end{aligned}$$

Consequently, the curvature vector $k(t) = -\frac{1}{2e^t}(\cos t + \sin t, \cos t - \sin t)$.

Lemma 1.13 *Suppose $\gamma : I \to \mathbb{R}^n$ is a regularly parametrised curve. The curvature vector attributed to γ is invariant under reparametrisation.*

Proof: Suppose $\tilde{k} : I \to \mathbb{R}^n$ is the curvature vector of the reparametrisation $\tilde{\gamma} : J \to \mathbb{R}^n$. Then,

$$\begin{aligned}
\tilde{k}(s) &= \frac{1}{||\tilde{\gamma}'(s)||^2}\Big(\tilde{\gamma}''(s) - \frac{\tilde{\gamma}'(s)\cdot\tilde{\gamma}''(s)}{||\tilde{\gamma}'(s)||^2}\tilde{\gamma}'(s)\Big)\\
&= \frac{1}{||\gamma'(\varphi)||^2\varphi'^2}\Big(\gamma''(\varphi)\varphi'^2 + \gamma'(\varphi)\varphi'' - \frac{\gamma'(\varphi)\varphi'\cdot[\gamma''(\varphi)\varphi'^2 + \gamma'(\varphi)\varphi'']}{||\gamma'(\varphi)||^2\varphi'^2}\gamma'(\varphi)\varphi'\Big)\\
&= \frac{1}{||\gamma'(\varphi)||^2\varphi'^2}\Big(\gamma''(\varphi)\varphi'^2 + \gamma'(\varphi)\varphi'' - \frac{[\gamma'(\varphi)\cdot\gamma''(\varphi)]\varphi'^4 + ||\gamma'(\varphi)||^2\varphi'^2\varphi'']}{||\gamma'(\varphi)||^2\varphi'^2}\gamma'(\varphi)\Big)\\
&= \frac{1}{||\gamma'(\varphi)||^2\varphi'^2}\Big(\gamma''(\varphi)\varphi'^2 - \frac{\gamma'(\varphi)\cdot\gamma''(\varphi)\varphi'^2}{||\gamma'(\varphi)||^2}\gamma'(\varphi)\Big)\\
&= \frac{1}{||\gamma'(t)||^2}\Big(\gamma''(t) - \frac{\gamma'(t)\cdot\gamma''(t)}{||\gamma'(t)||^2}\gamma'(t)\Big)\\
&= k(t),
\end{aligned}$$

where $t = \varphi(s)$ and we have used $\varphi = \varphi(s)$ to avoid a notation calamity. □

Definition 1.14 Let $\gamma : [a, b] \to \mathbb{R}^n$ be a regularly parametrised curve, with $k : [a, b] \to \mathbb{R}^n$ its

curvature vector. The total curvature of γ is defined as

$$\mu(\gamma) = \int_a^b ||k(t)||\ ||\gamma'(t)||\ dt.$$

Example 1.15 Following on from Example 1.12, we can compute the total curvature:

$$\mu(\gamma) = \int_0^{2\pi} \frac{1}{\sqrt{2}e^t} \cdot \sqrt{2}e^t\ dt = 2\pi.$$

Lemma 1.16 *Let $\gamma : [a, b] \to \mathbb{R}^n$ be a regularly parametrised curve. The total curvature $\mu(\gamma)$ is invariant under reparametrisation.*

Proof: Suppose $\tilde{\gamma} : [c, d] \to \mathbb{R}^n$ is such a reparametrisation, with parameter transformation φ and curvature vector $\tilde{k} : [c, d] \to \mathbb{R}^n$. Then,

$$\begin{aligned}
\mu(\tilde{\gamma}) &= \int_c^d ||\tilde{k}(s)||\ ||\tilde{\gamma}'(s)||\ ds \\
&= \int_c^d ||k(\varphi(s))||\ ||\gamma'(\varphi(s))||\varphi'(s)\ ds, \text{by Lemma 1.13 and using } \varphi'(s) > 0, \\
&= \int_{\varphi^{-1}(a)}^{\varphi^{-1}(b)} ||k(\varphi(s))||\ ||\gamma'(\varphi(s))||\varphi'(s)\ ds \\
&= \int_a^b ||k(t)||\ ||\gamma'(t)||\ dt, \text{by changing variables to } t = \varphi(s), \\
&= \mu(\gamma),
\end{aligned}$$

where we define $a = \varphi(c)$ and $b = \varphi(d)$. □

Definition 1.17 Let $\gamma : [a, b] \to \mathbb{R}^n$ be a parametrised curve. It is called closed if $\gamma(a) = \gamma(b)$ and $\gamma^{(k)}(a) = \gamma^{(k)}(b)$ for every $k \in \mathbb{Z}^+$. It is called simple if $\gamma|_{[a,b)}$ is injective.

Remark 1.18 Now, Definition 1.17 allows us to view a simple closed curve as a smooth injective map of the form $f : S^1 \to \mathbb{R}^n$, where S^1 is the one-dimensional sphere (or unit circle). This is a so-called embedding of the unit circle into real space, see Definition 1.35 for a generalisation of this concept. A number of texts on knot theory use such a function as the definition of a knot, where the co-domain is $\mathbb{R}^3$.

1.2 Topology and Isotopy

Topology is a powerful tool for the study of knots, in particular for defining what a mathematical knot is. We first recall some fundamental ideas from topology. Note that any text introducing

point-set topology worth its salt will include most of the definitions and results here (and many more) but we select only the ones most beneficial to us, proving them independently by definition-chasing. For the sake of completeness, see [May00].

Definition 1.19 A topology on a set X is a collection τ of subsets of X satisfying these:

(i) $\emptyset, X \in \tau$.

(ii) If $U, V \in \tau$, then $U \cap V \in \tau$.

(iii) If $\{U_\lambda\}_{\lambda \in \Lambda}$ is a family of subsets where $U_\lambda \in \tau$, for all $\lambda \in \Lambda$, then $\bigcup_{\lambda \in \Lambda} U_\lambda \in \tau$.

Example 1.20 Consider $\{1, 2, 3, 4, 5\}$. One possible topology we can endow upon this set is $\tau = \{\emptyset, \{1, 2\}, \{3, 4, 5\}, \{1, 2, 3, 4, 5\}\}$. It is quite trivial to verify that this is a topology, given that the only non-trivial subsets within this collection partition our superset.

Definition 1.21 Let (X, τ) be a topological space and $U \subseteq X$ some subset. The subset is said to be open if $U \in \tau$ and the subset is said to be closed if $X \setminus U \in \tau$.

Example 1.22 Consider the closed interval $[0, 1] \subseteq \mathbb{R}$. We better expect that this be closed in the standard Euclidean topology (the topology generated by open intervals). Indeed, this would be the case. However, $[0, 1] \subseteq [0, 1]$ is both open and closed in **any** topology we endow upon the interval (the whole space is always both open and closed by definition).

Note that openness and closure are *not* opposites of each other and not every subset can be classified as either of them, that is a subset can be open, closed, both or neither.

Definition 1.23 Let X and Y be topological spaces. A function $f : X \to Y$ is continuous if for all $U \subseteq Y$ open, it follows that $f^{-1}(U) \subseteq X$ is open.

Example 1.24 Consider the map $\pi : \mathbb{R}^2 \to \mathbb{R}$, defined as $\pi(x, y) = x$, where the topologies are induced by the standard Euclidean metric (meaning that the respective topologies consist of unions of open balls). This so-called projection map is continuous; take $U \subseteq \mathbb{R}$ an arbitrary open subset and note $\pi^{-1}(U) = \{(x, y) : x \in U\} = U \times \mathbb{R}$, which itself is open because $U \subseteq \mathbb{R}$ is open by assumption and $\mathbb{R} \subseteq \mathbb{R}$ is open by Definition 1.19.

Proposition 1.25 *Let X and Y be topological spaces. A function $f : X \to Y$ is continuous if and only if for all $C \subseteq Y$ closed, it follows that $f^{-1}(C) \subseteq X$ is closed.*

Proof: ($\Rightarrow$) Let $C \subseteq Y$ be closed. So, this means that $f^{-1}(Y \setminus C) = X \setminus f^{-1}(C) \subseteq X$ is open by continuity, because $Y \setminus C \subseteq Y$ is open. Thus, $f^{-1}(C) \subseteq X$ is closed by definition.

($\Leftarrow$) Let $U \subseteq Y$ be open. Then, it must be that $f^{-1}(Y \setminus U) = X \setminus f^{-1}(U) \subseteq X$ is closed by assumption, since $Y \setminus U \subseteq Y$ is closed. Hence, $f^{-1}(U) \subseteq X$ is open by definition. $\square$

Lemma 1.26 *Let X, Y, Z be topological spaces and suppose $f : X \to Y$ and $g : Y \to Z$ are continuous. Then, $f \circ g : X \to Z$ is continuous.*

Proof: Take $U \subseteq Z$ open. Then, by the continuity of g, it follows that $g^{-1}(U) \subseteq Y$ is open but then, by the continuity of f, it follows that $f^{-1}(g^{-1}(U)) \subseteq X$ is open. □

Definition 1.27 Let (X, τ) be a topological space and $A \subseteq X$. The subspace topology is defined as $\tau_A = \{U \cap A : U \in \tau\}$. The topological space (A, τ_A) is then called a subspace.

Example 1.28 We shall consider one example but we will prove it is indeed a subspace. Let's consider $\mathbb{Z} \subseteq \mathbb{R}$. The subspace topology induced by the standard Euclidean topology τ will be the so-called discrete topology, that is where every subset is open (and therefore also closed by Definition 1.21). Indeed, any interval of the form $(n-1/2, n+1/2) \subseteq \mathbb{R}$ is open, for every $n \in \mathbb{Z}$. As such, we have $(n - 1/2, n + 1/2) \cap \mathbb{Z} = \{n\} \in \tau_{\mathbb{Z}}$ by Definition 1.27.

Lemma 1.29 *Suppose X and Y are topological spaces, $A \subseteq X$ is a subspace and $f : X \to Y$ is continuous. Then, the restriction $f|_A : A \to Y$ is continuous.*

Proof: Consider the inclusion map $\iota_A : A \to X$, given by $\iota_A(x) = x$. It is enough to show that this is continuous. Indeed, take $U \subseteq X$ open. Then, $\iota_A^{-1}(U) = U \cap A$, which is open in the subspace by definition. Now, $f|_A = f \circ \iota_A$ and Lemma 1.26 gives the result. □

Lemma 1.30 *Let X and Y be topological spaces and $B \subseteq Y$ be a subspace. If $f : X \to Y$ is continuous and is such that $f(x) \in B$, for all $x \in X$, then $\hat{f} : X \to B$ is continuous.*

Proof: Take $U \subseteq B$ open. By definition, $U = V \cap B$, where $V \subseteq Y$ is open. Consequently, $\hat{f}^{-1}(U) = \hat{f}^{-1}(V \cap B) = \hat{f}^{-1}(V) \cap \hat{f}^{-1}(B) = f^{-1}(V)$, using the assumption that $f(x) \in B$, equivalent to $x \in f^{-1}(B)$. Thus, $f^{-1}(V) = \hat{f}^{-1}(U) \subseteq X$ is open by the continuity of f. □

Definition 1.31 Let (X, τ) be a topological space and $\sim$ be an equivalence relation on X. Then, the quotient topology on the set of equivalence classes is $\tau_q = \{U \subseteq {}^X/_\sim : q^{-1}(U) \in \tau\}$, where $q : X \to {}^X/_\sim$ given by $q(x) = [x]$ is the quotient map. We call $({}^X/_\sim, \tau_q)$ a quotient space.

A special type of continuous function is the analogue of an isomorphism between topological spaces. This will now be defined, but first the intuition: two topological spaces are the 'same' if one can be continuously deformed into the other without 'cutting' or 'glueing'.

Definition 1.32 Let X and Y be topological spaces. These spaces are homeomorphic if there exists a continuous bijection $f : X \to Y$ whose inverse is continuous, denoted $X \cong Y$. Such a function is then called a homeomorphism.

Example 1.33 Consider the unit circle S^1 and the interval $[0,1]$. These are *not* homeomorphic. However, we can define an equivalence relation between elements $x, y \in [0,1]$ as follows:

$$x \sim y \text{ if and only if } x = y \text{ or } x, y \in \{0,1\}.$$

Thus, we see that $^{[0,1]}/_{\sim}$ is a so-called quotient space consisting of the equivalence classes

$$[0] = [1] \text{ and } [z] = \{z\}, \text{ for all } z \in (0,1).$$

Now, we can construct a homeomorphism between $^{[0,1]}/_{\sim}$ and S^1, namely

$$f : {}^{[0,1]}/_{\sim} \to S^1, \text{ given by } f([x]) = (\cos(2\pi x), \sin(2\pi x)).$$

It is known that cos and sin are continuous; therefore f is continuous. As for the inverse, it is

$$f^{-1}((y_1, y_2)) = [\tan^{-1}(y_2/y_1)/2\pi].$$

By the continuity of $\tan^{-1}$, and noting that the quotient map is itself continuous and surjective, it must be that f^{-1} is a continuous inverse; this shows that f is a homeomorphism.

Lemma 1.34 *Let X, Y, Z be topological spaces and suppose $f : X \to Y$ and $g : Y \to Z$ are homeomorphisms. Then, $f \circ g : X \to Z$ is a homeomorphism.*

Proof: By definition, f^{-1} and g^{-1} are continuous and Lemma 1.26 applies, meaning both $f \circ g$ and $g^{-1} \circ f^{-1}$ are continuous. Finally, as the composition of bijections is a bijection, we have that $f \circ g$ is a continuous bijective function with continuous inverse $(f \circ g)^{-1}$. □

Definition 1.35 Suppose X and Y are topological spaces. An embedding of X into Y is a continuous injective map $f : X \to Y$ such that $f : X \to f(X)$ is a homeomorphism.

In fact, this is a slightly weaker notion than a homeomorphism.

Example 1.36 Consider the map $f : \mathbb{R} \to \mathbb{R}^2$ where $f(x) = (x, x^3)$. This is an embedding. Indeed, this map is continuous as it is a polynomial function and so Lemma 1.30 applies by considering $f(X) \subseteq Y$ as a subspace, implying that the restriction is continuous. Now, assuming $f(x) = f(y)$, we have that $(x, x^3) = (y, y^3)$ so comparing the first element of the two-tuples immediately gives that $x = y$, hence injectivity. The restriction is certainly surjective. Lastly, the inverse is the projection map $\pi : f(\mathbb{R}) \to \mathbb{R}$, given by $\pi(x, x^3) = x$. This is continuous by Example 1.24.

Definition 1.37 Let X and Y be topological spaces where $f, g : X \to Y$ are embeddings. An isotopy from f to g is a continuous map $F : X \times [0,1] \to Y$ where $F(x,0) = f(x)$, $F(x,1) = g(x)$

and $F(x,t)$ is an embedding for each $t \in [0,1]$.

Example 1.38 Consider $f, g : \mathbb{R} \to \mathbb{R}^2$ given by $f(x) = (x, 0)$ and $g(x) = (x, x^3)$, with standard Euclidean topologies. The map $F : \mathbb{R} \times [0,1] \to \mathbb{R}^2$ where $F(x,t) = (x, tx^3)$ is an isotopy. Indeed, Example 1.36 gives that g is an embedding and it is clear that f is also. Furthermore, we can see immediately that $F(x,0) = f(x)$ and $F(x,1) = g(x)$. Finally then, for any fixed $t \in [0,1]$, $F_t(x) = F(x,t)$ is a two-tuple consisting of polynomial functions, meaning it is continuous; it is injective since $F_t(x) = F_t(y)$ is to say $(x, tx^3) = (y, ty^3)$, thus $x = y$; it is surjective as $F_t : \mathbb{R} \to F_t(\mathbb{R})$ is the map $F_t(x) = (x, tx^3)$; its inverse is the projection map $\pi : F_t(\mathbb{R}) \to \mathbb{R}$, given by $\pi(x, tx^3) = x$, continuous by Example 1.24 and Lemma 1.29. Consequently, F_t is an embedding and thus F is an isotopy.

A stronger notion is the following, which will allow us to give a useful definition of what it means for a closed curve to be either knotted or unknotted.

Definition 1.39 Let X and Y be topological spaces where $f, g : X \to Y$ are homeomorphisms. An ambient isotopy from f to g is a continuous map $F : X \times [0,1] \to Y$ such that $F(x,0) = x$, $F(f(x),1) = g(x)$ and $F(x,t)$ is a homeomorphism for each $t \in [0,1]$.

Proposition 1.40 *Ambient isotopy defines an equivalence relation.*

Proof: Throughout the proof, suppose X and Y are topological spaces with $f, g, h : X \to Y$ homeomorphisms. First, it is clear that f is ambient isotopic to itself via $F(x,t) = f(x)$. So, we have reflexivity. Next, suppose f is ambient isotopic to g via $F(x,t)$. It then follows that g is ambient isotopic to f via $G(x,t) = F_1^{-1}(F(x,1-t))$. Indeed, from the definition, we have

$$G(x,0) = F_1^{-1}(F(x,1)) = F_1^{-1}(F_1(x)) = x$$

and

$$G(g(x),1) = F_1^{-1}(F(g(x),0)) = F_1^{-1}(g(x)) = f(x),$$

the final part of the definition of ambient isotopy a result of Lemma 1.34. Hence, we have proven symmetry. Finally, again suppose f is ambient isotopic to g via $F(x,t)$ and g is ambient isotopic to h via $G(x,t)$. Thus, f is ambient isotopic to h by $H(x,t) = G(F(x,t),t)$, since

$$H(x,0) = G(F(x,0),0) = G(x,0) = x$$

and

$$H(f(x),1) = G(F(f(x),1),1) = G(g(x),1) = h(x),$$

again applying Lemma 1.34 to complete the verification, which thus gives transitivity. □

2 Knots and Links

The theory developed in Section 1 suffices to now give a rigorous definition of a knot.

Definition 2.1 A knot is an equivalence class of closed curves, where the equivalence relation is ambient isotopy.

Definition 2.2 We say that K is knotted if there does **not** exist an ambient isotopy on $\mathbb{R}^3$ such that K is ambient isotopic to the unit circle S^1. Otherwise, we say that K is unknotted; we then identify any unknot with S^1.

We require *ambient isotopy* in Definition 2.1 since *isotopy* is not a strong enough condition; any embedding of a knot according to our definition is always isotopic to the unknot (this follows from a procedure called a bachelor's unknotting whereby 'pulling' on a curve makes the knot shrink to a point and vanish; this is mentioned in [Cro04]).

Remark 2.3 The literature makes a distinction between so-called tame and wild knots, they are knots that can either be represented as a *finite* polygonal chain (tame) or behave pathologically (wild). In fact, Definition 2.2 precludes wild knots since we specify that a knot is the image of smooth map (this is how we defined a curve) and wild knots fail to have well-defined derivatives, as noted in [Liv93].

2.1 Knot Diagrams and Reidemeister Moves

We next restrict to looking at knots from a projective point of view. There is a lot to be said about knot projections and isotopy; we will see that it is not at all trivial to determine if a given simple regular closed curve is knotted or unknotted.

Definition 2.4 Let $K_1, ..., K_n \subseteq \mathbb{R}^3$ be knots. Then, a link is the disjoint union of knots, that is $L = K_1 \sqcup ... \sqcup K_n$. The knots forming said link are called the components of L.

In particular, any knot is a link with a single component. It is also important to visualise knots and links, as will be possible by the next definition; this will be immensely useful throughout the rest of the discussion.

Definition 2.5 Let $L \subseteq \mathbb{R}^3$ be a link. A link diagram is a projection of L onto $\mathbb{R}^2$ with crossings consisting of **one** continuous curve (over-crossing) and **one** discontinuous curve (under-crossing).

Example 2.6 Consider the diagrams of the so-called unknot, trefoil knot and Hopf link:

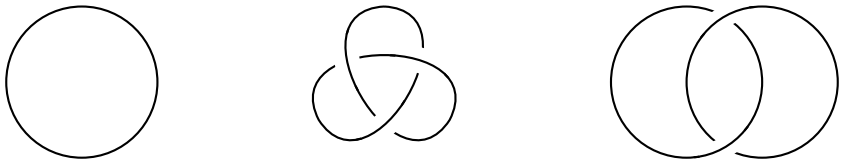

Figure 1: Respective diagrams of the unknot, trefoil knot and Hopf link.

Definition 2.7 Let L be a diagram of a link. An orientation of L is a choice of direction along each component of L in which the diagram is traversed.

Example 2.8 There are two possible orientations of the trefoil knot, shown in Figure 2 below.

Figure 2: The two orientations of the trefoil knot.

Definition 2.9 Let L be an oriented diagram of a link. The writhe of L is the sum of the signs of the crossings, denoted $\omega(L)$, subject to the following conventions of Figure 3.

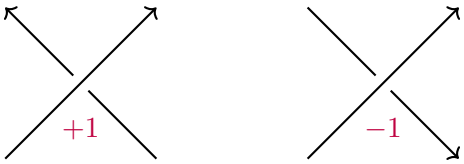

Figure 3: The signs of a link diagram's crossings.

Example 2.10 Consider the first of the orientations for the trefoil K as in Figure 2. One can easily compute $\omega(K) = -3$. Notice this is true irrespective of the orientation of K.

Lemma 2.11 *The writhe of a knot diagram is independent of its orientation.*

Proof: Let K be a diagram of a knot with some arbitrary orientation. By considering Figure 3, it is clear that changing said orientation preserves the sign at a crossing. □

Remark 2.12 Of course, Lemma 2.11 will fail if we instead refer to a diagram of a link with more than one component. An easy example is the Hopf link as in Example 2.6; it can have writhe either 2 or -2, depending on the orientation of each component.

Lemma 2.13 *Let K be the diagram of a knot and $\overline{K}$ its mirror image. Then, $\omega(\overline{K}) = -\omega(K)$.*

Proof: By taking mirror images, it is obvious that the types of crossing in Figure 3 will interchange roles, meaning that the sum of the signs of the crossings will be of opposite sign to $\omega(K)$, that is $\omega(\overline{K}) = -\omega(K)$ as needed. □

Now, we wish to develop some theory as a means of determining if two knots are ambient isotopic without the technical construction as in Definition 1.39. It will very quickly become clear that a vast majority of this paper is dedicated to building machinery for this very purpose. However, the technicality we face when studying a class of curves shan't be understated. We use the following definition which allows us to work only with knot diagrams; this is significantly nicer.

Definition 2.14 The Reidemeister moves are the following, applied to an arc of a link:

(**R0**) Planar isotopy of an arc.

(**R1**) Twisting part of an arc.

(**R2**) Moving an arc in front of or behind another arc.

(**R3**) Moving an arc in front of or behind a crossing.

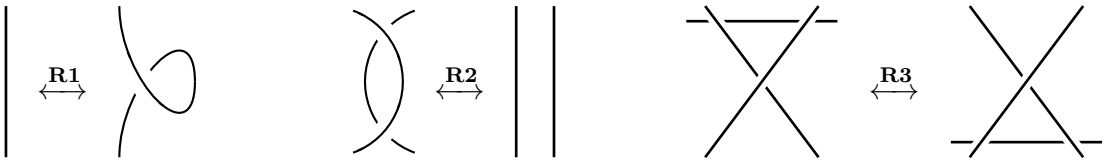

Figure 4: The Reidemeister moves from a knot diagram perspective.

Definition 2.15 Two link diagrams L and L' are called isotopic if they can be obtained from each other by a finite sequence of Reidemeister moves. They are called regularly isotopic if the they are isotopic via only the second and third Reidemeister moves.

Theorem 2.16 (Reidemeister's Theorem) *Two links L and L' are ambient isotopic if and only if their diagrams are related by a finite sequence of Reidemeister moves.*

The proof of this theorem is beyond the scope of this paper and is omitted but can be found in [Rei27]. Nevertheless, Reidemeister's work allows us to focus primarily on the three operations in Definition 2.14 and see how properties are affected by each of the Reidemeister moves.

Definition 2.17 A knot diagram K is called achiral if it is isotopic to its mirror image $\overline{K}$ and is called chiral if it is **not** isotopic to its mirror image.

Example 2.18 One of the most basic achiral knots is the figure-eight knot, which we can show directly by using the Reidemeister moves to get from the left-handed diagram to the right-handed diagram, and appealing to Theorem 2.16, as is done so in Figure 5.

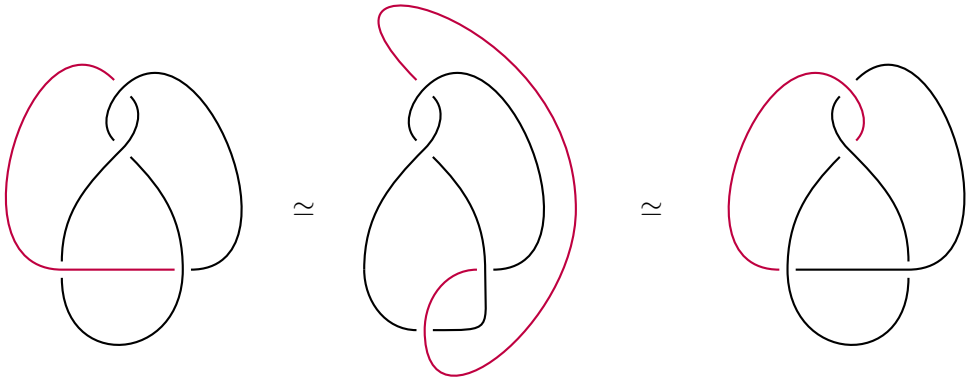

Figure 5: The ambient isotopy between mirrors of the figure-eight knot.

2.2 Arithmetic of Knots

One may ask if it be possible to join two links together in some way; it is. We will refer back to these notions later to show the interplay between properties of two links and this arithmetic.

Definition 2.19 Let L_1 and L_2 be two disjoint unoriented link diagrams. The connected sum of these diagrams, denoted $L_1 \# L_2$, is a combination of these diagrams in the following way:

(i) Find some quadrilateral region of $\mathbb{R}^2$ such that two of its sides are parts of arcs of each link diagram but otherwise it is disjoint from the diagrams.

(ii) Remove the parts of the arcs that coincide with the quadrilateral and add arcs on the other two sides of the quadrilateral.

Example 2.20 Let K_1 and K_2 be trefoil knots of opposite chirality. So, Figure 6 shows $K_1 \# K_2$.

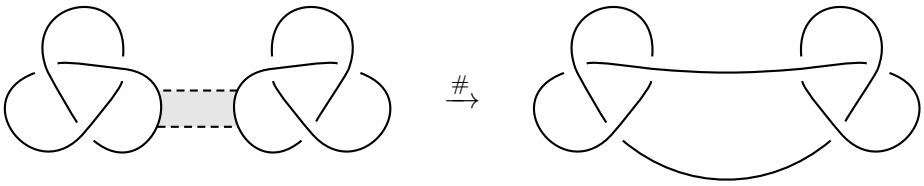

Figure 6: The connected sum of chiral-opposite trefoil knots.

Remark 2.21 The connected sum is more generally a topological operation which applies to manifolds. In the case where we deal with knots, the diagrams can be treated as one-manifolds. However, every knot is homeomorphic to S^1 so this more general connected sum fails to recognise the importance of the way our knots are embedded into $\mathbb{R}^3$.

We can adapt Definition 2.19 to account for the links being oriented. This situation has one additional condition; the quadrilateral chosen in the definition must be such that the orientation of the two sides which are parts of arcs oppose each other. We can then orientate the new arcs, the ones we add in (ii) of Definition 2.19. This is made visual by the next example.

Example 2.22 Let K_1 and K_2 be oriented trefoil knots of opposite chirality. Then, Figure 7 shows $K_1 \# K_2$.

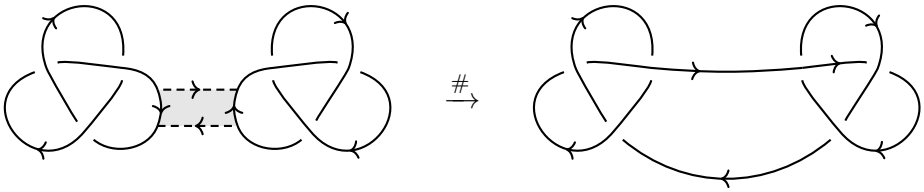

Figure 7: The connected sum of oriented chiral-opposite trefoil knots.

Theorem 2.23 *The set of knots with the operation connected sum forms a commutative monoid.*

Sketch of Proof: We must show that the connected sum is a commutative, associative binary operation and that there is an identity element. It is intuitively clear that $K \# \bigcirc = K$ by isotopy of the diagrams. This gives us the existence of the identity, namely the unknot.

For commutativity, let K_1 and K_2 be disjoint knot diagrams. Simply appeal to the **R2** and **R3** Reidemeister moves to 'push' K_1 along $K_1 \# K_2$ until it is to the right-hand side of K_2. By Reidemeister's Theorem, it follows that $K_1 \# K_2 = K_2 \# K_1$.

For associativity, suppose we have $(K_1 \# K_2) \# K_3$. Either K_3 is connected straight onto K_2, in which the result follows, or K_3 is not connected directly to K_2, in which we can proceed as with commutativity and 'pushing' K_3 along $(K_1 \# K_2) \# K_3$ until it is adjoined to K_2. Either way, it follows that $(K_1 \# K_2) \# K_3 = K_1 \# (K_2 \# K_3)$.

Finally, that the connected sum of any number of knots is also a knot is intuitively clear. $\square$

3 Knot Invariants

Now we begin the discussion on distinguishing between different knots and their diagrams by developing properties of knots that remain invariant under the Reidemeister moves.

Definition 3.1 A property preserved under the Reidemeister moves is an isotopy invariant.

We can now evaluate such invariants in comparison with others; as will soon be evident, some are much stronger than others. First we prove a small result which will be useful later.

Lemma 3.2 *The writhe is a regular isotopy invariant.*

Proof: The result is intuitive by considering Figure 4 prescribed with any orientations. Indeed, **R2** will remove two crossings of opposite sign, so said crossings are ignored when calculating the writhe anyway, and **R3** clearly doesn't change the writhe. □

3.1 Colourability

The first property considered is that of colourability. We will use results from linear algebra to define tri-colourability and prove that it is a knot invariant. The discussion will then be extended to p-colourability, for $p > 2$ any prime.

Definition 3.3 A knot diagram is tri-colourable if it can be coloured with three colours such that the following are satisfied:

(i) At least two colours are used.

(ii) If two colours meet at a crossing, they meet a third colour also.

Example 3.4 Consider a diagram of the trefoil knot. It is tri-colourable, as shown in Figure 8.

Figure 8: An example of a tri-colouring of the trefoil knot.

Example 3.5 The unknot is **not** tri-colourable as there is one arc so only one colour is used.

Theorem 3.6 *Tri-colourability is an isotopy invariant.*

Proof: We will simply demonstrate that for a given tri-coloured diagram of a knot, K say, the Reidemeister moves **R1**, **R2**, **R3** preserve the tri-colourability conditions of the diagram. For **R1**, note that an arc of K can only have one colour and inserting a twist introduces a crossing on that arc, but there is only one colour at that crossing, so the second condition of Definition 3.3 is satisfied. If K is tri-colourable, then the first condition of Definition 3.3 holds automatically. Hence, **R1** preserves tri-colourability. For **R2** and **R3**, there are two and five cases to consider, respectively. This is done by simply applying the moves locally to the pre-tri-coloured knot K and observing that tri-colourability still holds, as in Figure 9, which completes the proof. □

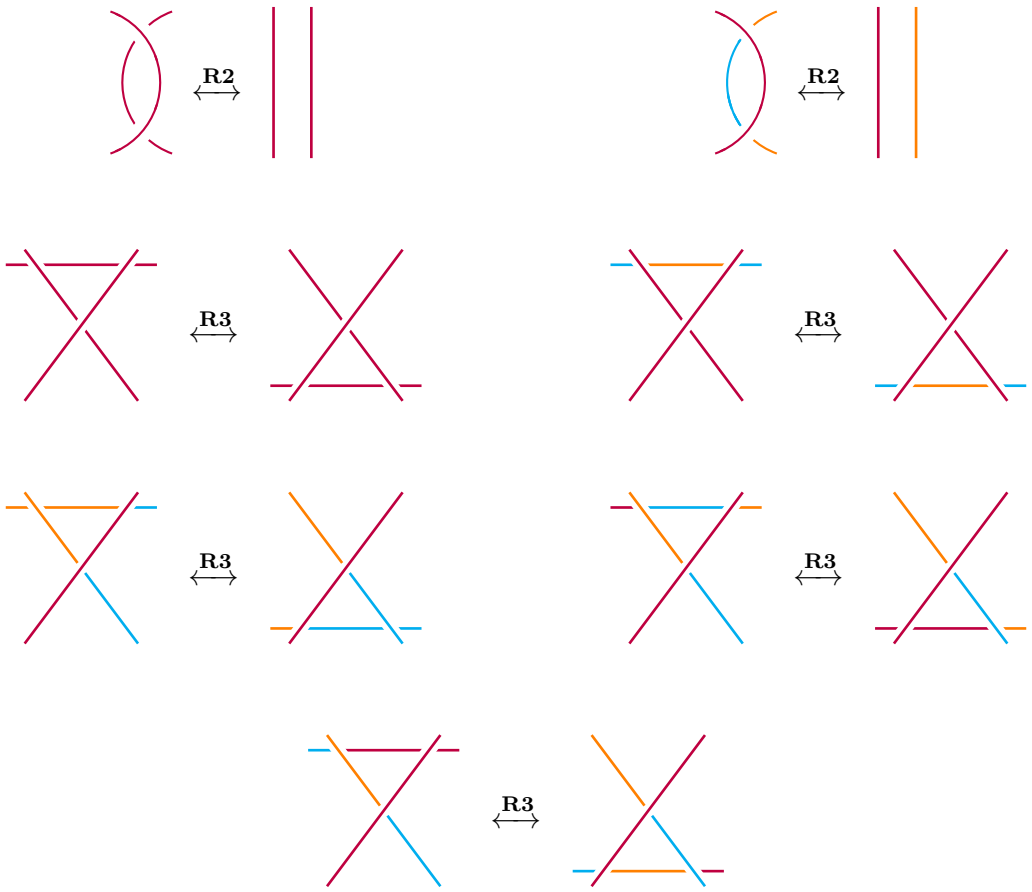

Figure 9: Tri-colourability being preserved under the Reidemeister moves.

Corollary 3.7 *If a knot is tri-colourable, then it is* ***not*** *ambient isotopic to the unknot.*

Note that Theorem 3.6 is somewhat useful for seeing if a knot is ambient isotopic to the unknot. However, there are a few immediate shortcomings. Firstly, some knots are **not** tri-colourable but are still **not** ambient isotopic to the unknot (the figure-eight knot for example). Secondly, two knot diagrams being tri-colourable does **not** mean they are ambient isotopic (the trefoil and its

mirror image, for example). However, we can improve on this notion slightly. In order to extend colourability of a knot diagram, as hinted at in [GP94], to a more general setting, define the set of n colours used in a colouring of a knot diagram to be $\mathbb{Z}_n$. We re-state the second condition of Definition 3.3. Indeed, let $x, y, z \in \mathbb{Z}_3$ where z is the colour of an over-crossing. Then, we have

$$x + y - 2z \equiv 0 \pmod 3.$$

The generalisation now follows, and underpins a very surprising numerical isotopy invariant.

Definition 3.8 Let $p > 2$ be prime. A knot diagram is p-colourable if it can be coloured with p colours such that the following are satisfied:

(i) At least two colours are used.

(ii) For $x, y, z \in \mathbb{Z}_p$, at any crossing with over-crossing z and under-crossings x and y, it must be that $x + y - 2z \equiv 0 \pmod p$.

Remark 3.9 We can solve an exercise in [Bos19] to see that no knot can be 2-colourable. Indeed, if $p = 2$ was allowed in Definition 3.8, it would mean that $x + y - 2z \equiv 0 \pmod 2$, which is to say $x \equiv y \pmod 2$. But then, we have $x \equiv z \pmod 2$. Here we have considered an arbitrary crossing, so only one colour is used; the first part of Definition 3.8 fails.

We can appeal to linear algebra to better understand the concept of p-colourability and the (somewhat limited) power it has. For that, we must define and prove a number of things.

Definition 3.10 Let K be a diagram of a knot with n crossings. A colouring matrix M_K of K is an $n \times n$ matrix with rows and columns representing the crossing and arcs of K, respectively, where an entry of 2 denotes an over-crossing, an entry of -1 denotes an under-crossing and an entry of 0 denotes exclusion from a crossing.

Remark 3.11 There is a particular case to discuss, that is when an arc crosses itself as in the **R1** move. Here, there is seemingly no well-defined notion of an over-crossing and under-crossing since one arc acts as both. As such, we assign an entry of 1 for such an occurrence.

Example 3.12 Consider the the trefoil knot as in Figure 1, with arcs labelled x_1, x_2, x_3 and crossings labelled $1, 2, 3$, anti-clockwise, with arc x_n leading to crossing n. The colouring matrix with respect to these conventions is

$$M_K = \begin{pmatrix} -1 & -1 & 2 \\ 2 & -1 & -1 \\ -1 & 2 & -1 \end{pmatrix}.$$

Remark 3.13 The colouring matrix can be viewed as a matrix of coefficients for a system of n equations, the so-called colouring equations. As is evident from Example 3.12, the rows and columns of the colouring matrix will sum to zero, meaning the rows and columns are linearly dependent as vectors in $\mathbb{R}^3$; linear algebra tells us that $\det(M_K) = 0$ as a result. Sadly then, this fails to be any form of invariant, as one may initially hope.

Definition 3.14 Let K be a diagram of a knot. The knot determinant $\det(K)$ of K is defined as the absolute value of **any** minor of the matrix M_K. The unknot has determinant 1 by convention.

Example 3.15 Continuing on from Example 3.12, we can consider the minor of M_K formed by removing the first row and second column, which gives us

$$\det(K) = \left| \det \begin{pmatrix} -1 & -1 \\ 2 & -1 \end{pmatrix} \right| = 3.$$

In fact, it is rather easy to see that all minors of the colouring matrix M_K coincide up to absolute value. We must be sure that this is always true and so this is what we demonstrate next.

Lemma 3.16 *The knot determinant is well-defined.*

Proof: We actually prove a stronger result as in [Cam08], namely if some $n \times n$ matrix M has the property that the entries along every row sum to zero, and the entries down every column sum to zero, then the absolute value of every minor is equal. Suppose that U is an $n \times n$ matrix consisting only of ones. We will compute $\det(M + U)$ in terms of an arbitrary minor M_{ij} of M. To do this, we will appeal to classical row operations as in linear algebra. If m_{ij} represents the entries of M, then

$$M + U = \begin{pmatrix} m_{11}+1 & \cdots & m_{1j}+1 & \cdots & m_{1n}+1 \\ \vdots & & \vdots & & \vdots \\ m_{i1}+1 & \cdots & m_{ij}+1 & \cdots & m_{in}+1 \\ \vdots & & \vdots & & \vdots \\ m_{n1}+1 & \cdots & m_{nj}+1 & \cdots & m_{nn}+1 \end{pmatrix}.$$

We assume that the rows and the columns of M each sum to zero, that is

$$\sum_{j=1}^{n} m_{ij} = 0, \text{ for fixed } i, \qquad \text{and} \qquad \sum_{i=1}^{n} m_{ij} = 0, \text{ for fixed } j,$$

respectively. We now proceed with elementary row and column operations on $M + U$ which transforms it into a matrix which is identical apart from the j^{th} column being all-zero except for an n on the i^{th} row down. See Appendix A for the explicit computations. If we call the resulting

matrix $\widetilde{M}$, we know $\det(M+U) = n\det(\widetilde{M})$, the factor of n a result of the elementary operations we used. But now, $\det(\widetilde{M}) = n(-1)^{i+j}\det(M_{ij})$, so $\det(M+U) = n^2(-1)^{i+j}\det(M_{ij})$. It must be that $\det(M_{ij})$ is independent of the choice of i and j up to sign. □

We are getting closer to being able to prove that the knot determinant is an isotopy invariant, which is surprising given that it is relatively simple to define and it is numerical. Before we do so, we shall show that there is a connection between knot determinants and the colourability of the corresponding knot.

Proposition 3.17 *Let K be a diagram of a knot. K is p-colourable if and only if $p \mid \det(K)$.*

Proof: Now, K is p-colourable if and only if the system of colouring equations has a solution, which occurs if and only if there exists $\mathbf{v} \in \mathbb{Z}_p^n$ where $\mathbf{v} \neq \lambda\mathbf{1}$, for any $\lambda \in \mathbb{Z}$, such that $M_K\mathbf{v} = \mathbf{0}$. By a classical result of linear algebra, it follows that $\text{rank}(M_K) < n$, since $\det(M_K) = 0$. Every solution of this system will lie in $\ker(M_K)$ yet we demand a non-zero solution, so $\text{null}(M_K) > 0$ which implies that $\text{rank}(M_K) < n-1$, by the Rank-Nullity Theorem. This is equivalent to saying that the determinant of each $(n-1) \times (n-1)$ minor vanishes modulo p by a result of [MZ19]. This is precisely the condition $\det(K) \equiv 0 \pmod{p}$ and so $p \mid \det(K)$. □

Example 3.18 Appealing to Proposition 3.17 in the context of Example 3.15, it is clear that the trefoil is tri-colourable but **not** $(5, 7, 11, ...)$-colourable; it is only tri-colourable.

The consequence of Example 3.18 shouldn't be so surprising; we can convince ourselves that it is not possible to colour the trefoil for $p \geq 5$ by looking at the usual diagram. However, this triviality is not always the case, as we will now see.

Example 3.19 Consider the following labelled diagram of the so-called endless knot:

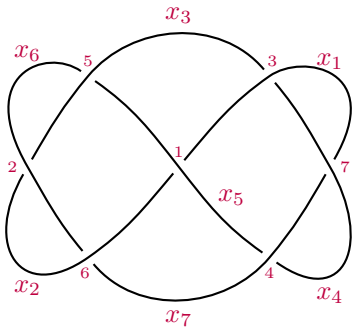

Figure 10: Labelling for the colouring matrix of the endless knot.

This gives rise to the colouring matrix

$$M_K = \begin{pmatrix} -1 & -1 & 0 & 0 & 2 & 0 & 0 \\ 0 & -1 & -1 & 0 & 0 & 2 & 0 \\ 2 & 0 & -1 & -1 & 0 & 0 & 0 \\ 0 & 0 & 0 & -1 & -1 & 0 & 2 \\ 0 & 0 & 2 & 0 & -1 & -1 & 0 \\ 0 & 2 & 0 & 0 & 0 & -1 & -1 \\ -1 & 0 & 0 & 2 & 0 & 0 & -1 \end{pmatrix}.$$

We need only calculate the determinant of a minor and take its absolute value. For the sake of time, we will state the result: $\det(K) = 15$. Accordingly, the endless knot is both 3-colourable and 5-colourable, as a result of Proposition 3.17.

We next state and prove another linear algebra result. It will provide us with the means of justifying why the knot determinant is invariant under the Reidemeister moves.

Lemma 3.20 *Let M be an $n \times n$ matrix. Adjoining an all-zero row and an all-zero column except for a one at their intersection, occurring on the leading diagonal, will* ***not*** *change* $\det(M)$.

Proof: Consider the determinant of M as an expansion by minors on the i^{th} row, that is

$$\det(M) = \sum_{j=1}^{n} (-1)^{i+j} m_{ij} \det(M_{ij}),$$

where m_{ij} is an entry of M and M_{ij} is the minor formed by removing the i^{th} row and j^{th} column. If M' is this extended matrix with the i^{th} row being all zero except for one on the diagonal, then

$$\det(M') = \sum_{j=1}^{n+1} (-1)^{i+j} m'_{ij} \det(M'_{ij}) = \det(M'_{ii}),$$

as the only position in which there is something non-zero is when $j = i$. Moreover, it follows that $\det(M'_{ii}) = \det(M)$ and this completes the proof. □

Theorem 3.21 *The knot determinant is an isotopy invariant.*

Proof: It suffices to show that the Reidemeister moves preserve the knot determinant. Let K be the knot on which such manipulations are performed. For **R1** and **R2**, let M_K be the knot's colouring matrix and $K_{\mathbf{R1}}$ and $K_{\mathbf{R2}}$ be the new diagrams formed by performing each of these moves. We claim that via the use of elementary row and column operations, the new matrices

will take the following form:

$$M_{K_{\mathbf{R1}}} \sim \begin{pmatrix} & & & 0 \\ & M_K & & \vdots \\ & & & 0 \\ 0 & \cdots & 0 & 1 \end{pmatrix} \quad \text{and} \quad M_{K_{\mathbf{R2}}} \sim \begin{pmatrix} & & 0 & 0 \\ & M_K & \vdots & \vdots \\ & & 0 & 0 \\ 0 & \cdots & 0 & 1 & 0 \\ 0 & \cdots & 0 & 0 & 1 \end{pmatrix}.$$

The full detail is given in Appendix B. As a result of Lemma 3.20, the determinant and nullity is unchanged; we know that the nullity of the original matrix is the dimension of the space of solutions to $M_K\mathbf{v} = \mathbf{0}$ and this is clearly preserved by the above forms of each colouring matrix. It follows from this that $\det(K_{\mathbf{R1}}) = \det(K) = \det(K_{\mathbf{R2}})$. Lastly, it is clear that an **R3** move on a diagram K, resulting in the diagram $K_{\mathbf{R3}}$, wouldn't change the knot determinant since $M_{K_{\mathbf{R3}}}$ is also an $n \times n$ matrix, obtainable from M_K by interchanging rows and columns. □

Example 3.22 We again consider our favourite trefoil and an equivalent diagram in Figure 11.

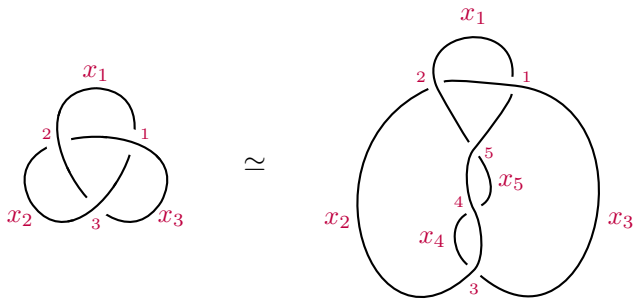

Figure 11: Applying the second Reidemeister move to the trefoil.

We have computed M_K in Example 3.15. It remains to compute $M_{K'}$ and in doing so we achieve

$$M_{K'} = \begin{pmatrix} -1 & -1 & 2 & 0 & 0 \\ 2 & -1 & -1 & 0 & 0 \\ 0 & 2 & -1 & -1 & 0 \\ 0 & 2 & 0 & -1 & -1 \\ -1 & 2 & 0 & 0 & -1 \end{pmatrix} \overset{\varphi}{\mapsto} \begin{pmatrix} -1 & -1 & 2 & 0 & 0 \\ 2 & -1 & -1 & 0 & 0 \\ -1 & 2 & -1 & 0 & 0 \\ 0 & 0 & 0 & 1 & 0 \\ 0 & 0 & 0 & 0 & 1 \end{pmatrix},$$

where φ represents the below sequence of row and column operations:

$$R_3 \mapsto R_3 + R_5, \quad R_3 \mapsto R_3 - R_4, \quad R_4 \mapsto R_4 - R_5,$$

$$C_1 \mapsto C_1 + C_4 - C_5, \quad C_2 \mapsto C_2 + 2C_5, \quad C_4 \mapsto -C_4, \quad C_5 \mapsto -C_5.$$

This example demonstrates the property we claimed in the proof of Theorem 3.21.

We now make a small deviation. It was proven in [Deh87] that the trefoil is chiral. There are a number of complicated arguments but we shall give a relatively modern result from which this follows rather quickly. Note however that the proof of this result does include some higher-level concepts but the base statement is rather accessible.

Proposition 3.23 *Let $p \equiv 3 \pmod 4$ be a prime number. If K is an achiral knot, then either*

$$p \nmid \det(K) \qquad \text{or} \qquad p^2 \mid \det(K).$$

Proof: The proof relies on so-called linking forms and homology. It is presented in [FMP17]. □

Corollary 3.24 *The trefoil is chiral.*

Proof: Recall from Example 3.15 that for the trefoil K, we have $\det(K) = 3$. As such, we use Proposition 3.23 with $p = 3$ and see that $p \mid \det(K)$ and $p^2 \nmid \det(K)$. As such, the contrapositive implies that K is not achiral, i.e. the trefoil is chiral. □

3.2 Alexander Polynomial

We use the work of the previous subsection to develop the Alexander polynomial in an intuitive manner. Alternatively, we could approach this from an algebraic angle in which we consider rings, ideals and the Wirtinger presentation as in Section 4 to derive the Alexander polynomial from a more general background. For simplicity, we shall state some interesting results but will not prove them yet as they require alternate discussion.

Definition 3.25 Let K be an oriented diagram of a knot. The Alexander polynomial $\Delta_K(t)$ of K is the knot determinant of K whereby the colouring matrix uses the conventions of Figure 12.

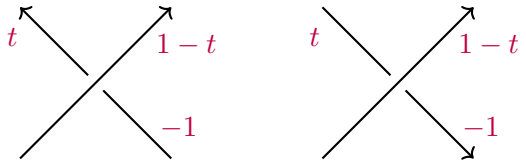

Figure 12: The colouring conventions for computing the Alexander polynomial.

Corollary 3.26 (of Theorem 3.21) *The Alexander polynomial is an isotopy invariant.*

Example 3.27 Consider the first oriented trefoil knot in Figure 2. We can easily compute the

colouring matrix with the conventions of Figure 12:

$$M_K = \begin{pmatrix} t & -1 & 1-t \\ 1-t & t & -1 \\ -1 & 1-t & t \end{pmatrix}.$$

Hence, we can now compute the Alexander polynomial, namely $\Delta_K(t) = t^2 - t + 1$.

Lemma 3.28 *Let K be an oriented diagram of a knot. Then, $|\Delta_K(-1)| = \det(K)$.*

Proof: Clearly, taking $t = -1$ in Figure 12 recovers Definition 3.10 from which the result follows. Note that we include the absolute value in the statement of the result because of a non-trivial multiplicative property of Alexander polynomials which is next discussed. □

We now appeal to the work of [Bad16] to understand the properties of the Alexander polynomial.

Proposition 3.29 *Let K be an oriented diagram of a knot and L an oriented diagram of a link. Then, we have the properties listed below.*

(i) *The Alexander polynomial is symmetric modulo $\pm t^n$, that is $\Delta_L(t) = \pm t^n \Delta_L(t^{-1})$.*

(ii) *The Alexander polynomial satisfies $\Delta_K(1) = 1$, possibly by using* (i).

(iii) *The Alexander polynomial satisfies $\Delta_{\overline{K}}(t) = \Delta_K(t)$.*

Proof: (of (iii) only) Consider the mirror images of the labelling convention in Figure 12 and note that the two are interchanged when reflecting across some line. This corresponds to elementary row and column operations on M_K which do not change the determinant. □

As such, the Alexander polynomial cannot be used to detect whether or not a knot is achiral.

Remark 3.30 We mentioned in the proof of Lemma 3.28 that we require an absolute value; this is because of part (i) of Proposition 3.29. Indeed, we computed the Alexander polynomial of the trefoil in Example 3.27 and we see that $\Delta_K(-1) = 3$, agreeing with Example 3.15 even in sign. However, suppose we had computed $\det(K)$ by considering a different minor, one that gives us $\Delta_K(t) = -t^2 + t - 1$, for example. In this case, we see that $\Delta_K(-1) = -3$.

3.3 Bracket and Jones Polynomials

There are a number of ways to assign a polynomial to a knot or link, one of the simplest being that of the bracket polynomial. Before we discuss the polynomial and its use, we will first construct it from an operation which acts on the crossings of a knot. Note that such a construction is possible for other polynomials as well, as will be seen.

Definition 3.31 Let L be a diagram of a link. A skein relation is an operation which establishes correspondence between the given diagram of L and the diagram of another link L' which differs from L at only one crossing.

Example 3.32 Consider the following, where L is a link diagram and A, B, C are indeterminate variables:

1. $\langle \bigcirc \rangle = 1$.
2. $\langle \bigcirc \sqcup L \rangle = C\langle L \rangle$.
3. $\langle \times \rangle = A\langle \asymp \rangle + B\langle)(\rangle$.

The first tells us that whenever we have the unknot under this skein relation, it evaluates to one and the second tells us that whenever we have the disjoint union of the unknot with a link, we can almost disregard the unknot, but with it comes a factor of the indeterminate C. The third (a skein relation) provides a means of removing a crossing of the form written on the left from a diagram of a link. What if we wanted to impose that this skein relation be invariant under regular isotopy? Well, this is precisely to force that

$$\langle \text{R1} \rangle = \langle)(\rangle \quad \text{and} \quad \left\langle \text{R2} \right\rangle = \left\langle \text{R2'} \right\rangle.$$

Working with the second Reidemeister move, we can use the skein relation to see that

$$\begin{aligned}
\langle \text{R1} \rangle &= A\langle \text{R2} \rangle + B\langle)(\rangle \\
&= A^2\langle \asymp \rangle + AB\langle \text{R2} \rangle + AB\langle)(\rangle + B^2\langle \asymp \rangle \\
&= (A^2 + ABC + B^2)\langle \asymp \rangle + AB\langle)(\rangle \\
&= \langle)(\rangle \text{ if and only if } AB = 1 \text{ and } A^2 + ABC + B^2 = 0,
\end{aligned}$$

which has solution $B = A^{-1}$ and $C = -A^2 - A^{-2}$. It turns out that this solution coincides with that when solving for the third Reidemeister move and thus we have enforced invariance under regular isotopy.

Definition 3.33 The bracket polynomial of a link diagram L is a polynomial given as follows:

1. $\langle \bigcirc \rangle = 1$.
2. $\langle \bigcirc \sqcup L \rangle = (-A^2 - A^{-2})\langle L \rangle$.
3. $\langle \times \rangle = A\langle \asymp \rangle + A^{-1}\langle)(\rangle$.

Lemma 3.34 *The bracket polynomial is invariant under regular isotopy but not isotopy.*

Proof: By construction, it is invariant under **R2**, so we need only show invariance under **R3**. Indeed, we calculate directly from Definition 3.33 and see that

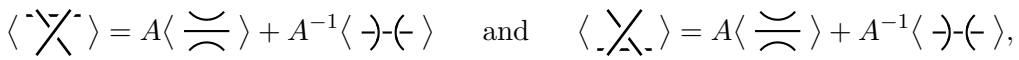

where we use the invariance under **R2** in the first bracket on the right side of the above equations. Clearly, these objects are equal and thus it is invariant under **R3** and thus regular isotopy. Finally, we expect that **R1** fails. Indeed, this is clear from direct computation:

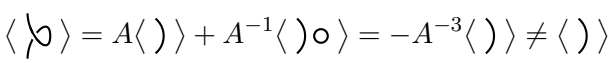

and thus the result is proven. □

Note that for a link diagram with k crossings, there are 2^k ways of removing the crossings under the skein relation of the bracket polynomial, which results in the unlink on k-components. In fact, we have this formula by applying the first and second rules of the bracket polynomial:

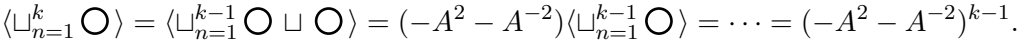

Definition 3.35 Let L be an oriented diagram of a link. The normalised bracket polynomial is

$$f_L(A) = (-A)^{-3\omega(L)}\langle L\rangle,$$

where $\langle L\rangle$ is the usual bracket polynomial, $\omega(L)$ is the writhe and A is an indeterminate variable.

Theorem 3.36 *The normalised bracket polynomial $f_L(A)$ is an isotopy invariant.*

Proof: The fact that $f_L(A)$ is invariant under **R2** and **R3** follows from Lemmata 3.2 and 3.34. Suppose that L' is an equivalent diagram of L, except we obtain L by applying **R1** to L', that is L' has a twist on one of its arcs. Then, we can see that

$$\omega(L') = \omega(L) \pm 1 \qquad \text{and} \qquad \langle L'\rangle = (-A)^{\mp 3}\langle L\rangle,$$

with sign depending on orientation. So, the definition of the normalised bracket polynomial gives

$$\begin{aligned} f_{L'}(A) &= (-A)^{-3\omega(L)\pm 3}\langle L'\rangle \\ &= (-A)^{-3\omega(L)}(-A)^{\pm 3}(-A)^{\mp 3}\langle L\rangle \end{aligned}$$

$$= (-A)^{-3\omega(L)}\langle L\rangle$$
$$= f_L(A).$$

and thus it is invariant under **R1** and so the result is proven. □

Example 3.37 Consider the diagram of the trefoil in Figure 2. It was Example 2.10 which showed us that the writhe of the trefoil is $\omega(K) = -3$. It remains to compute the corresponding bracket polynomial. We shall demonstrate this now:

$\langle$  $\rangle = A\langle$  $\rangle + A^{-1}\langle$  $\rangle$

$= A^2\langle$  $\rangle + \langle$  $\rangle + A^{-1}\langle$  $\rangle$

$= A^3\langle$  $\rangle + 2A\langle$  $\rangle + A^{-1}\langle$  $\rangle + \langle$  $\rangle + A^{-2}\langle$  $\rangle$

$= A^3\langle$  $\rangle + 3A\langle$  $\rangle + 3A^{-1}\langle$  $\rangle + A^{-3}\langle$ $\rangle$

$$= A^3(-A^2 - A^{-2})^2 + 3A(-A^2 - A^{-2}) + 3A^{-1} + A^{-3}(-A^2 - A^{-2})$$

$$= A^7 - A^3 - A^{-5}.$$

Finally then, it follows that $f_K(A) = (-A)^9(A^7 - A^3 - A^{-5}) = -A^{16} + A^{12} + A^4$.

Remark 3.38 If we proceed as in Example 3.37 with the diagram of the trefoil of opposite chirality, that is its mirror image, but **not** opposite orientation, it is natural to ask the question *what would happen?*. Indeed, if $\overline{K}$ is the mirror image of the diagram used in the above example, we would see that

$$f_{\overline{K}}(A) = -A^{-16} + A^{-12} + A^{-4}.$$

We soon discuss the connection between the normalised bracket polynomial and mirror images.

Definition 3.39 Let L be an oriented diagram of a link. The Jones polynomial of L is

$$V_L(t) = f_L(t^{-1/4}).$$

The advantage of this definition of the Jones polynomial is that it is relatively simple and we will soon see some immediate consequences. However, another definition will come from the study of

braid theory, as in Section 6, which has its own set of advantages, including a nice generalisation.

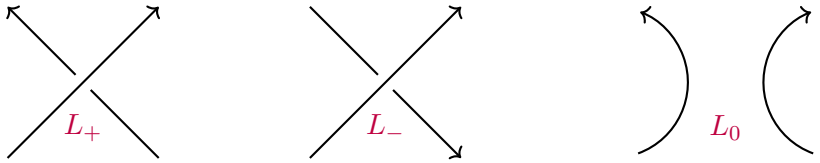

Figure 13: Types of crossing in oriented link diagrams, as in Proposition 3.40.

Proposition 3.40 *The Jones polynomial of the oriented diagram of link L satisfies these:*

(i) $V_{\bigcirc}(t) = 1$, *where* $\bigcirc$ *is an oriented unknot.*

(ii) $t^{-1}V_{L_+}(t) - tV_{L_-}(t) = (t^{1/2} - t^{-1/2})V_{L_0}(t)$, *where L_+, L_-, L_0 are as in Figure 13.*

Proof: It is clear that

$$f_{\bigcirc}(A) = (-A)^0\langle \bigcirc \rangle = 1,$$

which means the first formula in the statement of the proposition is recovered. As for the second, we will apply the definition of the bracket polynomial to the diagrams L_+ and L_- and substitute in the relevant variable. To begin, we see that

$$f_{L_+}(A) = -A^{-2}\langle \,)(\,\rangle - A^{-4}\langle \asymp \rangle \qquad \text{and} \qquad f_{L_-}(A) = -A^{4}\langle \asymp \rangle - A^{2}\langle \,)(\,\rangle.$$

Therefore, by making the substitution as in Definition 3.39, we see that

$$\begin{aligned} t^{-1}V_{L_+}(t) - tV_{L_-}(t) &= -t^{-1/2}\langle \,)(\,\rangle - \langle \asymp \rangle + \langle \asymp \rangle + t^{1/2}\langle \,)(\,\rangle \\ &= (t^{1/2} - t^{-1/2})V_{L_0}(t), \end{aligned}$$

by definition. Thus, we have the second formula and the result is proven. □

Example 3.41 Continuing on from Example 3.37, we see the Jones polynomial for the second trefoil diagram K as in Figure 2 is $V_K(t) = -t^4 + t^3 + t$.

Lemma 3.42 *Let K be a diagram of an oriented knot and $\widetilde{K}$ its reverse. Then, $V_{\widetilde{K}}(t) = V_K(t)$.*

Proof: It was Lemma 2.11 that established well-definedness for the writhe of an unoriented knot, since it is unchanged by reversing orientation. Further, the bracket polynomial ignores

orientation, so it is clear that $\omega(\widetilde{K}) = \omega(K)$ and $\langle \widetilde{K} \rangle = \langle K \rangle$, which means that $f_{\widetilde{K}}(A) = f_K(A)$ and as a consequence, we have $V_{\widetilde{K}}(t) = V_K(t)$. □

We end the discussion of these two polynomials with an immediate consequence of some earlier work. We will then briefly evaluate the invariants seen thus far.

Corollary 3.43 (of Theorem 3.36) *The Jones polynomial is an isotopy invariant.*

Of course, the bracket polynomial is not an isotopy invariant as was shown in Lemma 3.34 and thus its use is somewhat limited to developing intuition for skein relations and providing the basis of Definition 3.39. The benefit of distinguishing between Definitions 3.35 and 3.39 is that the Jones polynomial is, by design, a Laurent polynomial with integer coefficients in $t^{1/2}$, that is it lives in the ring $\mathbb{Z}[t^{1/2}, t^{-1/2}]$. This leads to generalisations that sadly we will not consider in this paper.

We conclude with an interesting result from the theory we have developed, that being a (more standard) sufficient test for chirality.

Lemma 3.44 *Let K be a diagram of an oriented knot and $\overline{K}$ its mirror. Then, $V_{\overline{K}}(t) = V_K(t^{-1})$.*

Proof: It was Lemma 2.13 that shows diagrams of opposing chirality have writhes of opposite sign, that is $\omega(\overline{K}) = -\omega(K)$. However, since the bracket polynomial ignores orientation, $\langle \overline{K} \rangle = \langle K \rangle$, it follows that $f_{\overline{K}}(A) = f_K(A^{-1})$ and, as a consequence, $V_{\overline{K}}(t) = V_K(t^{-1})$. □

Corollary 3.45 *If K is achiral, then $V_K(t) = V_K(t^{-1})$.*

Example 3.46 It was Example 2.18 that established the figure-eight knot was achiral. We will state but not prove that the Jones polynomial of this knot is $V_K(t) = t^2 - t + 1 - t^{-1} + t^{-2}$, by way of [Jon14]. We see that $V_K(t) = V_K(t^{-1})$, which demonstrates Corollary 3.45.

Example 3.47 We can use the Jones polynomial, specifically the contrapositive of Corollary 3.45 in conjunction with Example 3.41, to once again recover that the trefoil is chiral. Indeed, if K is the trefoil knot, we know that $V_K(t) = -t^4 + t^3 + t$ and we know that $V_{\overline{K}}(t) = -t^{-4} + t^{-3} + t^{-1}$ from Lemma 3.44. Therefore, $V_K(t) \neq V_K(t^{-1})$ implies that K is chiral.

This is better, in some senses, than the Alexander polynomial, since it can detect **some** chirality, but sadly the previous result isn't both necessary and sufficient; it may be that the mirror images of a diagram share the same Jones polynomial yet they are not isotopic. More generally, we may have two knots whose Jones polynomials coincide yet they are non-isotopic (the real killer comes in [Kan86], where we see an example of two knots whose Jones polynomials agree but are distinguished by the Alexander polynomial).

4 The Knot Group

Next, we concern ourselves with a more technical study of topological spaces. Indeed, we will develop the idea of the so-called fundamental group as to convincingly discuss the titular topic. We shall also consider an overview of free groups, generators and the Wirtinger presentation.

4.1 The Fundamental Group

The first path on the journey to defining the knot group is to understand a very important topological tool known as the fundamental group. This is now introduced, with a few useful results proven along the way.

Definition 4.1 Let X and Y be topological spaces and $f, g : X \to Y$ some maps. It is said that f and g are homotopic if there exists a continuous map $F : X \times [0,1] \to Y$ such that the following conditions hold:

(i) $F(x,0) = f(x)$.

(ii) $F(x,1) = g(x)$.

In this case, we write $f \simeq g$ to denote the fact these maps are homotopic.

Lemma 4.2 *Homotopy is an equivalence relation.*

Proof: Throughout, suppose that X and Y are topological spaces and $f, g, h : X \to Y$ are maps. It is clear that $f \simeq f$ via $F(x,t) = x$. Next, assuming that $f \simeq g$ via F, we also have $g \simeq f$ via $G(x,t) = F(x, 1-t)$. Finally, if $f \simeq g$ and $g \simeq h$ via F and G respectively, then $f \simeq h$ via

$$H(x,t) = \begin{cases} F(x,2t), & t \in [0,1/2] \\ G(x,2t-1), & t \in [1/2,1] \end{cases},$$

which completes the proof. □

Definition 4.3 Let X and Y be topological spaces. They are called homotopically equivalent if, for any $f : X \to Y$, there exists $g : Y \to X$ such that $g \circ f \simeq \mathrm{id}_X$ and $f \circ g \simeq \mathrm{id}_Y$.

Example 4.4 We solve an exercise in [GM12]. Let $\mathbb{R}^2$ be endowed with the standard Euclidean topology and consider S^1 and $\mathbb{R}^2 \setminus \{(0,0)\}$ as subspaces. Suppose that $f : S^1 \to \mathbb{R}^2 \setminus \{(0,0)\}$ is the inclusion map and that $g : \mathbb{R}^2 \setminus \{(0,0)\} \to S^1$ is given by $g(x) = x/||x||$. Then, these subspaces are homotopically equivalent. Indeed, we verify explicit homotopies below:

- $g \circ f \simeq \mathrm{id}_{S^1}$ via $F(x,t) = x$. Indeed, $F(x,0) = x = \mathrm{id}_{S^1}$ and $F(x,1) = x = (g \circ f)(x)$; as a matter of fact, this is exactly id_{S^1} since $||x|| = 1, \forall x \in S^1$.

- $f \circ g \simeq \mathrm{id}_{\mathbb{R}^2\setminus\{(0,0)\}}$ via $G(x,t) = tx/||x|| + (1-t)x$. Indeed, $G(x,0) = x = \mathrm{id}_{\mathbb{R}^2\setminus\{(0,0)\}}$ and $G(x,1) = x/||x|| = (f \circ g)(x)$.

Note that Definition 4.1 is very similar to that of Definition 1.37, that is the definition of isotopy. In fact, a homotopy can be thought of as a continuous deformation from one map to another without the embedding condition that we have for an isotopy. This is detailed in the next example.

Example 4.5 Consider the interval $[-3,3] \subseteq \mathbb{R}$ as a subspace and maps $f, g : [-3,3] \to \mathbb{R}$ where $f(x) = x$ and $g(x) = -x$. It is clear that these maps are homotopic via $F(x,t) = (1-2t)x$ but they are **not** isotopic because there is no such homotopy that is injective for all t. Take the one we stated here; at $t = 1/2$, the map is the zero-map $F(x,t) = 0$ which is certainly not injective.

Definition 4.6 Let X be a topological space. A path is a continuous map $\alpha : [0,1] \to X$, where $[0,1]$ has the subspace topology induced by the standard Euclidean topology on $\mathbb{R}$. A path is called a loop based at p if $\alpha(0) = p = \alpha(1)$.

Definition 4.7 Let X be a topological spaces and $\alpha, \beta : [0,1] \to X$ some paths with endpoints x and y. We call α and β path-homotopic if there is a continuous map $F : [0,1] \times [0,1] \to X$ such that the following conditions hold for all $s \in [0,1]$ and $t \in [0,1]$:

(i) $F(s,0) = \alpha(s)$.

(ii) $F(s,1) = \beta(s)$.

(iii) $F(0,t) = x$.

(iv) $F(1,t) = y$.

In this case, we write $\alpha \simeq \beta$ to denote the fact these paths are path-homotopic.

Example 4.8 Let $\alpha, \beta : [0,1] \to \mathbb{R}^n$ be any paths with end points x and y. Then, they are path-homotopic via the so-called straight-line homotopy, that is $F(s,t) = (1-t)\alpha(s) + t\beta(s)$.

Lemma 4.9 *Path-homotopy is an equivalence relation.*

Sketch of Proof: One can almost repeat the argument of the proof of Lemma 4.2 in the context of paths, taking care to verify the end-point conditions. □

Definition 4.10 Let X be a topological space. It is called path-connected if for every $x, y \in X$, there exists a path $\alpha : [0,1] \to X$ from x to y.

Example 4.11 The space $\mathbb{R}^n$ with the standard Euclidean topology is path-connected. Indeed, let $x, y \in \mathbb{R}^n$. Then, $\alpha(s) = (1-s)x + sy$ is a path from x to y. On the other hand, the space $\{(0,0)\} \cup \{(x, \sin(1/x)) : x \in (0,1]\}$ with topology induced from the Euclidean topology, commonly known as the *topologist's sine curve*, is famously not path-connected, since there is no way to continuously link the sine curve part of the space to the origin (proven in [Connd]).

The goal of this section is to explain and use this so-called knot group, so it will be good form to enter the mindset of a group-theorist at this point. The key to defining (the relevant objects needed to discuss) the knot group is to understand operations on paths, more specifically loops but these are just a special case by Definition 4.6.

Definition 4.12 Let X be a topological space along with $\alpha : [0,1] \to X$ a path from x to y and $\beta : [0,1] \to X$ be a path from y to z. Then, we define the following:

(i) The join of α and β is the path $\alpha * \beta : [0,1] \to X$ where $(\alpha * \beta)(s) = \begin{cases} \alpha(2s), & s \in [0, 1/2] \\ \beta(2s-1), & s \in [1/2, 1] \end{cases}$.

(ii) The reverse of α is the path $\overline{\alpha} : [0,1] \to X$ where $\overline{\alpha}(s) = \alpha(1-s)$.

(iii) The constant path at x is the path $e_x : [0,1] \to X$ where $e_x(s) = x, \forall s \in [0,1]$.

Proposition 4.13 *The join and reverse operations are well-defined on path homotopy equivalence classes. Also, we have associativity of the join and the existence of an identity and inverses.*

Proof: The proof consists of definition-chasing and some clever but not-too-difficult choices of path homotopies. We simply refer to [Rog18] for this result in its gory detail. □

As promised, Proposition 4.13 seems to give a group-like structure on the set of path homotopy equivalence classes. In fact, when we restrict to loops based at a specified point, we get just that.

Definition 4.14 Let X be a topological space and $\alpha : [0,1] \to X$ be some loop based at $x \in X$. The fundamental group is $\pi_1(X,x) = \{[\alpha] : \alpha \text{ is a loop based at } x\}$ with the join operation $*$. The literature also calls this the first homotopy group.

Remark 4.15 It is possible to also define the n^{th} homotopy group of a topological space X based at $x \in X$, which is $\pi_n(X,x) = \{[f] : f : S^n \to X \text{ is continuous with } f((1,0,...,0)) = x\}$. We will not dwell on this much because π_1 has much nicer properties and is better understood for our purposes. Notice that the fundamental group can be thought of in this way also; simply consider the equivalence relation we did in Example 1.33 which means the domain of our loops can be identified with S^1.

We next state a result by [McM13] and insert its proof, which was omitted in the original text.

Theorem 4.16 *Let X be a topological space and $\alpha : [0,1] \to X$ be a path from x to y. The map $\varphi : \pi_1(X,x) \to \pi_1(X,y)$ defined as $\varphi([\gamma]) = [\overline{\alpha} * \gamma * \alpha]$ is a group isomorphism.*

Proof: Let γ_1 and γ_2 be two loops based at x. Then, we see that

$$\varphi([\gamma_1]) * \varphi([\gamma_2]) = [\overline{\alpha} * \gamma_1 * \alpha] * [\overline{\alpha} * \gamma_2 * \alpha]$$

$$
\begin{aligned}
&= [\overline{\alpha} * \gamma_1 * \alpha * \overline{\alpha} * \gamma_2 * \alpha] \\
&= [\overline{\alpha} * \gamma_1 * e_x * \gamma_2 * \alpha] \\
&= [\overline{\alpha} * (\gamma_1 * \gamma_2) * \alpha] \\
&= \varphi([\gamma_1] * [\gamma_2]),
\end{aligned}
$$

which shows that the map is at least a group homomorphism. For bijectivity, it is enough to state and show that a certain map is its inverse; $\varphi^{-1} : \pi_1(X, y) \to \pi_1(X, x)$ defined as $\varphi^{-1}([\gamma]) = [\alpha * \gamma * \overline{\alpha}]$ will do. It is easy to see that $\varphi \circ \varphi^{-1} = \mathrm{id}_{\pi_1(X,y)}$ and $\varphi^{-1} \circ \varphi = \mathrm{id}_{\pi_1(X,x)}$. □

Corollary 4.17 *If X is a path-connected topological space, then π_1 is independent of the base point x. In this case, one may simply denote the fundamental group by $\pi_1(X)$.*

Definition 4.18 Let X be a path-connected topological space such that $\pi_1(X) \cong \{e\}$, that is it has trivial fundamental group. Then, it is called simply-connected.

Example 4.19 By Example 4.8, it is clear that $\pi_1(\mathbb{R}^n) \cong \{e\}$. Hence, $\mathbb{R}^n$ is simply-connected.

Lemma 4.20 *If $U \subseteq \mathbb{R}^n$ is convex, then $\pi_1(U) \cong \{e\}$, that is U is simply-connected.*

Proof: Let $\alpha : [0, 1] \to U$ be some loop based at $x \in U$. Then, $F(s, t) = (1 - t)\alpha(s) + tx$ is a path homotopy that maps into U by convexity. Hence, $\alpha \simeq e_x$ and so $\pi_1(U) \cong \{e\}$. □

We will not write a detailed proof of the classification of $\pi_1(S^1)$ since this would quickly become a surgery of homotopy theory as opposed to that of knot theory. Instead, we provide some of the groundwork which leads to the proof of this result.

Definition 4.21 Let X be a topological space. A covering space of X is a topological space C such that there exists a continuous surjective map $p : C \to X$ where, for each $x \in X$, there exists an open neighbourhood $U_x \subseteq X$ of x such that $p^{-1}(U_x) = \sqcup_{\lambda \in \Lambda} V_\lambda$ and $p|_{V_\lambda} : V_\lambda \to U_x$ is a homeomorphism for every $\lambda \in \Lambda$, where $(V_\lambda)_{\lambda \in \Lambda}$ is a family of open subsets of C. The terminology used is as follows:

(i) X is the base space.

(ii) p is the covering map.

(iii) $p^{-1}(x)$ is the fiber over x.

Example 4.22 Let $p : \mathbb{R} \to S^1$ be given as $p(x) = (\cos(2\pi x), \sin(2\pi x))$. Visually, this gives a helix with centre the real line. This map acts as the covering map from the covering space $\mathbb{R}$ to the base space S^1. It was Example 1.33 that this map is continuous. Moreover, it is clearly one periodic whereby the restriction $p|_{(y,y+1)} : (y, y + 1) \to S^1 \setminus \{p(y)\}$ is a homeomorphism.

Two important results are the so-called Path-Lifting and Homotopy-Lifting Lemmata. It is from these that we get the next result; full detail can be found in [Tho04].

Theorem 4.23 *The fundamental group* $\pi_1(S^1) \cong (\mathbb{Z}, +)$.

It would be immensely useful to be able to determine the fundamental group of a space which looks 'similar' to that of a space for which the fundamental group is already known. We first claim that the fundamental groups of the spaces in Figure 14 coincide.

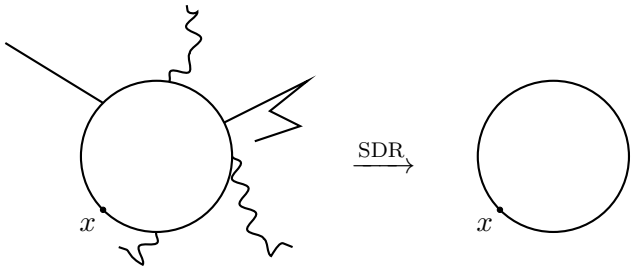

Figure 14: A contrived example of a strong deformation retract of S^1.

This can and will be proven using the next definition and a useful result that comes of it.

Definition 4.24 Let X and Y be topological spaces with $x \in X$ and $y \in Y$ and $h : X \to Y$ be continuous such that $h(x) = y$. Then, the induced homomorphism is $h_* : \pi_1(X, x) \to \pi_1(Y, y)$ which is given by $h_*([\alpha]) = [h \circ \alpha]$, where $\alpha : [0, 1] \to X$ is a loop based at x.

Proposition 4.25 *Let* X, Y, Z *be topological spaces with* $f : X \to Y$ *and* $g : Y \to Z$ *continuous. Inducing homomorphisms is functorial, that is* $(g \circ f)_* = g_* \circ f_*$ *and* $(\mathrm{id}_X)_* = \mathrm{id}_{\pi_1(X,x)}$, $\forall x \in X$.

Proof: Let $\alpha : [0, 1] \to X$ be a loop based at x. By definition, we have that $(g \circ f)_*([\alpha]) = [g \circ f \circ \alpha]$ and that $f_*([\alpha]) = [f \circ \alpha]$, which implies $g_*(f_*([\alpha])) = g_*([f \circ \alpha]) = [g \circ f \circ \alpha]$. Consequently, we see that $(g \circ f)_* = g_* \circ f_*$. Furthermore, $(\mathrm{id}_X)_*([\alpha]) = [\mathrm{id}_X \circ \alpha] = [\alpha]$, by definition. As a result, we see that $(\mathrm{id}_X)_* = \mathrm{id}_{\pi_1(X,x)}$. □

It is now possible to prove a result which will mean that our knot group is an isotopy invariant (see Theorem 4.46 for the full details, but note the heavy-lifting is done here).

Theorem 4.26 *The fundamental group is invariant under homeomorphism.*

Proof: Let X and Y be topological spaces and $f : X \to Y$ a homeomorphism such that $f(x) = y$, for some $x \in X$ and $y \in Y$. By definition, $f_* : \pi_1(X, x) \to \pi_1(Y, y)$ is a group homomorphism.

We now claim that $(f_*)^{-1} = (f^{-1})_*$. Indeed, both f and f^{-1} are continuous; we can appeal to the functorial property in Proposition 4.25 to obtain $f_*^{-1} \circ f_* = (\mathrm{id}_{\pi_1(X,x)})_*$ and $f_* \circ f_*^{-1} = (\mathrm{id}_{\pi_1(Y,y)})_*$. Therefore, it follows that f_* is bijective and thus a group isomorphism. □

Definition 4.27 Let X be a topological space and $A \subseteq X$ some subspace. It is said that A is a strong deformation retract (SDR) of X if there exists a continuous map $H : X \times [0,1] \to X$ called a strong deformation retraction such that the following conditions hold:

(i) $H(x,0) = x, \forall x \in A$.

(ii) $H(x,1) \in A, \forall x \in A$.

(iii) $H(a,t) = a, \forall a \in A, \forall t \in [0,1]$.

Example 4.28 An easy example is that the singleton $\{a\}$ is a strong deformation retract of the interval $[-a,a]$ via $H(x,t) = (1-t)x + ta$. Another such example is the map G we saw in Example 4.4; it implies that S^1 is a strong deformation retract of the punctured plane $\mathbb{R}^2 \setminus \{(0,0)\}$. This map also implies the more general result that S^{n-1} is a strong deformation retract of $\mathbb{R}^n \setminus \{\mathbf{0}\}$.

Proposition 4.29 *Let X be a topological space and $A \subseteq X$ a strong deformation retract of X. For all $a \in A$, the inclusion $\iota_A : A \to X$ induces the isomorphism $(\iota_A)_* : \pi_1(A,a) \to \pi_1(X,a)$.*

Proof: Suppose that H is the strong deformation retraction of A in X. For notation's sake, we define $h_1 : X \to A$ to be $h_1(x) = H(x,1)$. By definition, this is a continuous map. Furthermore, note that $h_1 \circ \iota_A : A \to A$ is the identity map on A, which means that $(h_1 \circ \iota_A)_* = (h_1)_* \circ (\iota_A)_*$ is the identity map on $\pi_1(A,a)$ by Proposition 4.25. Next, we consider $\iota_A \circ h_1 : X \to X$. Let $\alpha : [0,1] \to X$ be a loop based at a. Then, we see that $[\alpha] = [\iota_A \circ h_1 \circ \alpha]$ via the path homotopy $F(s,t) = H(\alpha(s),t)$. Therefore, we also have that $(\iota_A \circ h_1)_* = (\iota_A)_* \circ (h_1)_*$ is the identity map on $\pi_1(X,a)$. Consequently, $(\iota_A)_*^{-1} = (h_1)*$ and so $(\iota_A)_*$ is a group isomorphism. □

If we re-visit Figure 14, it is clear from Proposition 4.29 that the fundamental group of the space based anywhere on the circle coincides with the fundamental group of the circle, that is $(\mathbb{Z}, +)$.

Example 4.30 Consider the so-called Klein bottle (one of the coolest shapes in Mathematics). Although it is non-embeddable in three-dimensions, we consider its planar drawing in Figure 15.

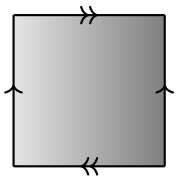

Figure 15: A planar drawing of the Klein bottle with gluing relations.

Remove one point from the Klein bottle, say the centre point without loss of generality. Applying a strong deformation retract takes us to a bouquet of two circles, as is shown in Figure 16.

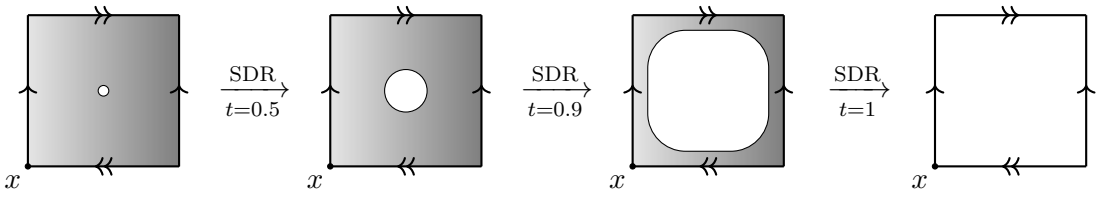

Figure 16: Performing a strong deformation retract on the punctured Klein bottle.

This lights the flame at the heart of the upcoming discussion in Section 5 on using such basic sketches as devices to build intuition and understand strange topological spaces.

4.2 Combinatorial Group Theory

It is now time to lay the groundwork which will lead to the Wirtinger presentation of a group, which is an immensely useful and relatively simple algorithmic tool for determining what we call the knot group.

Definition 4.31 Let $A = \{g_1, ..., g_n\}$, which we call the alphabet. A word is a finite concatenation of the symbols g_i and g_i^{-1}, where the empty word is denoted e, that is the word with no symbols.

It is possible to define two operations on the set of words of an alphabet:

- The product of two words is their concatenation.
- The inverse of a word is given by reversing the order and interchanging g_i and g_i^{-1}.

Example 4.32 Consider the English alphabet $A = \{a, b, ..., z\}$. From this, we construct the word $hello = hel^2o$, where we use the usual power notation to denote how many of that letter is concatenated. Then, we see that $(hello)^{-1} = o^{-1}l^{-2}e^{-1}h^{-1}$. Alternatively, another word we may construct is hel. Hence, the product $(hello)^{-1}hel = o^{-1}l^{-1} = (lo)^{-1}$. Overcoming the fact this example is somewhat perverse, the usefulness of these operations cannot be overstated.

Lemma 4.33 *Let $A = \{g_1, ..., g_n\}$ be an alphabet and $W = \{r_1, ..., r_m\}$ a finite set of words from the alphabet A. This is an equivalence relation: $r_1 \sim r_2$ if and only if r_1 is obtainable from r_2 by*

$$\textit{inserting/removing } g_i g^{-1} \textit{ and } g_i^{-1} g_i \qquad \textbf{or} \qquad \textit{concatenating/removing } r \textit{ and } r^{-1}.$$

Proof: It is clear that $r_1 \sim r_1$ simply by concatenating the empty word e at the end, say. If $r_1 \sim r_2$, then $r_2 \sim r_1$ because we can concatenate r^{-1} onto where an r had been concatenated or we can insert $g_i^{-1} g_i$ after a place where $g_i g_i^{-1}$ had been inserted. Finally, if $r_1 \sim r_2$ and $r_2 \sim r_3$, then $r_1 \sim r_3$ simply by performing the inserts/removals in one fell swoop. □

Proposition 4.34 *The quotient $^W/_\sim = \langle g_1, ..., g_n; r_1, ..., r_m \rangle$ is a group under concatenation.*

Hence, we now say that the g_i are generators and the r_j are relations. It may not always be that we have any relations. This is now explored and follows the framework of [MI02], culminating in a neat application to the theory of the fundamental group.

Definition 4.35 Let F be a group and $S \subseteq F$ some subset. We say that S is a free basis of F if, for any group G and any map $\varphi : S \to G$, there exists a unique group homomorphism $\widetilde{\varphi} : F \to G$ such that $\widetilde{\varphi}|_S = \varphi$. In this case, F is called a free group.

Example 4.36 The group $(\mathbb{Z}, +)$ is a free group with basis $\{1\}$. Indeed, if $\varphi : \{1\} \to G$ is a map where $\varphi(1) = g$, then $\widetilde{\varphi} : \mathbb{Z} \to G$ defined as $\widetilde{\varphi}(n) = g^n$ is a group homomorphism with $\widetilde{\varphi}|_{\{1\}} = \varphi$.

A free group can now be understood as in Proposition 4.34, that is a free group F with basis S has presentation $\langle S; \cdot \rangle$, that is where the set of relations is empty. But why can we make such an identification? Because an application of the First Isomorphism Theorem to the unique group homomorphism $\widetilde{\varphi}$ in Definition 4.35 gives

$$F/\ker(\widetilde{\varphi}) \cong G.$$

Because of this combinatorial approach to defining free groups, it is possible to state the celebrated Seifert-van Kampen Theorem in this way, as is done in [Bignd].

Theorem 4.37 (Seifert-van Kampen Theorem) *Let X be a topological space where $U, V \subseteq X$ are open, path-connected subsets with $X = U \cup V$ and $U \cap V \neq \emptyset$ also path-connected. Suppose that $\iota_U : U \cap V \to U$ and $\iota_V : U \cap V \to V$ are inclusion maps and that for $x \in U \cap V$, we have these group presentations:*

$$\begin{aligned} \pi_1(U, x) &\cong \langle a_1, ..., a_n; r_1, ..., r_i \rangle \\ \pi_1(V, x) &\cong \langle b_1, ..., b_m; s_1, ..., s_j \rangle \\ \pi_1(U \cap V, x) &\cong \langle c_1, ..., c_l; t_1, ..., t_k \rangle. \end{aligned}$$

Then, it is possible to write the presentation for the fundamental group of X as follows:

$$\pi_1(X,x) \cong \langle a_1,...,a_n,b_1,...,b_m; r_1,...,r_i,s_1,...,s_j,(\iota_U)_*(c_1)(\iota_V)_*(c_1)^{-1},...,(\iota_U)_*(c_l)(\iota_V)_*(c_l)^{-1}\rangle.$$

Example 4.38 Let $X = S^1 \sqcup S^1$ and identify one point on each circle via some equivalence relation $\sim$. Then, $X/\sim$ is the so-called bouquet of two circles that intersect only at the identified point, $[p] \in X/\sim$, say. The goal is to apply the Seifert-van Kampen Theorem; this can be done with the open sets shown in Figure 17.

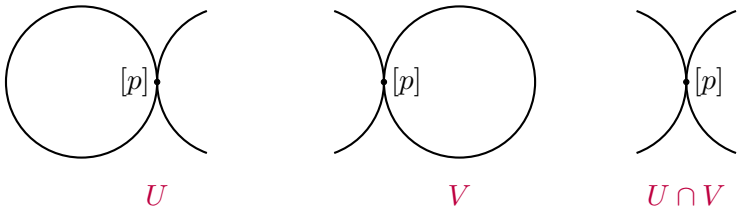

Figure 17: One choice of open subsets of the bouquet of two circles.

We see that U and V are open and path-connected, with non-empty path-connected intersection. Furthermore, S^1 is a deformation retract of both U and V, meaning $\pi_1(U) \cong \pi_1(S^1) \cong \pi_1(V)$. Example 4.36 implies $\pi(S^1) \cong \langle a; \cdot \rangle$, where a is some generator for loops based in S^1. Therefore,

$$\pi_1(U) \cong \langle a; \cdot \rangle \text{ and } \pi_1(V) \cong \langle b; \cdot \rangle.$$

Also, $U \cap V$ will deformation retract to a point, which means $\pi_1(U \cap V) \cong \langle \cdot; \cdot \rangle$. It then follows from the Seifert-van Kampen Theorem that

$$\pi_1(X/\sim) \cong \langle a, b; \cdot \rangle.$$

Remark 4.39 The work of Example 4.38 can be applied inductively, that is to discuss the so-called bouquet of n-circles with an equivalence relation identifying one point on each copy. It turns out that if $X/\sim$ is our bouquet, then $\pi_1(X/\sim) \cong \langle a_1, ..., a_n; \cdot \rangle$, the free group of n generators.

Example 4.40 Let us make use of Example 4.30 in order to calculate $\pi_1(K^2)$, where K^2 is a Klein bottle. We can find two open subsets of K^2, drawn as planar projections in Figure 18.

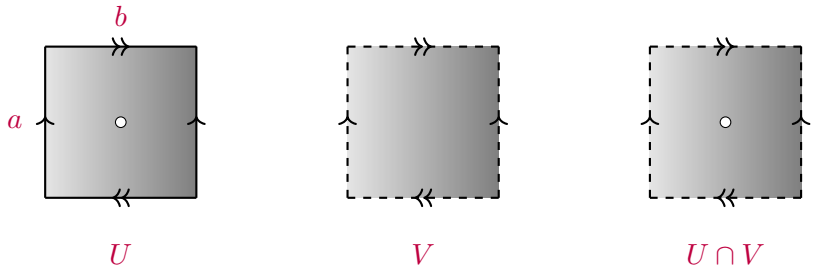

Figure 18: One choice of open subsets of the Klein bottle.

It was Example 4.30 that established the bouquet of two circles was a deformation retract of U, so $\pi_1(U) \cong \langle a, b; \cdot \rangle$ by Example 4.38. Furthermore, it is clear that V is simply connected, so $\pi_1(V) \cong \langle \cdot; \cdot \rangle$. Finally, $U \cap V$ will deformation retract to S^1, meaning that $\pi_1(U \cap V) \cong \langle c; \cdot \rangle$. If we consider the inclusion maps as in the Seifert-van Kampen Theorem, it is clear that $(\iota_V)_*(c) = e$ since V is simply connected and that $(\iota_U)_*(c) = aba^{-1}b$. Consequently,

$$\pi_1(K^2) \cong \langle a, b; aba^{-1}b \rangle.$$

4.3 The Knot Group

The work on combinatorial group theory allows for us to comfortably introduce the so-called Wirtinger presentation, which turns out to be a very useful device when considering the knot group; this is equivalent to computing a fundamental group, a point discussed further towards the end of this section. But first, let us finally live up to the name of Section 4 and discuss the knot group.

Definition 4.41 Let K be a diagram of a knot. The knot group is $\mathrm{gr}(K)$.

This is far from a useful definition, but we will soon prove a useful form of the knot group, which can then be interpreted geometrically and topologically.

Definition 4.42 Let K be an oriented diagram of a knot with n arcs labelled x_i and m crossings. The Wirtinger presentation is $\mathrm{gr}(K) \cong \langle x_1, ..., x_n; r_1, ..., r_m \rangle$, with relations given in Figure 19.

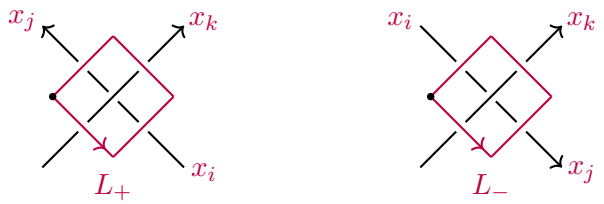

$x_k x_i x_k^{-1} x_j^{-1} = e$ $\qquad$ $x_k x_j^{-1} x_k^{-1} x_i = e$

Figure 19: The Wirtinger relations as loops above positive and negative crossings.

Example 4.43 Yet again, we consider the first trefoil knot as in Figure 2, i.e. with clockwise orientation. The Wirtinger relations are as follows:

$$\begin{aligned} x_3 x_2^{-1} x_3^{-1} x_1 = e \quad &\Rightarrow \quad x_1 = x_3^{-1} x_2 x_3 \\ x_1 x_3^{-1} x_1^{-1} x_2 = e \quad &\Rightarrow \quad x_2 = x_1^{-1} x_3 x_1 \\ x_2 x_1^{-1} x_2^{-1} x_3 = e \quad &\Rightarrow \quad x_3 = x_2^{-1} x_1 x_2 \end{aligned}$$

Thus, $\mathrm{gr}(K) \cong \langle x_1, x_2, x_3; x_3 x_2^{-1} x_3^{-1} x_1, x_1 x_3^{-1} x_1^{-1} x_2, x_2 x_1^{-1} x_2^{-1} x_3 \rangle$. It is possible to eliminate one of the relations by substituting in one of the above expressions. We will do so for x_3:

$$x_1 = x_2^{-1} x_1^{-1} x_2 x_1 x_2 \qquad \text{and} \qquad x_2 = x_1^{-1} x_2^{-1} x_1 x_2 x_1.$$

Therefore,

$$\begin{aligned}
\mathrm{gr}(K) &\cong \langle x_1, x_2; x_1^{-1} x_2^{-1} x_1^{-1} x_2 x_1 x_2, x_2^{-1} x_1^{-1} x_2^{-1} x_1 x_2 x_1 \rangle \\
&= \langle x_1, x_2; (x_1 x_2 x_1)^{-1} x_2 x_1 x_2, (x_2 x_1 x_2)^{-1} x_1 x_2 x_1 \rangle \\
&= \langle x_1, x_2; x_1 x_2 x_1 = x_2 x_1 x_2 \rangle \\
&= \langle a, b; a^2 = b^3 \rangle,
\end{aligned}$$

where we define $a = x_2 x_1 x_2$ and $b = x_1 x_2$.

Remark 4.44 It is possible to imagine the trefoil as embedded on the surface of a torus, where the trefoil winds twice around the meridian (in the direction of the longitude) and thrice around the longitude (in the direction of the meridian). This is visualised in Figure 20. Note that the picture is a sort-of *push-off* of the knot, in that it is slightly lifted away from the torus so we can better see how it is embedded. As such, the trefoil may be named the $(2, 3)$-torus knot. Note the naming convention with regard to the indices that appear in the Wirtinger presentation in Example 4.43. Our goal is to prove that this is no coincidence.

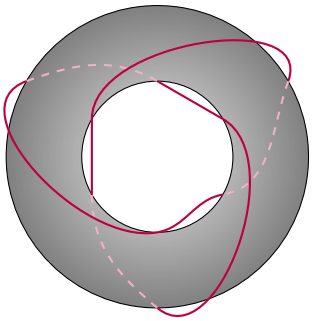

Figure 20: A birds-eye view of the trefoil embedded onto T^2, with a slight push-off.

Proposition 4.45 *Let K be a diagram of a knot. Then,* $\mathrm{gr}(K) \cong \pi_1(\mathbb{R}^3 \setminus K)$.

Proof: Let $p \in \mathbb{R}^3 \setminus K$. Then, it is possible to consider loops based at p that enclose each of the arcs in the crossing drawn in Figure 19 such that they have positive signs at each crossing in the sense of Definition 2.9. Let the loop that encircles arc x_i be denoted α_i. Then, we deal with three such loops, namely $\alpha_i, \alpha_j, \alpha_k$. We now show that the Wirtinger presentation coincides with the

path homotopy class involving these loops. Indeed then, Figure 21(a) demonstrates this in one case. From this, we see that $\alpha_k * \alpha_i * \alpha_k^{-1} \simeq \alpha_j$, which agrees with the first Wirtinger relation. We next consider Figure 21(b) from which we see that $\alpha_k^{-1} * \alpha_j * \alpha_k \simeq \alpha_i$, which agrees with the second Wirtinger relation.

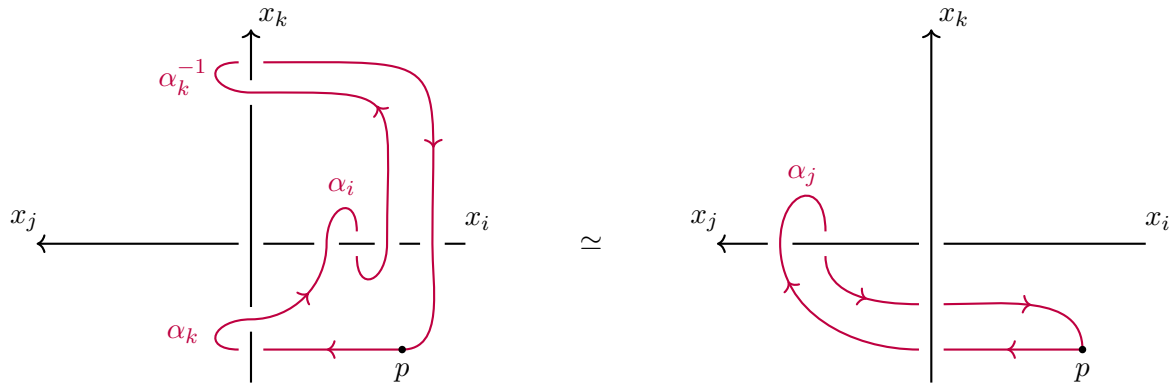

(a) A positive crossing and the join of loops that encode the presentation.

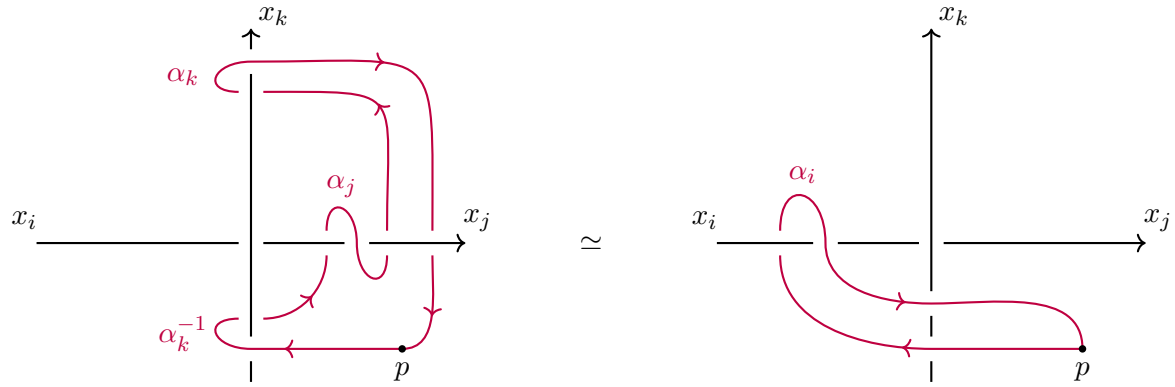

(b) A negative crossing and the join of loops that encode the presentation.

Figure 21: Wirtinger relations encoded by loops in the space $\mathbb{R}^3 \setminus K$.

From here, it is possible to appeal to the Seifert-van Kampen Theorem with strategically chosen open and path-connected subsets on which the generators $\alpha_1, ..., \alpha_n$ have relations $r_1, ..., r_m$ as in Definition 4.42, establishing our correspondence between the groups in the statement. □

Theorem 4.46 *The knot group is an isotopy invariant.*

Proof: Recall that homeomorphic spaces have isomorphic fundamental groups, via Theorem 4.26 If K_1 and K_2 are isotopic knots, that is $K_1 \simeq K_2$, then this implies $\mathbb{R}^3 \setminus K_1 \cong \mathbb{R}^3 \setminus K_2$ and so

$\pi_1(\mathbb{R}^3 \setminus K_1) \cong \pi_1(\mathbb{R}^3 \setminus K_2)$. We then appeal to Proposition 4.45 to see that $\mathrm{gr}(K_1) \cong \mathrm{gr}(K_2)$. $\square$

Example 4.47 We will determine the knot group of the unknot. We know that $\pi_1(S^1) \cong (\mathbb{Z}, +)$ but we must determine $\pi_1(\mathbb{R}^3 \setminus S^1)$. We proceed as in the proof of Proposition 4.45, by choosing some base point $p \in \mathbb{R}^3 \setminus S^1$ of classes of loops. Of course, if a loop at p doesn't link with S^1, then the loop is contractible to the constant path e_p. But of course, if a generates the loop α that links with S^1 once, then another loop β that links with S^1 twice, say, will be generated by a^2, as in Figure 22. Therefore, we see a familiarity with Example 4.36 and conclude that $\pi_1(\mathbb{R}^3 \setminus S^1) \cong \langle a; \cdot \rangle \cong (\mathbb{Z}, +)$.

Figure 22: Representatives of two classes of loops that appear in $\pi_1(\mathbb{R}^3 \setminus S^1)$.

Proposition 4.48 *Let K be a diagram of a knot. Then, K is p-colourable if and only if there exists a group homomorphism $\varphi : \mathrm{gr}(K) \to D_{2p}$ to the dihedral group of order $2p$.*

Proof: Recall that $D_{2p} = \langle a, b; a^p, b^2, abab \rangle$, where a generates rotations and b generates reflections, by way of a result in [CSW16]. We flesh out the homomorphism briefly mentioned in this source. Define $\varphi(x_i) = a^{c_i} b$ where c_i is the colour of the arc x_i. We must now verify that this is a group homomorphism. Indeed, we apply this to the Wirtinger presentation of $\mathrm{gr}(K)$:

$$\begin{aligned} & \varphi(x_j) = \varphi(x_k x_i x_k^{-1}) \\ \Leftrightarrow \quad & a^{c_j} b = a^{c_k} b a^{c_i - c_k} \\ \Leftrightarrow \quad & b a^{c_j} b = b a^{c_k} b a^{c_i - c_k} \\ \Leftrightarrow \quad & a^{-c_j} = a^{c_i - 2c_k}. \end{aligned}$$

But now, this is true if and only if $c_i + c_j - 2c_k \equiv 0 \pmod{p}$, which is precisely the p-colourability condition (note that the Wirtinger presentation has arc x_k as the over-crossing). Conversely, all non-trivial homomorphisms between these groups arise in this way by tracing the above chain of implications in reverse. $\square$

We took some time in Remark 4.44 to introduce the concept of a torus knot, where we also alluded to a deeper interplay between these such knots and the Wirtinger presentation of their

knot groups. Proving this will allow us to conclude our work having an idea on how to use the objects looked at throughout this section. First, we will define these special knots properly.

Definition 4.49 Let K be the diagram of a knot. It is called a (p, q)-torus knot if it is embeddable on the surface of a torus such that it winds p times around the meridian and q times around the longitude, where also $\gcd(p, q) = 1$. In the case that $\gcd(p, q) \neq 1$, we have a (p, q)-torus link, with number of components $\gcd(p, q)$. Such a knot will be denoted $T_{p,q}$.

Lemma 4.50 *Let $T_{p,q}$ be an oriented (p, q)-torus knot. Then, the following are true:*

(i) $T_{-p,-q} \simeq \widetilde{T}_{p,q}$, *i.e. it has reversed orientation.*

(ii) $T_{p,-q} \simeq \overline{T}_{p,q}$, *i.e. it is its mirror image.*

(iii) $T_{p,q} \simeq T_{q,p}$.

Sketch of Proof: Now, (i) is intuitive and trivial. For (ii) we refer to [Kaw96]. As for (iii), we follow the process as done in [Ada04] but generalising to arbitrary (p, q)-torus knots. Indeed, suppose $D \subseteq T^2$ is a closed disk of a torus such that $D \cap T_{p,q} = \emptyset$. Then, $T^2 \setminus D$ deformation retracts to a bouquet of two circles, but as T^2 is deformed in this way, $T_{p,q}$ ends up being carried by this deformation to two closed strips. It is possible to invert these (turn them inside out); the roles of meridian and longitude thus swap roles during this process. Therefore, inserting back the removed disk gives a torus on which the knot is a (q, p)-torus knot; a lovely illustration can be found in the aforementioned source. □

We are ready to reap the rewards of studying the knot group and Seifert-van Kampen Theorem. As with some of the previous knot-theoretic concepts, we turn to [GP94], adapting their proof slightly.

Theorem 4.51 *The knot group $\pi_1(\mathbb{R}^3 \setminus T_{p,q}) \cong \langle a, b; a^p = b^q \rangle$.*

Proof: Let T be the solid torus, which has boundary T^2, and take some (p, q)-torus knot $T_{p,q} \subseteq T^2$ as in Definition 4.49. For some $\varepsilon > 0$, let $N_\varepsilon \subseteq \mathbb{R}^3$ be the tubular neighbourhood of $T_{p,q}$. Notice that the closure $\overline{N}_\varepsilon$ deformation retracts to $T_{p,q}$, meaning $\pi_1(\mathbb{R}^3 \setminus \overline{N}_\varepsilon) \cong \pi_1(\mathbb{R}^3 \setminus T_{p,q})$ by Proposition 4.29. We next define the following:

$$U = T \setminus \overline{N}_\varepsilon \qquad \text{and} \qquad V = (\mathbb{R}^3 \setminus T) \setminus \overline{N}_\varepsilon$$

Geometrically, U is the solid part of our solid torus with a groove carved into it where which the tubular neighbourhood would otherwise occupy; we can see that it deformation retracts to the longitudinal circle at the centre of the solid part of the torus, that is $\pi_1(U) \cong \langle a; \cdot \rangle$. Next, we see that the fundamental group of V is generated by a loop through the hole of the torus,

from which it follows that $\pi_1(V) \cong \langle b; \cdot \rangle$, with b being a generating loop passing through the hole formed by removing the point x. Finally, we see that $U \cap V$ is an open annulus which therefore has a circle as a deformation retract, so $\pi_1(U \cap V) \cong \langle c; \cdot \rangle$. The hypotheses of the Seifert-van Kampen Theorem are satisfied:

$$\pi_1(\mathbb{R}^3 \setminus \overline{N}_\varepsilon) \quad \cong \quad \langle a, b; (\iota_U)_*(c)(\iota_V)_*(c)^{-1} \rangle \quad \cong \quad \langle a, b; a^p b^{-q} \rangle,$$

which occurs since the generator c corresponds to loops at the centre of the open annulus, winding p times in the longitudinal direction and q times in the meridional direction. □

Sadly, the knot group isn't a complete isotopy invariant, in that there are instances of non-ambient isotopic knots whose knot groups are isomorphic; we will show this by way of an example.

Example 4.52 The mirror image of our trefoil knot $T_{2,3}$ is the knot $T_{2,-3}$ by Lemma 4.50. As such, we can appeal to Theorem 4.51 to see that

$$\mathrm{gr}(T_{2,-3}) \;\cong\; \langle a, b; a^2 = b^{-3} \rangle \;\cong\; \langle c, d; c^2 = d^3 \rangle \;\cong\; \mathrm{gr}(T_{2,3}).$$

where the isomorphism in the above equation comes from mapping $a \mapsto c$ and $b \mapsto d^{-1}$. But as we have mentioned prior to this, we know that the trefoil is chiral, something which the knot group fails to detect here.

Remark 4.53 The only knot groups with non-trivial centres are those of the torus knots, which is a result discussed in [BZ66]. This is not a group theory paper and thus we stop here, but it is interesting nevertheless.

5 Seifert Surfaces

We can use the classification of surfaces to discuss the interesting question *what can we say about a surface whose boundary is a given knot?*. First, we will discuss the necessary theory as to develop the titular concept in a rigorous manner.

Definition 5.1 A (topological) surface without boundary is a topological space Σ such that for any $x \in \Sigma$, there exists an open neighbourhood $U_x \subseteq \Sigma$ of x such that $U_x \cong \mathbb{R}^2$. The boundary $\partial\Sigma$ of a topological surface Σ is defined to be the set of points whose open neighbourhood is homeomorphic to $\mathbb{R}^2_{\geq 0}$.

Example 5.2 It follows that $\mathbb{R}^2 \subseteq \mathbb{R}^3$ is a surface. Indeed, for any $x \in \mathbb{R}^2$, a simply-connected open neighbourhood $U_x \subseteq \mathbb{R}^2$ will certainly be homeomorphic to $\mathbb{R}^2$, a consequence of the well-known Riemann Mapping Theorem of complex analysis, where we make the identification $\mathbb{R}^2 \cong \mathbb{C}$, which gives a bijection between such a neighbourhood to the open unit disk.

We now deviate the discussion to the study of surfaces and will emerge with the required knowledge to understand how knots relate to this area. This will be done in a more general context by appealing to homological methods before restricting to the two-dimensional case that we need. But first, we note one property of general topological spaces that we relate to surfaces.

Definition 5.3 Let X be a topological space and $(U_\lambda)_{\lambda\in\Lambda}$ a collection of open subsets.

- The sets $(U_\lambda)_{\lambda\in\Lambda}$ form an open cover if $\bigcup_{\lambda\in\Lambda} U_\lambda = X$.
- The sets $(U_\lambda)_{\lambda\in\Lambda'}$ form a finite subcover if $\Lambda' \subseteq \Lambda$ has finite size and $\bigcup_{\lambda\in\Lambda'} U_\lambda = X$.

The topological space X is called compact if every open cover admits a finite subcover.

Remark 5.4 When we talk about compact surfaces, we mean precisely that it is a compact topological space with the property stated in Definition 5.1. In the case that a surface is both compact and has no boundary, we call it closed and in the case that they have boundary, we can think of them as being closed yet having a finite number of open disks removed. This idea will be re-visited in Theorems 5.35 and 5.41; having boundary is formalised in Definition 5.39.

5.1 Combinatorial Topology

We now discuss the so-called triangulation of a surface; this delves into what is called homology. This provides a means of defining orientability and will lay the groundwork for these Seifert surfaces we wish to study.

Definition 5.5 Let $p_1, ..., p_{n+1} \in \mathbb{R}^n$ be affinely independent, that is $p_2 - p_1, ..., p_{n+1} - p_1$ are

linearly independent. The n-simplex generated by these points is the set

$$\Delta^n = \{\lambda_1 p_1 + ... + \lambda_{n+1} p_{n+1} : \lambda_1 + ... + \lambda_{n+1} = 1 \text{ and } \lambda_i \geq 0\}.$$

A neat way to think about these n-simplices are as complete graphs on $n+1$ vertices with a convex hull, that is the graph is the 'frame' of a polytope. This becomes evident by looking at Example 5.6. Although we only require low-dimensional forms for the relation of surfaces to knots, it is interesting to remain as general as possible.

Example 5.6 We can consider a number of simple examples which are sketched in Figure 23:

(i) The 0-simplex is a point (or vertex).

(ii) The 1-simplex is a line (or edge).

(iii) The 2-simplex is a triangle (or face).

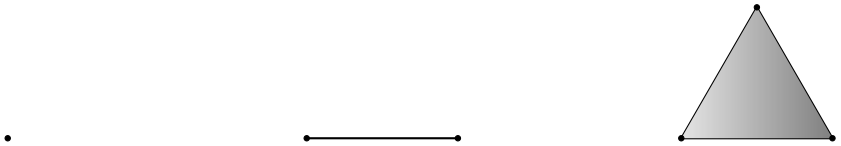

(a) The 0-simplex. **(b)** The 1-simplex. **(c)** The 2-simplex.

Figure 23: The simplices up to two-dimensions viewed pictorially.

We aim to relate this discussion to surfaces; although Definition 5.5 is general for any dimension, it is redundant for the purpose of our work to consider $n > 3$.

Definition 5.7 A k-face of an n-simplex is a subset of Δ^n, where $k \leq n$. It is proper when it is a proper subset, that is **not** an n-face.

Example 5.8 Consider the 2-simplex. It is clear that it has three 0-faces (vertices) and three 1-faces (edges) and only one 2-face (the simplex itself).

It is possible to take a number of simplices and 'glue' them together on corresponding faces, by which we mean identify faces via homeomorphisms.

Definition 5.9 An n-dimensional pseudo-simplicial complex (or n-complex) is a finite collection $\widetilde{\Delta}$ of simplices, where $n = \max\{k : \Delta^k \subseteq \widetilde{\Delta}\}$, that satisfy the following:

(i) For any simplex in $\widetilde{\Delta}$, all faces of that simplex are in $\widetilde{\Delta}$.

(ii) The intersection of any two simplices in $\widetilde{\Delta}$ is either a common face or is empty.

Example 5.10 We form a 3-complex by adjoining a 2-simplex to a 3-simplex as in Figure 24:

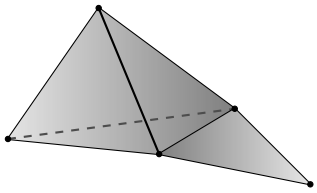

Figure 24: One possible three-dimensional complex.

Definition 5.11 A triangulation of a surface Σ is a homeomorphism between the topological space Σ and some simplicial complex.

Definition 5.12 Let Σ_1 and Σ_2 be surfaces. We say they are isomorphic if there is a bijection between the vertices of the triangulation of Σ_1 and the vertices of the triangulation of Σ_2 such that triangles map to triangles and the identification of sides is preserved.

Example 5.13 The sphere S^2 can be identified in the two slightly different ways shown below.

(a) The first gluing relation of S^2.

(b) The second gluing relation of S^2.

Figure 25: Triangulations of S^2.

It turns out these gluing relations are **not** isomorphic as noted in [Rob15], despite the obvious fact that $S^2 \cong S^2$. Therefore, something similar to but stronger than isomorphism is needed if we are to classify surfaces in this combinatorial way. Another thing to note: although the images above represent a surface via triangles, they are **not** triangulations. Look at the first one, say; each 2-simplex shares three edges and three points; the picture is not that of a 2-complex since their intersection is non-empty and is not a common face, so the second condition of Definition 5.9 fails. In fact, this is an example of a CW-complex, which has a less-restrictive definition than that of our simplicial complexes.

Definition 5.14 Let Σ be a surface defined by some gluing relation. A subdivision of the gluing relation is a decomposition into triangles.

Example 5.15 Consider the gluing relation in Figure 26 applied to a hexagon. By subdividing, it is clear the surface is that of a torus T^2.

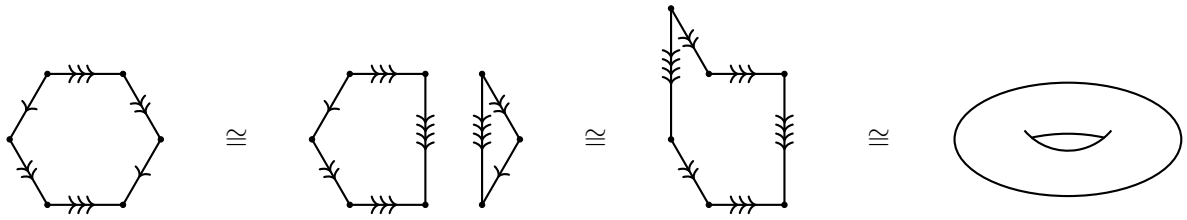

Figure 26: A subdivision which yields the usual projection of the torus T^2.

We now introduce the way in which we identify two surfaces by only their gluing relations.

Definition 5.16 Two gluing relations are called equivalent if there exists a finite sequence of isomorphisms and subdivisions relating them.

The next result is useful for subsequent proofs but is difficult to show rigorously; it is mentioned and used in [Pet07].

Theorem 5.17 *Two surfaces Σ_1 and Σ_2 are homeomorphic if and only if their gluing relations are equivalent.*

Definition 5.18 An orientation of a surface Σ is an assignment of a clockwise or anti-clockwise circulation to each face of a triangulation such that circulations across any edge oppose one another. In this case, Σ is called orientable.

Example 5.19 The sphere S^2 is orientable. Indeed, consider the following triangulation with the assigned circulations (and note that the condition laid out in Definition 5.18 is satisfied).

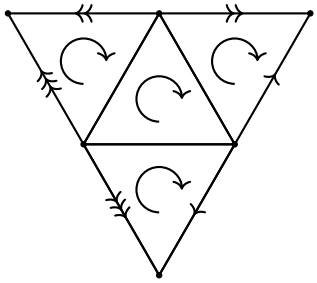

Figure 27: An orientation of the sphere, given via triangulation.

Furthermore, we see that the Möbius strip M^2 is non-orientable. Indeed, take a triangulation of M^2 and apply a circulation to one face; we immediately see a contradiction to Definition 5.18 if we try to extend this across neighbouring faces – the orientation across the identified edges at either end oppose each other.

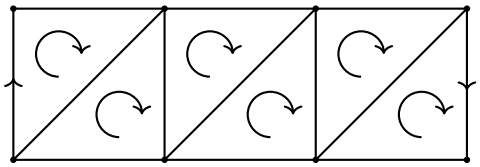

Figure 28: An attempt at an orientation of the Möbius strip, given via triangulation.

Proposition 5.20 *Orientability is a topological invariant.*

Proof: It suffices by Theorem 5.17 to show that orientability is preserved under the equivalence of gluing relations, in particular triangulations. Indeed, let Σ be an orientable surface have some gluing relation. Any subdivision is also orientable; this is achieved by prescribing the same circulation to any triangle of the face which it comes from. Of course, isomorphisms will preserve circulations and thus we are done. □

Definition 5.21 Let Σ be a surface. A subsurface of Σ is that which is obtained by deleting some faces and their gluing instructions from the gluing relation of Σ.

Remark 5.22 It is useful to now assume a graph-theoretic approach in the style of [Rob15]. Given the gluing relations, we can very naturally introduce two different graphs which are defined as follows (see Appendix C for further details on this):

- The identification graph G is one whose vertices and edges represent the vertices and edges of the gluing relation, respectively.
- The identification dual graph G^* is one whose vertices and edges represent faces and adjacency of faces given by the gluing relation, respectively.

Lemma 5.23 *A surface Σ is non-orientable if and only if the Möbius strip is a subsurface of Σ.*

Proof: ($\Leftarrow$) If M^2 is a subsurface, then Σ is non-orientable by Example 5.19.

($\Rightarrow$) We proceed with a proof using graph-theoretic methods. Consider the identification dual graph G^* of Σ. Because this graph is connected, it is possible to choose some spanning tree T of G^*. Now, simply choose a circulation on one face and extend this along the edges of T, that

is to the other faces in the gluing relation. Let G be the identification graph of Σ and H the subgraph of G where we removes the edges of G that intersect those of T. If the circulations across any edge of H do **not** oppose each other, then Σ is non-orientable. If this occurs, then we have a cycle in G^*, which corresponds to a cycle of faces and thus the existence of M^2 as a subsurface. □

Example 5.24 Consider the so-called projective plane $\mathbb{P}^2$ as now sketched (we can think of it as antipodal points of S^1 identified but we consider it also as a quotient of $[0,1] \times [0,1]$, which is slightly more useful in this context).

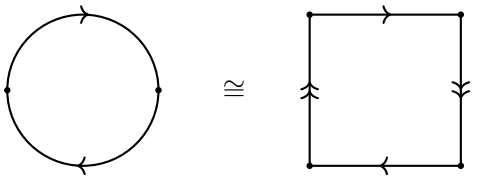

Figure 29: Two representations of the projective plane $\mathbb{P}^2$.

Now, it is possible to subdivide the second image of Figure 29, which is shown in Figure 30. We can then see that M^2 is a subsurface and so Lemma 5.23 applies, giving that $\mathbb{P}^2$ is non-orientable.

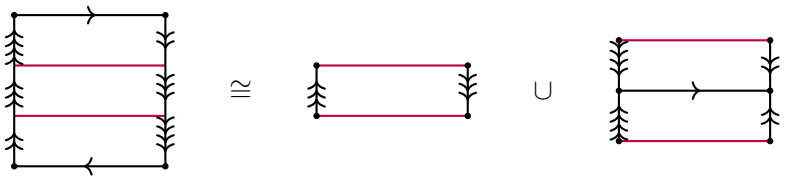

Figure 30: A pictorial justification that $\mathbb{P}^2 = M^2 \cup D$, where D is a closed disk.

We are getting close to being able to classify topological surfaces. But first, there is an important concept that must be discussed.

Definition 5.25 Let $\widetilde{\Delta}$ be an n-complex. The Euler characteristic of $\widetilde{\Delta}$ is defined as

$$\chi(\widetilde{\Delta}) = \sum_{k=0}^{n} (-1)^k \left|\widetilde{\Delta}^{(k)}\right|,$$

where $\widetilde{\Delta}^{(k)}$ represents the set of k-faces of $\widetilde{\Delta}$.

Example 5.26 Consider the 3-simplex Δ^3. Then, $\chi(\Delta^3) = 4 - 6 + 4 = 2$. This should be familiar to those with a knowledge on the Platonic solids. However, Definition 5.25 is a deeper generalisation which holds in arbitrary dimensions.

Example 5.27 Consider a truncated icosahedron X consisting of p pentagons and h hexagons. Then, there are $(5p+6h)/3$ vertices and $(5p+6h)/2$ edges and $p+h$ faces. As such, $\chi(X) = p/6$. But now, this is a convex shape, so it must be that $\chi(X) = 2$, meaning that $p = 12$. We have just proven that every football consists of precisely 12 pentagonal faces.

Lemma 5.28 *Let $X = A \cup B$, where A and B are n-complexes. Then,*

$$\chi(X) = \chi(A) + \chi(B) - \chi(A \cap B).$$

Proof: Using Definition 5.25, we formulate the right-hand-side of the equation in the statement:

$$\chi(A) + \chi(B) - \chi(A \cap B) = \sum_{k=0}^{n} (-1)^k \Big(\big|A^{(k)}\big| + \big|B^{(k)}\big| - \big|(A \cap B)^{(k)}\big| \Big) + (-1)^n \big|(A \cap B)^{(n)}\big|,$$

but $A \cap B$ is an $(n-1)$-complex, meaning it has no n-faces, that is the final term above vanishes. The Inclusion-Exclusion Principle gives $|A \cup B| = |A| + |B| - |A \cap B|$, which applies to the above:

$$\chi(A) + \chi(B) - \chi(A \cap B) = \sum_{k=0}^{n} (-1)^k \big|(A \cup B)^{(k)}\big| = \sum_{k=0}^{n} (-1)^k \big|X^{(k)}\big| = \chi(X),$$

which is precisely the formula we require. □

Proposition 5.29 *The Euler characteristic is a topological invariant.*

Proof: It again suffices by Theorem 5.17 to show that the Euler characteristic is preserved under the equivalence of gluing relations; a subdivision adds an edge and adds a vertex but it also splits another edge into two and adds a face. Thus, if Σ is a surface with Euler characteristic $\chi(\Sigma) = V - E + F$, then the Euler characteristic of the subdivision of this surface is

$$(V + 1) - (E + 2) + (F + 1) = V - E + F,$$

so $\chi(\Sigma)$ is preserved. Finally, isomorphisms trivially preserve $\chi(\Sigma)$ and thus we are done. □

Example 5.30 Let $X = S^2 \sqcup S^2$. Then, Lemma 5.28 gives that

$$\chi(X) = \chi(S^2) + \chi(S^2) - \chi(S^2 \cap S^2) = 2 + 2 - 0 = 4,$$

using that the copies of S^2 are disjoint. Note that Example 5.26 gives the Euler characteristic of

S^2, since the 3-simplex is the triangulation of the sphere and Proposition 5.29 means they have equal Euler characteristic. Inductively, $\chi(S^2 \sqcup \cdots \sqcup S^2) = 2n$, where there are n copies of S^2.

Another useful property of surfaces that can be discussed are that of through-holes. It seems reasonable to assert that a torus cannot be homeomorphic to a sphere because a sphere has no through-holes yet the torus has one. This concept can now be made rigorous.

Definition 5.31 Let Σ be a surface. The genus of the surface $g(\Sigma)$ is the supremum of the number of non-intersecting simple closed curves on Σ that preserve connectedness of the surface.

Example 5.32 Any closed curve on T^2 that is homotopically equivalent to a point will disconnect the surface. However, one closed curve through the hole of the torus will preserve connectedness (and a second such curve will give a disconnection). Therefore, $g(T^2) = 1$.

Recall in Section 2 we defined the connected sum of link diagrams; we noted in Remark 2.21 that this is a specific case of a more general topological operation, which is next discussed.

Definition 5.33 Let Σ_1 and Σ_2 be surfaces. The connected sum of these surfaces, denoted $\Sigma_1 \# \Sigma_2$, is found by identifying the boundary of a single face in each gluing relation.

Lemma 5.34 *Let A and B be n-complexes. Then,*

$$\chi(A \# B) = \chi(A) + \chi(B) - \chi(S^n).$$

Proof: (of the $n = 2$ case) We shall prove this result for two surfaces Σ_1 and Σ_2. Let X_1 and X_2 be the surfaces' respective triangulations, that is they are 2-complexes. By Definition 5.33, the connected sum of these complexes comes about by identifying two 2-faces, one from each of X_1 and X_2. If we say that X is the 2-complex representing $\Sigma_1 \# \Sigma_2$, then we have the following:

- The number of vertices $V_X = V_{X_1} + V_{X_2} - 3$.
- The number of edges $E_X = E_{X_1} + E_{X_2} - 3$.
- The number of faces $F_X = F_{X_1} + F_{X_2} - 2$.

Therefore, we can easily see that $\chi(\Sigma_1 \# \Sigma_2) = \chi(\Sigma_1) + \chi(\Sigma_2) - 2$. The general case follows by doing a similar analysis of the vertices, edges and faces of higher-dimensional complexes. □

Theorem 5.35 (Classification of Surfaces without Boundary) *Every closed connected surface Σ can be represented in precisely one of the following ways:*

(i) *As a sphere, in which $\chi(\Sigma) = 2$.*

(ii) *As the connected sum of n-tori, in which $\chi(\Sigma) = 2 - 2n$.*

(iii) *As the connected sum of n-projective planes, in which $\chi(\Sigma) = 2 - n$.*

Remark 5.36 We omit the proof since it would detract from the intentions of this paper; we can however see the full detail in [Zee66]. We shall note that the facts about the Euler characteristics in the statement of Theorem 5.35 follow from inductively applying Lemma 5.34, using $\chi(T^2) = 0$ and $\chi(\mathbb{P}^2) = 1$.

Definition 5.37 If $\mathbb{P}^2$ is a subsurface of a surface Σ, then we say that it is a cross-cap of Σ.

From Theorem 5.35, we can state formulae for the genera of closed surfaces Σ without boundary:

$$g(\Sigma) = \begin{cases} 1 - \frac{1}{2}\chi(\Sigma), & \text{if } \Sigma \text{ is orientable} \\ 2 - \chi(\Sigma), & \text{if } \Sigma \text{ is non-orientable} \end{cases}. \qquad (\dagger)$$

Example 5.38 We know that the torus T^2 is orientable by Lemma 5.23 and we easily compute $\chi(T^2) = 1 - 2 + 1 = 0$ and so $g(T^2) = 1$ (this agrees with our previous answer in Example 5.32).

Definition 5.39 Let $D \subseteq \mathbb{R}^2$ be a closed disk and Σ a surface. We say that D is a cuff of the surface $\Sigma \# D$. In other words, $\Sigma \# D$ is a surface with one boundary component.

Corollary 5.40 (of Lemma 5.34) *Let Σ be a surface and D a cuff on the surface. Then,*

$$\chi(\Sigma \# D) = \chi(\Sigma) - 1.$$

Proof: It is clear that $\chi(D) = 1$. Therefore, $\chi(\Sigma \# D) = \chi(\Sigma) + 1 - 2 = \chi(\Sigma) - 1$. □

Theorem 5.41 (Classification of Surfaces with Boundary) *Every connected surface Σ can be represented in precisely one of the following ways:*

(i) *As a sphere with k-cuffs, in which $\chi(\Sigma) = 2 - k$.*

(ii) *As the connected sum of n-tori with k-cuffs, in which $\chi(\Sigma) = 2 - 2n - k$.*

(iii) *As the connected sum of n-projective planes with k-cuffs, in which $\chi(\Sigma) = 2 - n - k$.*

Remark 5.42 It is clear that a topological surface Σ is completely determined by the Euler characteristic, its orientability and the number of boundary components. It is also clear that formula (†) for the genus holds for surfaces with boundary, noting that n in the statement of Theorem 5.41 is the (un-)orientable genus.

5.2 Seifert Surfaces

We can now relate the work done in Section 5 thus far to knot theory, in which we consider special types of surfaces which also yield some useful knot invariants.

Definition 5.43 Let K be a knot and Σ_K be a connected orientable surface with singular boundary component $\partial\Sigma_K = K$. Then, Σ_K is called the Seifert surface of K.

Proposition 5.44 *For any knot K, there exists a Seifert surface Σ_K.*

Sketch of Proof: We leave it to [Dan15] for the details; we shall discuss what is known as Seifert's Algorithm, that is the procedure which yields a Seifert surface and indeed this works with any knot. The algorithm proceeds as follows:

(i) Choose an orientation of K.

(ii) Connect every arc entering a crossing to the adjacent arc leaving the crossing.

(iii) Connect these disks with half-twist bands at each crossing.

Choosing an orientation on one disk and propagating via the half-twist bands to the other disks will yield a consistent orientation. □

Example 5.45 We shall apply Seifert's Algorithm to the usual trefoil diagram K and appeal to the Classification of Surfaces with Boundary as to identify it with a more 'standard' surface.

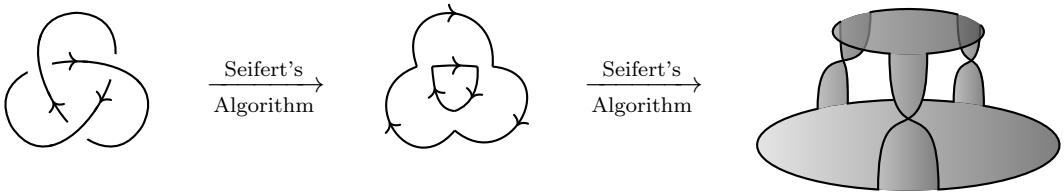

Figure 31: Applying Seifert's Algorithm to the trefoil.

Given what we have in Figure 31, we can see the Euler characteristic is $\chi(\Sigma_K) = 2\chi(D) + 3\chi(B)$, where D is the disk and B is the half-twist band. But now, we know that $\chi(D) = 1$ and we can see that $\chi(B) = -1$. Therefore, $\chi(\Sigma_K) = -1$. Furthermore, we know that this surface has one cuff by definition of Seifert surface. Because it is orientable, it can only be the connected sum of n-tori with one cuff, by the Classification of Surfaces with Boundary. Substituting the known values into the equation given in the statement of the theorem, we see that $n = 1$. Consequently, the Seifert surface of the trefoil is a punctured torus.

Definition 5.46 Let K be a knot. The genus of K is defined to be the non-negative integer

$$g(K) = \inf\{g(\Sigma_K) : \Sigma_K \text{ is a Seifert surface of } K\}$$

The genus of a knot is trivially an isotopy invariant since it is a topological invariant. The main problem comes from determining the genus of a knot; it is not at all trivial to do so. That being said, one interesting point shall now be mentioned.

Lemma 5.47 *Let K be a knot. Then, $g(K) = 0$ if and only if K is the unknot.*

Proof: Well, $g(K) = 0$ if and only if K is the boundary of a disk. □

Therefore, given some complicated diagram of a knot, the genus immediately tells us if that class of closed curve is indeed knotted. We can refer to Lemma 5.47 to acquire the genus of what can only be described as our favourite knot.

Example 5.48 By Example 5.45, we see that the genus of that particular Seifert surface of K is $g(\Sigma_K) = 1$. By Lemma 5.47, $g(K) \neq 0$ so taking the infimum must give that $g(K) = 1$.

We have used [Rob15] as a basis for some of this discussion. However, there are a number of exercises left to the reader, which we will now solve in the next few results as to deepen our understanding of the genus of a knot.

Proposition 5.49 *Let K be a knot and Σ_K the corresponding Seifert surface. If Σ_K consists of d disks and b half-twist bands, then $\chi(\Sigma_K) = d - b$.*

Proof: This is a generalisation of the Euler characteristic argument of Example 5.45. Indeed, $\chi(\Sigma_K) = d\chi(D) + b\chi(B)$, again where D is a disk and B is a half-twist band. We know already that $\chi(D) = 1$ and $\chi(B) = -1$. □

Corollary 5.50 *Let K be a knot with n crossings. Then, $g(K) \leq n/2$.*

Proof: Let Σ_K be the corresponding Seifert surface. Because it has boundary, the number of disks $d \geq 1$, which is to say $0 \geq 1 - d$. Using the formula established for the genus, we know that $g(\Sigma_K) = 1 - \frac{1}{2}\chi(\Sigma_K)$ which can be written as $g(\Sigma_K) = \frac{1}{2}(1 - d + n)$. Hence, using the inequality we have just established, it must be that $g(\Sigma_K) \leq \frac{1}{2}n$. Minimising the crossing number over all diagrams of K preserves this bound. As such, we have that $g(K) \leq \frac{1}{2}n$. □

The next result is rather powerful but a full proof is beyond the scope of our discussion. Despite this, we fully detail half the argument and sketch the rest.

Theorem 5.51 *Let $K = K_1 \# K_2$ be a knot. Then, $g(K) = g(K_1) + g(K_2)$.*

Sketch of Proof: We first show the more simple inequality $g(K) \leq g(K_1) + g(K_2)$. Indeed, let Σ_{K_1} and Σ_{K_2} be Seifert surfaces of the respective knots with minimal genera. We can apply the more general connected sum to these surfaces, which gives us a surface $\Sigma_{K_1 \# K_2}$ whose

boundary is $K_1 \# K_2$. Indeed, we now proceed with a quick study on the genus of this new surface. By Lemma 5.34, we have $\chi(\Sigma_{K_1 \# K_2}) = \chi(\Sigma_{K_1}) + \chi(\Sigma_{K_2}) - 1$. Then, using the formula relating the genus to the Euler characteristic as presented in Theorem 5.41, it is clear that $g(\Sigma_{K_1 \# K_2}) = g(\Sigma_{K_1}) + g(\Sigma_{K_2})$. As such,

$$g(K_1 \# K_2) \leq g(\Sigma_{K_1 \# K_2}) = g(\Sigma_{K_1}) + g(\Sigma_{K_2}) = g(K_1) + g(K_2),$$

where we use the assumption that the Seifert surfaces for each knot are minimal.

We now sketch the proof to show the more difficult $g(K) \geq g(K_1) + g(K_2)$, following the structure of [Rin14]. Here, we start with $\Sigma_{K_1 \# K_2}$ being the Seifert surface of the connected sum of knots which has minimal genus. This part of the proof hinges on the study of intersecting surfaces in $\mathbb{R}^3$. We construct a sphere S containing K_1 but not K_2; we should have S intersecting $K_1 \# K_2$ in exactly two points p and q, say. From here, we consider $S \cap \Sigma_{K_1 \# K_2}$. It is certainly non-empty because $p, q \in S \cap \Sigma_{K_1 \# K_2}$. Also, we can construct a path between p and q on this intersection. The technical part now follows: we can suppose that this path is the only arc in the intersection and that there are no loops in the intersection; this is achieved by repeatedly modifying S. If we then 'cut' along this arc, we get the disjoint union of connected orientable surfaces with boundary K_1 and K_2 respectively, i.e. Seifert surfaces for each knot. Call them Σ_{K_1} and Σ_{K_2}. Then,

$$g(K_1 \# K_2) = g(\Sigma_{K_1 \# K_2}) = g(\Sigma_{K_1}) + g(\Sigma_{K_2}) \geq g(K_1) + g(K_2),$$

which completes the proof. □

Definition 5.52 Let K be a knot. It is called composite if there exist non-trivial knots K_1 and K_2 such that $K = K_1 \# K_2$. Otherwise, it is called prime.

Proposition 5.53 *Let K be a knot where $g(K) = 1$. Then, K is prime.*

Proof: Suppose to the contrary that $K = K_1 \# K_2$ for non-trivial knots K_1 and K_2. We can use Theorem 5.51 to see that $g(K) = g(K_1) + g(K_2) = 1$ which implies that either $g(K_1) = 0$ or $g(K_2) = 0$, so one of them is trivial, a contradiction. □

Corollary 5.54 *Any composite knot K has a factorisation into prime knots.*

Proof: By definition, there exist non-trivial knots K_1 and K_2 such that $K = K_1 \# K_2$. If each of K_1 and K_2 are prime, we are done. Otherwise, proceed to decompose the composite knots in the connected sum. Note that this process will terminate because Theorem 5.51 guarantees that K cannot be the connected sum of greater than $g(K)$ non-trivial knots. □

Corollary 5.55 (of Theorem 2.23) *The only invertible knot under connected sum is the unknot.*

Proof: Suppose K_1 and K_2 are arbitrary knots. If $K_1 \# K_2 = \bigcirc$, then Theorem 5.51 gives that

$$0 = g(\bigcirc) = g(K_1) + g(K_2).$$

As such, it must be that $g(K_1) = 0$ and $g(K_2) = 0$; both K_1 and K_2 are trivial. This shows the only way to obtain the unknot through connected sum is via the connected sum of the unknot with itself. This is why knots only form a commutative monoid under connected sum. □

There are other ways to argue for the next result, but we will use the theory of Seifert surfaces (in particular the idea of the knot genus) to show we can create any number of distinct knots.

Theorem 5.56 *There are infinitely many distinct knots.*

Proof: Let K be any non-trivial knot and define a sequence $(K_n)_{n \in \mathbb{Z}^+}$ of knots whereby K_n is the connected sum of n-copies of K. Then $g(K_n) = ng(K)$ by Theorem 5.51. But now, the K_n are pairwise distinct because $g(K_n) \neq g(K_m)$, whenever $n \neq m$ by the fact that K is non-trivial and Corollary 5.55 implies that the connected sum of non-trivial knots remains non-trivial. □

We conclude this subsection with an example that not only shows how to compute the Seifert surface of a link, but that a diagram can have more than just the one Seifert surface.

Example 5.57 Consider the link L as drawn in Figure 32.

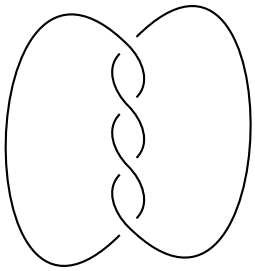

Figure 32: An alternating diagram of some two-component link L.

Depending on the orientation we prescribe (of which there are four), we can generate different Seifert surfaces. This is shown considering two possible orientations, one in which each component is traversed clockwise and one in which they oppose each other. Call the Seifert surfaces $\Sigma_{L,1}$ and $\Sigma_{L,2}$ respective of the ordering of the figures below.

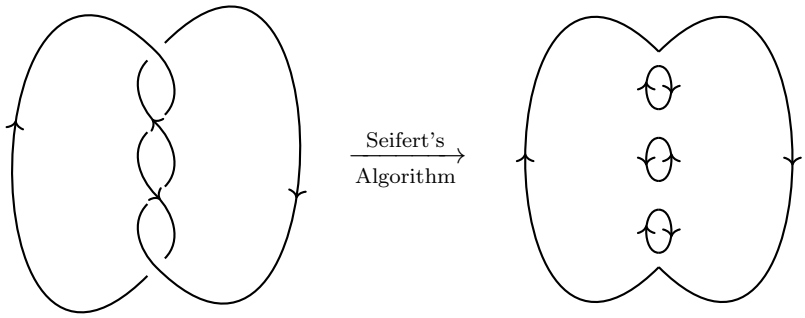

Figure 33: The Seifert surface $\Sigma_{L,1}$.

Using Proposition 5.49, we see that $\chi(\Sigma_{L,1}) = 4 - 4 = 0$ and, because L is has two components, $g(\Sigma_{L,1}) = 0$. We proceed similarly with the second orientation.

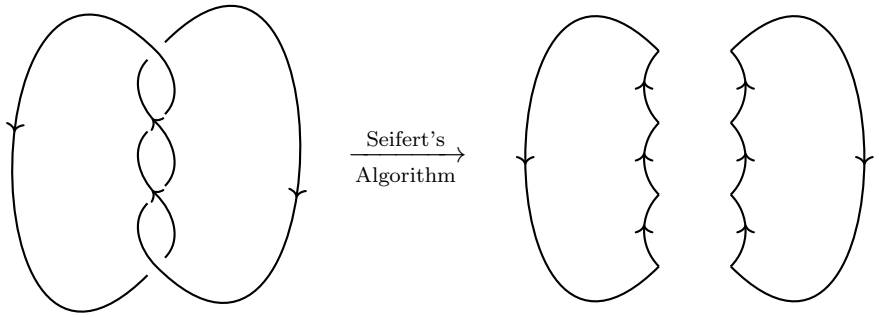

Figure 34: The Seifert surface $\Sigma_{L,2}$.

Again by Proposition 5.49, we have $\chi(\Sigma_{L,2}) = 2 - 4 = -2$ and $g(\Sigma_{L,2}) = 1$. Hence, $\Sigma_{L,1} \ncong \Sigma_{L,2}$ since the genera do not agree, yet we have $\partial\Sigma_{L,1} = L = \partial\Sigma_{L,2}$ by construction. Thus, this example proves that a link diagram can have more than one corresponding Seifert surface.

Remark 5.58 Another approach considered was to attack this section from the point of view of simplicial homology. Given some n-simplex Δ^n as in Definition 5.5 on vertices $\{p_1, ..., p_{n+1}\}$, we can consider the free Abelian groups C_n which are generated by the n-faces (more specifically, they are linear combinations over $\mathbb{Z}$ of the n-faces); we call the elements of each of these groups n-chains. This provides a means to define the boundary of a combinatorial surface without

referring to homeomorphisms as in Definition 5.1. Indeed, we say that the boundary maps are

$$\partial_n : C_n \to C_{n-1}, \quad \partial_n([p_1, ..., p_{n+1}]) = \sum_{i=1}^{n+1} (-1)^i [p_1, ..., p_{i-1}, p_{i+1}, ..., p_{n+1}].$$

From here, we can define the k^{th} homology group of some n-simplex as follows:

$$H_k(\Delta^n) = \frac{\ker(\partial_k)}{\mathrm{im}(\partial_{k+1})}.$$

The intuition here is that these groups can detect any k-dimensional holes in a topological space. Perhaps this is a little naïve and it is better to think of the k^{th} homology group as detecting cycles that are not boundary components.

5.3 Seifert Matrices

We will now discuss yet another knot-related matrix. Given a knot K and Seifert surface Σ_K, we saw that such a surface can be constructed using only disks and half-twist bands. In fact, we can construct a Seifert surface of a knot using only one disk with (possibly more than half-twist) bands attached to that disk. For this, we shall loosely follow [Mur07] but prove a number of things independently.

Example 5.59 Consider Figure 31. We can slide the middle half-twist band along one of the others, the right one say, so that it ends on the bottom disk which results in a one-twist band. Then, we can shrink the top disk slightly to a strip which connects the ends of the left and right half-twist bands. This results in another one-twist band. We see the end result in Figure 35.

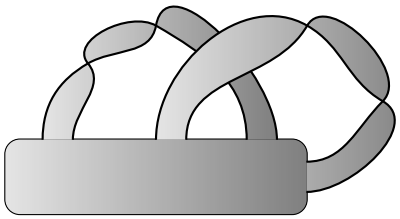

Figure 35: A modified version of the Seifert surface of the trefoil.

Definition 5.60 Let L be an oriented link with at least two components, C_i and C_j say. Then, the linking number of these components $\mathrm{lk}(C_i, C_j)$ is defined as half the sum of the signs of the crossings between these components.

Example 5.61 Consider our most basic link, the Hopf link as in Figure 1. Then, if we orientate

both clockwise, we see that $\mathrm{lk}(C_1, C_2) = -1$.

Definition 5.62 Let K be a knot and Σ_K the modified one-disk Seifert surface as discussed above. A Seifert matrix of the knot is $S_K = [\mathrm{lk}(x_i, x_j^+)]_{i,j}$, where x_i, x_j are loops based on the disk which circumnavigate the i^{th} and j^{th} bands respectively, where x_j^+ is the push-off of such a loop, i.e. where we have lifted x_j a distance ε away from the surface at each point in the direction of the normal vector.

Example 5.63 Let us consider two loops on our modified Seifert surface from Example 5.59 (we will be very well acquainted with this example by the end of this section); call them x_1 and x_2 and say they travel around the centre of their respective bands. With a bit of careful thought, we can compute the Seifert matrix as follows:

$$S_K = \begin{pmatrix} 1 & 1 \\ 0 & 1 \end{pmatrix}.$$

Remark 5.64 This remark is very much paired with Remark 5.58 in that there is a significant homological angle that can be taken here; the loops we defined in Definition 5.62 are actually generators of the first homology group of the Seifert surface, denoted $H_1(\Sigma_K)$. Again, we shall not discuss this too much (unfortunately) but we are clearly aware of this deeper approach. We will however refer to the loops as first homology generators.

Given some knot K, the Seifert matrix S_K isn't remotely invariant; we can choose a different set of first homology generators from which to get a Seifert matrix. In fact, Example 5.57 demonstrates that the Seifert surface may not always be unique (yes, this was done for a link but everything we discuss here also extends to links with more than one component as is discussed in [Cro04]). That aside, Seifert matrices do lead to a number of invariants.

Example 5.65 We again consider the usual trefoil K. We can use Example 5.63 to see that

$$S_K = \begin{pmatrix} 1 & 1 \\ 0 & 1 \end{pmatrix} \quad \text{and} \quad S_K^T = \begin{pmatrix} 1 & 0 \\ 1 & 1 \end{pmatrix} \quad \text{which means} \quad S_K + S_K^T = \begin{pmatrix} 2 & 1 \\ 1 & 2 \end{pmatrix}.$$

The eagle-eyed reader will notice that $|\det(S_K + S_K^T)| = 3 = \det(K)$. This is not a coincidence.

Proposition 5.66 *Let K be a knot. Then,* $\det(K) = |\det(S_K + S_K^T)|$.

Note that the vast majority of the literature uses Proposition 5.66 as a definition so we shall omit a proof for now. Recall in Section 3 that we saw the Alexander polynomial as a generalisation of the knot determinant. In a similar vein, we can define the Alexander polynomial in terms of a Seifert matrix of a knot and it does coincide with that of Definition 3.25.

Definition 5.67 Let K be a knot. Then, the Alexander polynomial is $\Delta_K(t) = \det(S_K - tS_K^T)$.

We can now finally prove part (i) of Proposition 3.29 using this alternate definition.

Proof: From our equivalent definition, we can quickly see that

$$\Delta_K(t) = \det(S_K + tS_K^T) = \det(tS_K^T - S_K),$$

since the transpose doesn't affect the determinant. As such, we can remove a factor of t, giving us $\Delta_K(t) = t^{2g(\Sigma_K)} \det(S_K^T - t^{-1}S_K) = t^{2g(\Sigma_K)}\Delta_K(t^{-1})$, where $g(\Sigma_K)$ is the genus. □

We make one observation: the Seifert matrix S_K constructed using Σ_K will be of dimension $2g(\Sigma_K) \times 2g(\Sigma_K)$; this is justified by Remark 5.58 in that the first homology group will detect cycles on a surface that aren't boundary components (also thought of as the number of holes $g(\Sigma_K)$) and we can use the formula relating the genus and Euler characteristic along with Proposition 5.49 with $d = 1$ to conclude that the number of bands $b = 2g(\Sigma_K)$.

Definition 5.68 Let M be a symmetric matrix. Then, the signature $\sigma(M)$ of M is defined as the number of positive entries minus the number of negative entries on the leading diagonal of the diagonalisation of M.

From linear algebra, we know that this is just the difference between the number of positive and negative eigenvalues of a matrix. It will not be much of a surprise to see how we can relate this to Seifert matrices and knot theory.

Example 5.69 We proceed with a quick bout of linear algebra; the characteristic polynomial of $S_K + S_K^T$, where K is the usual trefoil, is $\lambda^2 - 4\lambda + 3$ which has roots $\lambda = 1$ and $\lambda = 3$. Hence, the diagonalisation of the matrix is

$$\begin{pmatrix} 1 & 0 \\ 0 & 3 \end{pmatrix}.$$

We can immediately read off that $\sigma(S_K + S_K^T) = 2$, since there are no negative eigenvalues.

Definition 5.70 Let K be a knot. The signature $\sigma(K)$ of K is the usual signature of $S_K + S_K^T$.

Theorem 5.71 *The signature of a knot is an isotopy invariant.*

Sketch of Proof: This result is fully proven in our motivating reference [Mur07]. The idea is that we use so-called S-equivalence of Seifert matrices which corresponds to performing surgery on the surface Σ_K, i.e. adding a handle under certain conditions. The punchline is that Seifert matrices can be changed through congruence or enlargement; showing that the signature remains unchanged when one of these occurs will give that it is an isotopy invariant. □

We now proceed with proving some exercises left to us in [Liv93].

Lemma 5.72 *Let K be a knot and $\overline{K}$ its mirror image. Then, $\sigma(\overline{K}) = -\sigma(K)$.*

Proof: Let S_K be a Seifert matrix of K. Then, taking mirror images interchanges positive and negative crossings, meaning that the linking numbers change sign. As such, we have $S_{\overline{K}} = -S_K$. Diagonalising will preserve this change of sign, meaning we have $D_{\overline{K}} = -D_K$ for the diagonalised matrices. Consequently, the number of positive and negative eigenvalues have swapped roles and so the signature will change sign. □

Corollary 5.73 *If K is achiral, then $\sigma(K) = 0$.*

Proof: If K is achiral, then $\overline{K} \simeq K$ and Theorem 5.71 implies that $\sigma(\overline{K}) = \sigma(K)$. Using this in Lemma 5.72 means that we have $\sigma(K) = -\sigma(K)$, so the only option is to have $\sigma(K) = 0$. □

Proposition 5.74 *Let K_1 and K_2 be knots. Then, we have that $\det(K_1 \# K_2) = \det(K_1)\det(K_2)$ and that $\sigma(K_1 \# K_2) = \sigma(K_1) + \sigma(K_2)$.*

Proof: Let Σ_{K_1} and Σ_{K_2} be respective Seifert surfaces on which Seifert matrices will be computed. Note that the orientable surface formed by joining these via connected sum will give a Seifert surface which we call $\Sigma_{K_1 \# K_2}$. As such, the Seifert matrix of the connected sum of knots will have the form

$$S_{K_1 \# K_2} = \begin{pmatrix} S_{K_1} & 0 \\ 0 & S_{K_2} \end{pmatrix},$$

since the first homology generators of Σ_{K_1} will not interact with those of Σ_{K_2} and vice versa. As such, we can compute the symmetric matrix formed by adding the transpose, namely

$$S_{K_1 \# K_2} + S_{K_1 \# K_2}^T = \begin{pmatrix} S_{K_1} + S_{K_1}^T & 0 \\ 0 & S_{K_2} + S_{K_2}^T \end{pmatrix}.$$

Therefore, the non-trivial entries in the diagonalisation of the above matrix will be those from the diagonalisations of $S_{K_1} + S_{K_1}^T$ and $S_{K_2} + S_{K_2}^T$. As such, we can immediately read off the additivity of the signature, i.e. $\sigma(K_1 \# K_2) = \sigma(K_1) + \sigma(K_2)$. As for multiplicity of the determinant, by basic linear algebra, $\det(S_{K_1 \# K_2} + S_{K_1 \# K_2}^T)$ is merely the product of the entries on the leading diagonal of its diagonalisation. As we already noted, this will consist only of the leading diagonal entries of the other two matrices, which means we have $\det(K_1 \# K_2) = \det(K_1)\det(K_2)$. □

Corollary 5.75 *Let K_1 and K_2 be knots. Then, $\Delta_{K_1 \# K_2}(t) = \Delta_{K_1}(t)\Delta_{K_2}(t)$.*

We conclude this section by proving a somewhat surprising result, which will provide us with another means to argue why no knot can be 2-colourable.

Theorem 5.76 *Let K be a knot. Then, $\det(K)$ is odd and $\sigma(K)$ is even.*

Proof: By Proposition 3.29, we know that $\Delta_K(1) = 1$, which is to say that $\det(S_K - S_K^T) = 1$. As such, we can see that $S_K + S_K^T \equiv S_K - S_K^T \pmod 2$ and so taking determinants of both sides gives that $\det(K) \equiv 1 \pmod 2$. From this, it must follows that the diagonalisation of $S_K - S_K^T$ contains no zeros on the leading diagonal. Because it is a matrix of even dimension, if there is an even (or odd) number of positive eigenvalues, there must be an even (or odd) number of negative eigenvalues. As such, the signature is always even. □

Remark 5.77 We gave a reason in Remark 3.9 as to why it is never going to be possible to colour a knot with only two colours; we have made this notion rigorous. Indeed, Theorem 5.76 implies that $\det(K)$ is never even, so $2 \nmid \det(K)$ but Proposition 3.17 implies therefore that K is never 2-colourable.

6 Braid Theory

The topic of knot theory, although relatively new, is still very deep. As such, there are a number of interesting related areas that can be discussed. We will look at one of these closely related disciplines called braid theory from geometric, algebraic and topological viewpoints, after which we explain why these give equivalent notions of the same thing. We conclude with a constructive proof of Alexander's Theorem and explain how to use it in the context of some of our favourite knots.

Definition 6.1 A braid on n-strings (or an n-braid) consists of n arcs $x_1, ..., x_n$ with integer endpoints $1, ..., n$. More specifically, each x_i connects a point $P_i^+ = (i, 0, 1)$ in the so-called upper plane to a point $P_{\pi(i)}^- = (i, 0, 0)$ in the so-called lower plane, where $\pi \in S_n$ is a permutation. In the case that π is trivial, we call it a pure braid on n-strings (or a pure n-braid).

To avoid 'nasty' braids, we stipulate that the strands of an n-braid must cross at a finite number of places and must not intersect, with crossings occurring on different hyperplanes (i.e. different z-values). As with links, two n-braids σ and σ' are equivalent if there exists an ambient isotopy of $\mathbb{R}^3$ taking σ to σ'. We draw these as planar drawings, analogous to Definition 2.5.

Example 6.2 Consider the following 4-braid diagram, in which the permutation $\pi = (1)(3)(24)$.

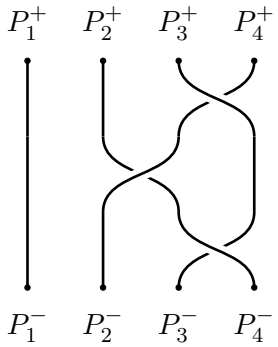

Figure 36: An example of a 4-braid.

6.1 The Braid Group

Naturally, one may consider what would happen if we identify the upper and lower planes of a braid diagram. This will become clear soon, but first we discuss properties of braids in an algebraic context. We can use the structure of a group to describe interactions between n-braids. This will be done as in the work of [Art47] before branching into a more topological approach.

Definition 6.3 The n-braid alphabet is the set $A = \{\sigma_k, \sigma_k^{-1} : 1 \leq k \leq n\}$, where the symbols are given in Figure 37 below. An n-braid word is the concatenation of the symbols σ_k and σ_k^{-1},

where the trivial n-braid is denoted e_n, taken in order from the upper plane to the lower plane.

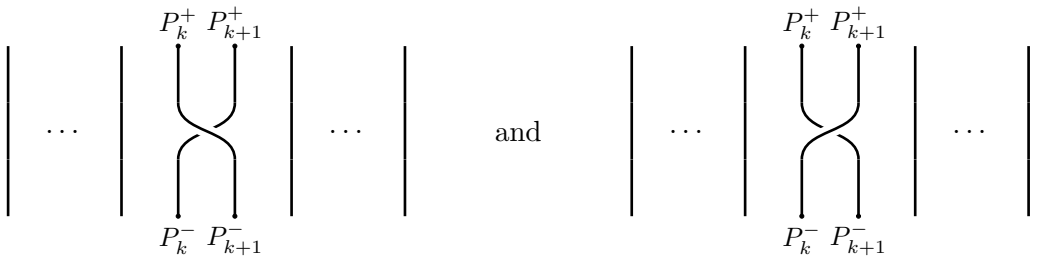

Figure 37: The geometric interpretations of σ_k and σ_k^{-1} respectively.

This looks similar to Definition 4.31 and it will come as little surprise that this will give us a presentation of a group whose underlying set consists of n-braids.

Example 6.4 The word corresponding to the 4-braid σ in Example 6.2 is $\sigma = \sigma_3\sigma_2^{-1}\sigma_3$.

Intuitively, the concatenation of these symbols corresponds to identifying the points at the ends of each braid diagram, that is they are 'stacked' onto each other; this is shown in Figure 38.

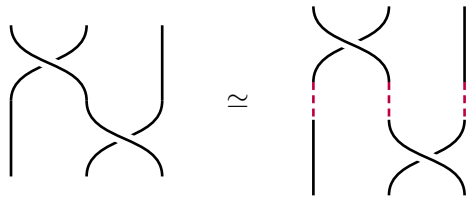

Figure 38: The join of σ_1 and σ_2.

We shall now develop the theory of equivalence of braids. We begin with three important moves, the latter two of which seem to correspond with the Reidemeister moves **R2** and **R3** respectively.

Definition 6.5 The Artin moves are the following, applied to arcs of a braid:

(**A1**) We have $\sigma_i\sigma_j = \sigma_j\sigma_i$ whenever $|i - j| > 1$.

(**A2**) We have $\sigma_i\sigma_i^{-1} = e = \sigma_i^{-1}\sigma_i$.

(**A3**) We have $\sigma_i\sigma_{i+1}\sigma_i = \sigma_{i+1}\sigma_i\sigma_{i+1}$.

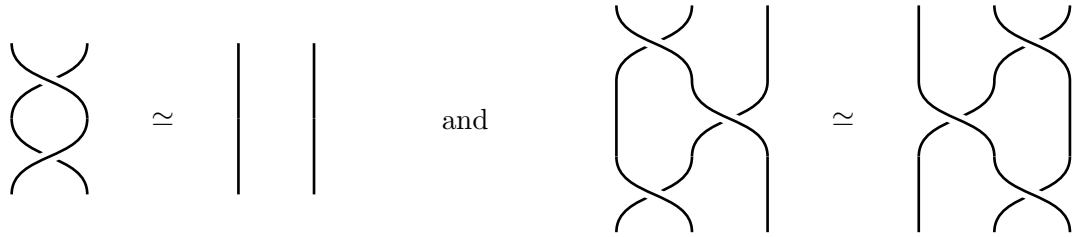

Figure 39: The geometric interpretations of **A2** and **A3**.

Example 6.6 Consider the 4-braid given by $\sigma = \sigma_2^{-1}\sigma_1\sigma_3^{-1}\sigma_1^{-1}\sigma_2$. Thus, the Artin moves give

$$\sigma \simeq \sigma_2^{-1}\sigma_1\sigma_1^{-1}\sigma_3^{-1}\sigma_2 \simeq \sigma_2^{-1}\sigma_3^{-1}\sigma_2.$$

Definition 6.7 Let σ be some n-braid. We can define an equivalence relation $\sim$ on the braid diagram, given by $P_i^+ \sim P_j^-$ if and only if $i = j$, to get the link via braid closure $L_{\overline{\sigma}}$.

Example 6.8 Any section of this paper would be incomplete without our favourite knot so we will show that, by closing the following 2-braid, we achieve the trefoil.

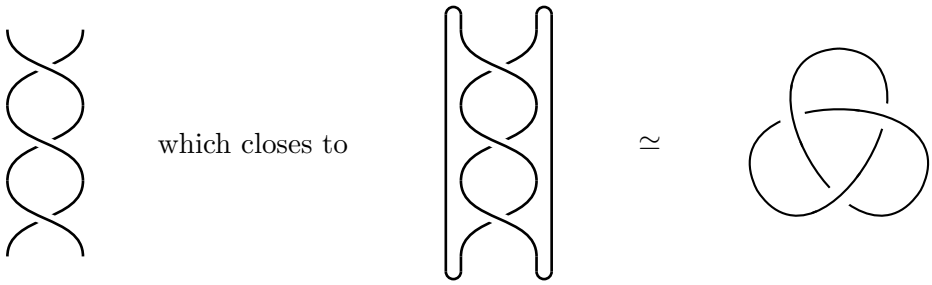

Figure 40: The trefoil via braid closure.

Naturally, we may wonder *can we close two different braids to the same link?*. The answer is yes and there are two relatively simple justifications. Indeed, let σ be an n-braid represented by the word w. Then, $L_{\overline{\sigma}}$ can also be formed from the $(n+1)$-braid σ' represented by $w\sigma_{n+1}$, that is $L_{\overline{\sigma}}$ and $L_{\overline{\sigma'}}$ are ambient isotopic. Alternatively, $L_{\overline{\sigma}}$ can be formed from the n-braid σ'' represented by $\sigma_i w \sigma_i^{-1}$, that is $L_{\overline{\sigma}}$ and $L_{\overline{\sigma''}}$ are ambient isotopic.

Definition 6.9 Let σ be an n-braid represented by word w. The Markov moves are the above adaptations of an n-braid, called stabilisation and conjugation, respectively.

We will now state a result by Markov but we do not include the complicated proof; see [MJ36].

Theorem 6.10 (Markov's Theorem) *Two words represent the same link via braid closure if and only if they can be obtained from each other via a finite sequence of Markov and Artin moves.*

Example 6.11 Consider a braid and apply the stabilisation move. We clearly see that the links via braid closures are indeed ambient isotopic (each is a Hopf link); we apply **R1** to the coloured sections in Figure 41 and stretch/shrink them slightly to pass between the diagrams.

Figure 41: Applying the stabilisation Markov move to the closure of a braid.

Definition 6.12 The braid group on n-strands with respect to the Artin presentation is

$$B_n = \langle \sigma_1, ..., \sigma_{n-1}; \sigma_i\sigma_{i+1}\sigma_i = \sigma_{i+1}\sigma_i\sigma_{i+1}\ \forall i,\ \ \sigma_i\sigma_j = \sigma_j\sigma_i\ \forall |i-j|>1 \rangle.$$

We see the braid group on n-strands is a group on $n-1$ generators with relations **A1** and **A3**.

Proposition 6.13 *Artin's presentation of B_n is equivalent to the geometric interpretation of defining an equivalence relation identifying the upper and lower planes of braid diagrams.*

Proof: Because we stipulate that a braid diagram has crossings for different z-values, it is possible to identify an n-braid with the joining of multiple diagrams of the form of Figure 37. This is precisely a concatenation of members of the n-braid alphabet, by Definition 6.3. Conversely, the identification of the upper and lower planes of multiple braid diagrams will yield an n-braid word. The fact that different braid diagrams correspond to the same braid differ by the relations in Definition 6.12 is clearly a result of Markov's Theorem. □

We now develop a more topological viewpoint of braid groups. However, we will also need to refer to some deeper group-theoretic content in order to achieve this.

Definition 6.14 For a topological space X, the ordered configuration space of X on n points is $\text{Conf}_n(X) = \{(x_1, ..., x_n) \in X^n : x_i \neq x_j\ \forall i \neq j\}$, with subspace topology induced by X^n, which in turn has the product topology induced by X.

Definition 6.15 Let G be a group and X a set. We have a left G-action on X if there exists a map $\rho : G \times X \to X$ given by $\rho_g(x)$ satisfying the following, for all $g, h \in G$ and $x \in X$:

- $(\rho_g \circ \rho_h)(x) = \rho_{gh}(x)$.

- $\rho_{e_G}(x) = x$.

Of course, we could define a right G-action similarly but generally, we just say G *acts on* X. We can apply Definition 6.15 to a context involving the ordered configuration space as is now done.

Lemma 6.16 *For a topological space X, we have an action of S_n on the set* $\mathrm{Conf}_n(X)$.

Proof: Define the map $\rho : S_n \times \mathrm{Conf}_n(X) \to \mathrm{Conf}_n(X)$ by $\rho_\pi((x_1, ..., x_n)) = (x_{\pi(1)}, ..., x_{\pi(n)})$. We need only verify the conditions of Definition 6.15. Indeed,

$$(\rho_{\pi_1} \circ \rho_{\pi_2})((x_1, ..., x_n)) = (x_{(\pi_1 \circ \pi_2)(1)}, ..., x_{(\pi_1 \circ \pi_2)(n)}) = \rho_{\pi_1 \circ \pi_2}((x_1, ..., x_n)),$$

noting that $\pi_1 \circ \pi_2 \in S_n$ by closure. As for the second condition, we see that

$$\rho_e((x_1, ..., x_n)) = (x_1, ..., x_n),$$

where e is the trivial permutation. □

For some group G acting on a set X, we can define an equivalence relation on X whereby we say two elements are equivalent precisely when the action maps one to the other. In particular, for $x, y \in X$, we say $x \sim y$ if and only if there exists $g \in G$ such that $\rho_g(x) = y$.

Definition 6.17 Let some group G act on a set X and $x \in X$. The G-orbit of x is the set $\mathrm{Orb}_G(x) = \{\rho_g(x) : g \in G\}$, i.e. the equivalence class of x under the previous relation.

Example 6.18 Consider the group action in Lemma 6.16 and let $(x_1, ..., x_n) \in \mathrm{Conf}_n(X)$. Then, $\mathrm{Orb}_{S_n}((x_1, ..., x_n)) = \{(x_{\pi(1)}, ..., x_{\pi(n)}) : \pi \in S_n\}$, which is the set of n-tuples containing precisely $x_1, ..., x_n$ in any order.

Definition 6.19 For a topological space X, the unordered configuration space of X on n points is $\mathrm{UConf}_n(X) = {}^{\mathrm{Conf}_n(X)}/_{S_n}$, that is the set of S_n-orbits equipped with the quotient topology.

From [Coh13], we get the next definition, which finally ties the group theory we have done back to the titular concept of Section 6. We then prove it is consistent with that which came before.

Definition 6.20 The braid group on n-strands with respect to the theory of fundamental groups is $B_n = \pi_1(\mathrm{UConf}_n(\mathbb{R}^2))$, where $\mathbb{R}^2$ is endowed with the standard Euclidean topology.

Proposition 6.21 *The topological interpretation of B_n agrees with the geometric interpretation of defining an equivalence relation identifying the upper and lower planes of braid diagrams.*

Sketch of Proof: Consider a loop in the space $\mathrm{UConf}_n(\mathbb{R}^2)$. We can see that such a loop will trace n curves in space-time, that is a subset of $\mathbb{R}^2 \times [0, 1]$, which do not intersect. As such,

one recovers an n-braid. Conversely, an n-braid can be thought of in this way because a loop in $\mathrm{UConf}_n(\mathbb{R}^2)$ will act as a representative of a class of loops in $\pi_1(\mathrm{UConf}_n(\mathbb{R}^2))$. □

6.2 Alexander's Theorem

We finish this section with an important result by Alexander, as is found in [BZ13].

Theorem 6.22 (Alexander's Theorem) *Every link is isotopic to a closed braid.*

Sketch of Proof: Let L be the diagram of an oriented link and $p \in \mathbb{R}^2 \setminus L$ some point through which we draw the so-called braid-axis (not passing through a crossing of L). Choose a circulation (orientation) of $\mathbb{R}^2$. If all arc of L agree in orientation with that of $\mathbb{R}^2$, we are done. Otherwise, suppose that (part of) an arc x_i is opposed to the orientation of $\mathbb{R}^2$. Then, we can apply Reidemeister moves to adjust x_i in such a way that its orientation agrees with that of the plane. Doing this for all such arcs and tracing the arcs that protrude from the braid-axis will yield a braid, from which its closure is L. □

Example 6.23 Consider the best knot to come out of Mathematics (we know which one we're talking about). We shall apply the constructive proof of Alexander's Theorem to demonstrate how to get a braid from which the trefoil is obtained via braid closure.

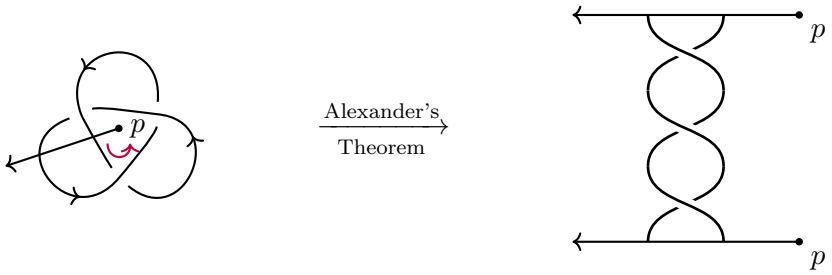

Figure 42: Applying Alexander's Theorem to the trefoil.

With p chosen as in Figure 42 and anti-clockwise circulation, we see that all arcs of K agree with this orientation of $\mathbb{R}^2$. Thus, we can immediately trace the arcs from the braid-axis, sweeping said axis around in the orientation given. Notice that our conclusion agrees with Example 6.8.

Example 6.24 Consider the usual diagram of the figure-eight knot as in Figure 5 and choose an anti-clockwise circulation. Then, with the point p chosen as in Figure 43, we see that an arc is in opposition to the orientation of $\mathbb{R}^2$. As such, we can manoeuvre it via ambient isotopy so that the arc is traced anti-clockwise around p.

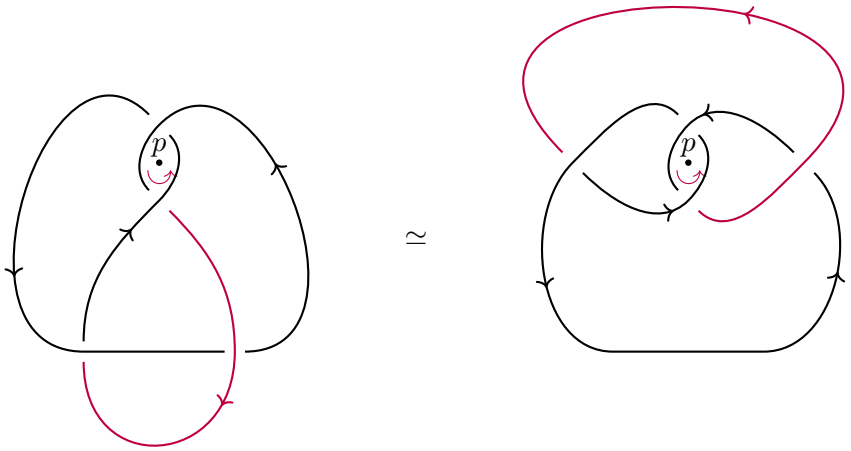

Figure 43: Adjusting the figure-eight knot so that we can use Alexander's Theorem.

Then, we need only trace the arcs from the braid-axis as we did in Example 6.23 and this gives us what we see in Figure 44 below.

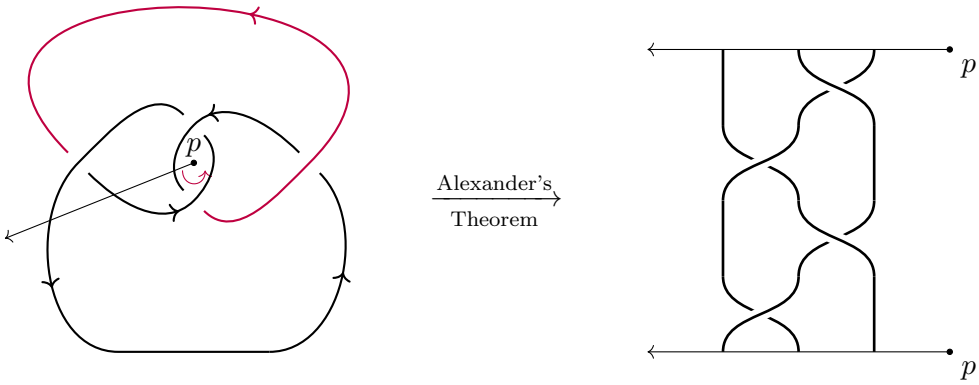

Figure 44: Applying Alexander's Theorem to the modified figure-eight knot.

7 The Fáry-Milnor Theorem

One of the most fascinating results in the study of knots comes from differential geometry. It provides a relationship between the knottedness of a curve and its curvature, which is not at all obvious. We have to develop some theory in the style of Section 1 if we have any hope of proving the titular result but without further ado, we state the theorem of [Mil50].

Theorem 7.1 (Fáry-Milnor Theorem) *Suppose $\gamma : [0,1] \to \mathbb{R}^3$ is a simple regular closed curve. If the total curvature $\mu(\gamma) \leq 4\pi$, then γ is ambient isotopic to S^1.*

The intuition here is that any knot will wrap around itself at least twice, exhibiting a total curvature bounded below by 4π, so it seems very plausible. The proof will require some additional theory first, and we will even prove a slightly lesser result which is nevertheless interesting and is perhaps the first step on the journey to the Fáry-Milnor Theorem.

7.1 The Tangent Indicatrix

We now introduce another curve-theoretic concept which allows for some lateral movement in understanding the problem, the use of which will soon become clear.

Definition 7.2 Let $\gamma : [0,1] \to \mathbb{R}^n$ be a regular closed curve. The tangent indicatrix is the curve

$$\Gamma : [0,1] \to S^{n-1} \text{ given by } \Gamma(t) = \frac{\gamma'(t)}{||\gamma'(t)||}.$$

We shall begin with some intuition on the tangent indicatrix; it will become an immensely useful tool for the proving of our main theorem.

Proposition 7.3 *Let $\gamma : [0,1] \to \mathbb{R}^n$ be a regular closed curve. Then, the total curvature of γ coincides with the length of the tangent indicatrix, that is $\mu(\gamma) = L(\Gamma)$.*

Proof: First, Lemmata 1.10 and 1.16 imply $L(\Gamma)$ and $\mu(\gamma)$ are invariant under reparametrisation. As such, let γ be a unit speed curve without loss of generality, meaning that $||\gamma'(t)|| = 1$. Under this hypothesis, we see that the unit tangent vector is $\gamma'(t)$ and the curvature vector is $\gamma''(t)$. Consequently, we see that

$$\begin{aligned}
\mu(\gamma) &= \int_0^1 ||k(t)||\, ||\gamma'(t)||\, dt \\
&= \int_0^1 ||\gamma''(t)||\, dt \\
&= \int_0^1 ||\Gamma'(t)||\, dt
\end{aligned}$$

$$= L(\Gamma),$$

where we note that $\Gamma'(t) = \gamma''(t)$ by the unit speed assumption. □

We can now relate the tangent indicatrix to n-dimensional spheres, following the work of [Kok18] but expanding on the ideas present in this source by inserting proofs where they are omitted.

Definition 7.4 Let $\gamma : [0,1] \to S^{n-1}$ be a regular closed curve. Then γ is a great circle if it is of the form $\gamma(t) = \cos(2\pi t)\mathbf{e_1} + \sin(2\pi t)\mathbf{e_2}$, where $\mathbf{e_1}, \mathbf{e_2} \in S^{n-1}$ are orthonormal vectors.

Definition 7.5 Let γ be a great circle on S^{n-1} and $p, q \in \text{im}(\gamma)$; these points disconnect γ into two arcs, γ_1 and γ_2 say. The spherical distance between them is $d_{S^{n-1}}(p,q) = \min\{L(\gamma_1), L(\gamma_2)\}$.

Lemma 7.6 *Let $\gamma : [0,1] \to S^{n-1}$ be some closed curve. If $L(\gamma) < 2\pi$, then there exists $p \in S^{n-1}$ such that for every $q \in \text{im}(\gamma)$, the spherical distance satisfies $d_{S^{n-1}}(p,q) \leq L(\gamma)/4$.*

Proof: Let $x, y \in \text{im}(\gamma)$ split the curve into arcs of equal length and p be the midpoint with respect to the spherical distance. For every $q \in \text{im}(\gamma)$ with $d_{S^{n-1}}(p,q) < \pi/2$, it follows that

$$2d_{S^{n-1}}(p,q) \quad \leq \quad d_{S^{n-1}}(x,q) + d_{S^{n-1}}(y,q) \quad \leq \quad L(\gamma_1) + L(\gamma_2) \quad = \quad L(\gamma)/2,$$

where γ_1 and γ_2 are arcs between x & q and y & q, respectively. Here, we use the fact that the spherical distance is a lower bound on the length of a curve between two points on the sphere (in fact, one can define the spherical distance between two points as the infimum over all curves with those endpoints). □

Remark 7.7 If we change the hypothesis of Lemma 7.6 to have $L(\Gamma) = 2\pi$ and that Γ is **not** the union of two great semi-circles, then the bound still holds. Furthermore, the spherical distance is a known metric, meaning it satisfies the Triangle Inequality.

Now, suppose we have two points $p, q \in S^{n-1}$. If we consider the plane which contains both p and q as well as the origin, then the angle θ between p and q will satisfy $\cos(\theta) = p \cdot q$ and the infimum over all arcs between these points will have length θ. As such, $d_{S^{n-1}}(p,q) = \cos^{-1}(p \cdot q)$. This is a simple case of the so-called Haversine Formula.

Lemma 7.8 *Perpendicular vectors on S^{n-1} have spherical distance $\pi/2$.*

Proof: Suppose that $p \cdot q = 0$. Then, $d_{S^{n-1}}(p,q) = \cos^{-1}(p \cdot q) = \cos^{-1}(0) = \pi/2$. □

Theorem 7.9 (Fenchel-Borsuk Theorem) *Let $\gamma : [0,1] \to \mathbb{R}^n$ be a simple regular closed curve. Then, the total curvature $\mu(\gamma) \geq 2\pi$ with equality if and only if γ is plane convex.*

Proof: Assume to the contrary that $L(\Gamma) < 2\pi$. Then, Lemma 7.6 applies, giving the existence of $p \in S^{n-1}$ such that for every $t \in [0,1]$, the spherical distance $d_{S^{n-1}}(p, \Gamma(t)) \leq L(\Gamma)/4 < \pi/2$. Next, we define the function $f(t) = p \cdot \gamma(t)$. Because γ is a closed curve, we can assume it is 1-periodic, meaning that $f(t)$ is also 1-periodic. By the Extreme Value Theorem, there exists $s \in [0,1]$ such that $f'(s) = 0$. Therefore, differentiating at $t = s$ gives us

$$p \cdot \gamma'(s) = 0 \quad \Rightarrow \quad p \cdot \Gamma(s) = 0 \quad \Rightarrow \quad d_{S^{n-1}}(p, \Gamma(s)) = \frac{\pi}{2},$$

the final implication a consequence of Lemma 7.8. This contradicts the strict inequality just established. By Proposition 7.3, $L(\Gamma) = \mu(\gamma) \geq 2\pi$. We shall omit the proof of the equality case since it requires use of other results – the Hopf Index Theorem and the Whitney-Graustein Theorem – but we leave it to [Eva10] for the full details. □

7.2 Crofton's Formula

We give one final auxiliary result which leads directly to the proof of the Fáry-Milnor Theorem. This will be done by following the work of [Che67] for both Crofton's Formula and the proof, which we expand upon through more detailed explanations than were provided in this source.

Definition 7.10 Let $C : [0,1] \to S^2$ be an oriented great circle. We call the unique point $P \in S^2$ a pole if it is positive-normal to the plane containing the great circle which has a norm induced by the orientation. As such, we may identify the great circle with said unique pole by C_P.

Proposition 7.11 (Crofton's Formula) *Let $\gamma : [0,1] \to S^2$ be a regularly parametrised curve and $C : [0,1] \to S^2$ an oriented great circle. Then, the length of γ will satisfy*

$$\iint n_\gamma(C)\, dA = 4L(\gamma),$$

where $n_\gamma(C)$ is the number of intersection points of γ and C and the domain of the integral is the set of poles of all oriented great circles.

Proof: Without loss of generality, assume γ has unit speed parametrisation and let $\gamma(s) \coloneqq \mathbf{e_1}(s)$, which we can complete to a positively-oriented orthonormal basis $\{\mathbf{e_1}(s), \mathbf{e_2}(s), \mathbf{e_3}(s)\}$ for our curve $\gamma(s)$ at each $s \in [0, L(\gamma)]$. We can use properties of orthogonality and bases to see that

$$\mathbf{e_i} \cdot \mathbf{e_i} = 1 \quad \Rightarrow \quad \mathbf{e_i'} \cdot \mathbf{e_i} = 0.$$

Furthermore, for every $i \neq j$, we also see that

$$\mathbf{e_i} \cdot \mathbf{e_j} = 0 \quad \Rightarrow \quad \mathbf{e_i'} \cdot \mathbf{e_j} = -\mathbf{e_i} \cdot \mathbf{e_j'},$$

that is we have the skew-symmetric property. Combining these properties gives the following:

$$\begin{aligned}\mathbf{e_1'} &= a_2\mathbf{e_2} + a_3\mathbf{e_3},\\ \mathbf{e_2'} &= -a_2\mathbf{e_1} + a_1\mathbf{e_3},\\ \mathbf{e_3'} &= -a_3\mathbf{e_1} - a_1\mathbf{e_2},\end{aligned}$$

where the coefficients are real number depending on s, i.e. functions $a_i : [0, L(\gamma)] \to \mathbb{R}$. At some time, choose a point on the curve given by $\mathbf{e_1}$. As such, the oriented great circles that contain $\mathbf{e_1}$ have poles on the equator, which is the $\mathbf{e_2e_3}$-plane, since this is the tangent plane. Therefore, each pole will be of the form

$$P_{\varphi,s} = \cos(\varphi)\mathbf{e_2} + \sin(\varphi)\mathbf{e_3}, \tag{$*$}$$

where $\varphi \in [0, 2\pi)$. As such, we have parametrised the domain of these such poles in terms of the local coordinates (φ, s). Additionally, note that $a_2^2 + a_3^2 = 1$, which means, for some angle $\theta \in [0, 2\pi)$ depending on s, we have the following forms for the coefficient functions:

$$a_2 = \cos(\theta(s)) \qquad \text{and} \qquad a_3 = \sin(\theta(s)).$$

Using partial differentiation on ($*$) in conjunction with the above expressions, the area element corresponding to these local coordinates is $dA_{\varphi,s} = ||\partial_\varphi P \times \partial_s P||\, d\varphi ds$. Explicitly, we get

$$\begin{aligned}dA_{\varphi,s} &= |a_2\cos(\varphi) + a_3\sin(\varphi)|\, d\varphi ds,\\ &= |\cos(\theta)\cos(\varphi) + \sin(\theta)\sin(\varphi)|\, d\varphi ds\\ &= |\cos(\varphi - \theta)|\, d\varphi ds,\end{aligned}$$

by a standard trigonometric identity. Let C_P be the oriented great circle with pole $P_{\varphi,s}$. Then,

$$\begin{aligned}\iint n_\gamma(C_P)\, dA &= \iint 1\, dA_{\varphi,s}\\ &= \int_0^{L(\gamma)}\int_0^{2\pi} |\cos(\varphi - \theta)|\, d\varphi ds\\ &= \int_0^{L(\gamma)}\int_0^{2\pi} |\cos(x)|\, dx ds,\\ &= \int_0^{L(\gamma)}\int_0^{\pi/2} 4\cos(x)\, dx ds\\ &= \int_0^{L(\gamma)} 4\, ds\\ &= 4L(\gamma),\end{aligned}$$

where we made the substitution $x = \varphi - \theta$ which is such that $dx = d\varphi$. □

Remark 7.12 The tangent indicatrix of a closed space curve satisfies the conditions of Crofton's Formula, which in conjunction with Proposition 7.3 gives us a means to tackle Theorem 7.1.

Proof of the Fáry-Milnor Theorem: Let γ have unit speed parametrisation and P be the pole of great circle C_P. We wish to analyse the value $n_\Gamma(C_P)$, where Γ is the tangent indicatrix of γ on S^2. Assume without loss of generality that the curvature of γ is non-vanishing; this is equivalent to Γ being regular. We can now make two very useful observations:

- $n_\Gamma(C_P)$ is positive on $[0, 2\pi] \times [0, L(\gamma)]$.
- $n_\Gamma(C_P)$ is even. The intuition is that if Γ crosses over C_P, then it must cross back because it is closed. The situation where Γ is tangential to C_P will occur at an isolated number of points, meaning the measure of such oriented great circles as in Crofton's Formula is 0.

Define the so-called height map $h_P : [0, L(\gamma)] \to \mathbb{R}$ given by $h_P(s) = \gamma(s) \cdot P$. We can clearly see that $h_P'(s) = \gamma'(s) \cdot P$, which means any critical point of the height map occurs precisely when P is orthogonal to some tangent plane of γ, i.e. when the tangent indicatrix intersects C_P. As such, $n_\Gamma(C_P)$ is the number of extrema of the height map. By Proposition 7.3, the hypothesis of Theorem 7.1 is to say $L(\Gamma) < 4\pi$ and so Crofton's Formula implies that

$$\iint n_\Gamma(C_P)\, dA < 16\pi.$$

Recall the surface area of S^2 is 4π, meaning there exists a pole $\overline{P}$ where $n_\Gamma(C_{\overline{P}}) < 4\pi$. If not,

$$\iint 4\, dA < 16\pi \quad \Rightarrow \quad \iint dA < 4\pi,$$

contradicting the area of the sphere. It can only be that $n_\Gamma(C_{\overline{P}}) = 2$. This means $h_{\overline{P}}$ has two extrema. We can suppose that $\overline{P} = (0, 0, 1)$. In this case, since the height map is defined on a compact set, the Extreme Value Theorem implies there is precisely one maximum and one minimum point. These points divide our original curve γ into two arcs, along one of which the vertical component increases and along the other of which it decreases. Hence, taking a plane Σ orthogonal to $\overline{P}$ and considering its intersection whilst varying it between the extremal points yield sets consisting of only two points. Connecting each point via a line segment generates a surface bounded by γ which is homeomorphic to the closed disk. Therefore, Lemma 5.47 implies that γ thought of as a knot has genus zero and must be the unknot. □

Remark 7.13 We have shown a weaker version of the Fáry-Milnor Theorem, that is $\mu(\gamma) < 4\pi$ implies that γ is the unknot. For the equality case, we refer to the original paper [Mil50] by Milnor

who proved the stronger result by estimating curves with closed polygons. In this estimation, he defines the total curvature as the infimum of the polygonal curvature over all possible inscribed polygons. He then showed that, for the bound we proved above, namely $\mu(\gamma) \geq 4\pi$ for a knotted curve, it is always possible to reduce the total curvature. The implication is that for non-trivial isotopy classes of closed curves, the infimum 4π is never attained (if it was, it could be reduced, contradicting the lower bound). These examples are found in [Coo19].

Example 7.14 We see from [Cla02] that any (p, q)-torus knot can be parametrised as follows:

$$\gamma_{T_{p,q}}(t) = (\cos(pt)\cos(qt) + 2\cos(pt), \sin(pt)\cos(qt) + 2\sin(pt), -\sin(qt)).$$

More specifically, let us consider for the final time the knot that has been our friend through the thick and thin of this paper; I am obviously talking about the trefoil knot which we recall is a $(2, 3)$-torus knot. As such, the trefoil has parametrised equation

$$\gamma_{T_{2,3}}(t) = (\cos(2t)\cos(3t) + 2\cos(2t), \sin(2t)\cos(3t) + 2\sin(2t), -\sin(3t)).$$

We use software to compute the total curvature to be $\mu(\gamma_{T_{2,3}}) \approx 17.822 > 12.567 \approx 4\pi$ so the conditions of the Fáry-Milnor Theorem hold, as expected.

Going back to Corollary 3.7 for instance, we know that the trefoil is distinct from the unknot, but the Fáry-Milnor Theorem does **not** guarantee this at all – we have only demonstrated the contrapositive of Theorem 7.1 in Example 7.14.

Example 7.15 Consider the $(1, 4)$-torus knot, which is ambient isotopic fo S^1. However, using

$$\gamma_{T_{1,4}}(t) = (\cos(t)\cos(4t) + 2\cos(t), \sin(t)\cos(4t) + 2\sin(t), -\sin(4t)),$$

we can compute the total curvature to be $\mu(\gamma_{T_{1,4}}) \approx 24.274 > 4\pi$, so the Fáry-Milnor Theorem certainly doesn't give us both a necessary and sufficient condition on the knottedness of a parametrised curve in terms of its total curvature, since there exist unknots that have total curvature larger than 4π.

8 Summary

The discussion on knot theory is concluded and we now summarise the findings established in this paper and make comment on the areas we could develop further given the time.

We have seen a number of link invariants, ranging from numerical ones (number of components, p-colourability, the knot determinant, the genus, the signature) to polynomial invariants (bracket polynomial, normalised bracket and Jones polynomials) and even topological ones (knot group). However, we haven't discussed anything that can be considered a complete knot invariant; there were always examples showing the limitations of the invariants we have. It would have been nice to delve into some additional technicality, studying at least one complete invariant, but alas we have developed sufficient theory to show that many of the knots and links we have used are indeed distinct.

Arguably the most powerful tool to come of this paper is the fundamental group; we have seen that it encodes information on the knot group, p-colourability and braid presentations. Its outreach is surprising and it is relatively easy to gain intuition on this object.

One riveting aspect was the discussion on braid theory. Given more time, it would have been preferable to flesh out Section 6 more. One possible route would be to use [Fas05] as a basis of the extended discussion which would have seen us re-discover the Jones polynomial through the so-called Temperley-Lieb Algebra. It would also have been preferable to elaborate on Remarks 5.58 and 5.64 given more time; homology is an interesting concept in topology and, as we saw on a rudimentary level, it can even be used to discuss Alexander polynomials and Seifert matrices. Nevertheless, we included the aforementioned remarks as a way to note that this alternative route exists.

One of the most interesting results was the Fáry-Milnor Theorem. The fact this requires no real intuition beyond *a knot will be quite twisted* is rather impressive; we could prove this theorem (given the auxiliary results) pretty much at the end of Section 1. That being said, leaving the statement and its resolution until the end hopefully gives any admirer of differential geometry an opportunity to finish this paper with a sense of joy, having endured a lengthy discussion mostly on knot diagrams.

References

[Ada04] Colin Adams. *The Knot Book*. American Mathematical Society, 2004.

[Art47] Emil Artin. Theory of Braids. *Annals of Mathematics*, 48(1):101–126, 1947.

[Bad16] Nate Bade. *Properties of the Alexander Polynomial*. Northeastern University, 2016. URL: https://web.northeastern.edu/beasley/MATH7375/Lecture18.pdf.

[Bignd] Alessandro Bigazzi. *The Seifert-van Kamepn Theorem*. University of Warwick, n.d.

[Bos19] Anthony Bosman. Knot theory, 2019. URL: https://drive.google.com/file/d/1fPwXmiYRhR3ZMa_7p8RNP0zBQRzoXFGz/view.

[BZ66] Gerhard Burde and Heiner Zieschang. Eine Kennzeichnung der Torusknoten. *Mathematische Annalene*, 167:169–176, 1966. doi:10.1007/BF01362170.

[BZ13] Gerhard Burde and Heiner Zieschang. *Knots*, volume 5 of *De Gruyter Studies in Mathematics*. Walter de Gruyter, 2013.

[Cam08] Peter Cameron. *Matrices with Zero Row and Column Sum*. Queen Mary University of London, 2008. URL: http://www.maths.qmul.ac.uk/~pjc/odds/zero.pdf.

[Che67] Shiing Shen Chern. Curves and Surfaces in Euclidean Spaces. *Studies in Global Geometry and Analysis*, 4(3):16–56, 1967.

[Cla02] David Clark. *Transforming Trigonometric Knot Parameterizations into Rational Knot Parameterizations*. Mount Holyoke College, 2002. URL: https://www.mtholyoke.edu/~adurfee/reu/02/dc.pdf.

[Coh13] Fred Cohen. *Introduction to Configuration Spaces and their Applications*. University of Rochester, 2013. URL: https://www.mimuw.edu.pl/~sjack/prosem/Cohen_Singapore.final.24.december.2008.pdf.

[Connd] Keith Conrad. *Spaces that are Connected but not Path-Connected*. Stanford University, nd. URL: https://kconrad.math.uconn.edu/blurbs/topology/connnotpathconn.pdf.

[Coo19] John Cook. *Total Curvature of a Knot*. 2019. URL: https://www.johndcook.com/blog/2019/10/01/total-curvature-of-a-knot/.

[Cro04] Peter Cromwell. *Knots and Links*. Cambridge University Press, 2004.

[CSW16] Scott Carter, Daniel Silver, and Susan Williams. *Three Dimensions Of Knot Coloring*. 2016. URL: https://arxiv.org/pdf/1301.5378.pdf.

[Dan15] Supreedee Dangskul. *A Construction of Seifert Surfaces by Differential Geometry*. University of Edinburgh, 2015.

[Deh87] Max Dehn. *Papers on Group Theory and Topology*. Springer-Verlag New York, 1987.

[Eva10] Charles M. Evans. *Curves, Knots and Total Curvature*. Wake Forest University, 2010. URL: https://pdfs.semanticscholar.org/d035/84eab92242313c316a34d19ca74d0f7bbd30.pdf.

[Fas05] Jordan Fassler. *Braids, the Artin Group and the Jones Polynomial*. University of California Los Angeles, 2005. URL: https://www.math.ucla.edu/~radko/191.1.05w/jordan.pdf.

[FMP17] Stefan Friedl, Allison N. Miller, and Mark Powell. *Determinants of Amphichiral Knots*. University of Regensburg, 2017. URL: http://www.mathematik.uni-regensburg.de/friedl/papers/determinant-of-amphichiral-knots-june-19-2017.pdf.

[GM12] Moritz Groth and Ieke Moerdijk. *Homotopy Theory Exercise Sheet 1*. Radboud University, 2012. URL: https://www.math.ru.nl/~mgroth/teaching/htpy13/Exercise01.pdf.

[GP94] Nick Gilbert and Timothy Porter. *Knots and Surfaces*. Oxford University Press, 1994.

[Jon14] Vaughan Jones. *The Jones Polynomial for Dummies*. University of California Berkley, 2014. URL: https://math.berkeley.edu/~vfr/jonesakl.pdf.

[Kan86] Taizo Kanenobu. Examples on Polynomial Invariants of Knots and Links. *Mathematische Annalen*, 275(42):555–572, 1986. doi:10.1007/BF01459137.

[Kaw96] Akio Kawauchi. *A Survey of Knot Theory*. Birkhäuser Verlag, 1996.

[Kok18] Gerasim Kokarev. *MATH5113M: Advanced Differential Geometry*. University of Leeds, 2018.

[Liv93] Charles Livingston. *Knot Theory*, volume 24. Cambridge University Press, 1993.

[May00] J. Peter May. *An Outline Summary of Basic Point Set Topology*. University of Chicago, 2000. URL: http://www.math.uchicago.edu/~may/MISC/Topology.pdf.

[McM13] Curtis McMullen. *Topology*. Harvard University, 2013. URL: http://people.math.harvard.edu/~ctm/papers/home/text/class/harvard/131/course/course.pdf.

[MI02] Charles Miller III. *Combinatorial Group Theory*. Heriot-Watt University, 2002. URL: http://www.macs.hw.ac.uk/~lc45/Teaching/kggt/miller.pdf.

[Mil50] John Milnor. On the Total Curvature of Knots. *Annals of Mathematics*, 52(2):248–257, 1950. doi:10.2307/1969467.

[MJ36] Andrey Andreyevich Markov Jr. On the Free Equivalence of Closed Braids. *Matematicheskii Sbornik*, 43(1):73–78, 1936.

[Mur07] Kunia Murasugi. *Knot Theory and Its Applications*. Springer Science and Business Media, 2007.

[MZ19] Andreas Müller and Dimiter Zlatanov. *Singular Configurations of Mechanisms and Manipulators*, volume 589 of *CISM International Centre for Mechanical Sciences*. Springer, 2019.

[Pet07] Carlo Petronio. *Combinatorial and Geometric Methods in Topology*. 2007. URL: https://arxiv.org/pdf/0706.4368.pdf.

[Rei27] Kurt Reidemeister. *Elementare Begründung der Knotentheorie*, volume 5. Springer Berlin Heidelberg, 1927. doi:10.1007/BF02952507.

[Rin14] Andrea Rincon. *Seifert Surfaces and Genus*. 2014. URL: https://www.mathi.uni-heidelberg.de/~lee/Andrea.pdf.

[Rob15] Justin Roberts. *Knots Knotes*. University of California San Diego, 2015. URL: http://math.ucsd.edu/~justin/Papers/knotes.pdf.

[Rog18] John Rognes. *Lecture Notes on Topology for MATH3500/4500*. University of Oslo, 2018. URL: https://www.uio.no/studier/emner/matnat/math/MAT4500/h18/dokumenter/topology.pdf.

[Tho04] Anne Thomas. *Covering Spaces*. University of Chicago, 2004. URL: http://math.uchicago.edu/~womp/2004/athomas04.pdf.

[Wil96] Robin J. Wilson. *Introduction to Graph Theory*. Longman, 4th edition, 1996.

[Zee66] Erik Christopher Zeeman. *An Introduction to Topology*. University of Warwick, 1966.

Appendices

A The Proof of Lemma 3.16

Here, we will explicitly compute the row operations discussed in the proof of Lemma 3.16. Indeed,

$$
\begin{aligned}
M+U &= \begin{pmatrix} m_{11}+1 & \cdots & m_{1j}+1 & \cdots & m_{1n}+1 \\ \vdots & & \vdots & & \vdots \\ m_{i1}+1 & \cdots & m_{ij}+1 & \cdots & m_{in}+1 \\ \vdots & & \vdots & & \vdots \\ m_{n1}+1 & \cdots & m_{nj}+1 & \cdots & m_{nn}+1 \end{pmatrix} \\
&\overset{1.}{\longmapsto} \begin{pmatrix} m_{11}+1 & \cdots & n & \cdots & m_{1n}+1 \\ \vdots & & \vdots & & \vdots \\ n & \cdots & n^2 & \cdots & n \\ \vdots & & \vdots & & \vdots \\ m_{n1}+1 & \cdots & n & \cdots & m_{nn}+1 \end{pmatrix} \\
&\overset{2.}{\longmapsto} \begin{pmatrix} m_{11}+1 & \cdots & n & \cdots & m_{1n}+1 \\ \vdots & & \vdots & & \vdots \\ 1 & \cdots & n & \cdots & 1 \\ \vdots & & \vdots & & \vdots \\ m_{n1}+1 & \cdots & n & \cdots & m_{nn}+1 \end{pmatrix} \\
&\overset{3.}{\longmapsto} \begin{pmatrix} m_{11} & \cdots & 0 & \cdots & m_{1n} \\ \vdots & & \vdots & & \vdots \\ 1 & \cdots & n & \cdots & 1 \\ \vdots & & \vdots & & \vdots \\ m_{n1} & \cdots & 0 & \cdots & m_{nn} \end{pmatrix},
\end{aligned}
$$

where we have applied the following elementary matrix operations numbered as follows:

1. $R_i \mapsto R_i + R_{k_1}$ for every $k_1 \neq i$ and $C_j \mapsto C_j + C_{k_2}$ for every $k_2 \neq j$.
2. $R_i \mapsto \frac{1}{n} R_i$.
3. $R_k \mapsto R_i - R_k$ for every $k \neq i$.

It is clear that the determinant of the resulting matrix can be written as an expansion by minors down the j^{th} column, which is all-zero bar one entry, as we wrote in the proof of Lemma 3.16.

B The Proof of Theorem 3.21

We give the linear algebra details as to how we arrived at the conclusions regarding the colouring matrices of a knot which has had the Reidemeister moves applied to it. First, we see that the original colouring matrix will be of the form

$$M_K = \begin{array}{c} \\ n-1 \\ n \end{array} \begin{array}{c} \begin{array}{ccc} x_{n-1} & x_n & \end{array} \\ \begin{pmatrix} & & \\ -1 & -1 & \\ & -1 & \end{pmatrix} \end{array}.$$

We apply **R1** to the n^{th} arc of a knot diagram K to form $K_{\mathbf{R1}}$, assuming this arc passes between the $(n-1)^{\text{th}}$ and n^{th} crossings. This gives us the following:

$$M_{K_{\mathbf{R1}}} = \begin{array}{c} \\ n-1 \\ n \\ n+1 \end{array} \begin{array}{c} \begin{array}{ccccccc} & & & x_{n-1} & x_n & x_{n+1} \end{array} \\ \begin{pmatrix} & & & & & 0 \\ & & & & & \vdots \\ & & & & & 0 \\ & & & -1 & 0 & -1 \\ & & & & -1 & 0 \\ 0 & \cdots & 0 & 0 & -1 & 1 \end{pmatrix} \end{array}$$

$$\overset{1.}{\longmapsto} \begin{array}{c} \\ n-1 \\ n \\ n+1 \end{array} \begin{array}{c} \begin{array}{ccccccc} & & & x_{n-1} & x_n & x_{n+1} \end{array} \\ \begin{pmatrix} & & & & & 0 \\ & & & & & \vdots \\ & & & & & 0 \\ & & & -1 & -1 & -1 \\ & & & & -1 & 0 \\ 0 & \cdots & 0 & 0 & 0 & 1 \end{pmatrix} \end{array}$$

$$\overset{2.}{\longmapsto} \begin{array}{c} \\ n{-}1 \\ n \\ n{+}1 \end{array} \begin{array}{c} \begin{array}{cccccc} & & & x_{n-1} & x_n & x_{n+1} \end{array} \\ \begin{pmatrix} & & & & & 0 \\ & & & & & \vdots \\ & & & & & 0 \\ & & & -1 & -1 & 0 \\ & & & & -1 & 0 \\ 0 & \cdots & 0 & 0 & 0 & 1 \end{pmatrix} \end{array},$$

where we have applied the following elementary matrix operations numbered as follows:

1. $C_n \mapsto C_n + C_{n+1}$.
2. $R_{n-1} \mapsto R_{n-1} + R_{n+1}$.

We apply **R2** to the $(n-1)^{\text{th}}$ and n^{th} arcs of a knot diagram K to form $K_{\mathbf{R2}}$, where the n^{th} arc now passes underneath the $(n-1)^{\text{th}}$ arc. This gives us the following:

$$
M_{K_{\mathbf{R2}}} = \begin{array}{c} \\ n{-}1 \\ n \\ n{+}1 \\ n{+}2 \end{array}
\begin{array}{c}
\begin{array}{ccccccc} & & & x_{n-1} & x_n & x_{n+1} & x_{n+2} \end{array} \\
\begin{pmatrix}
 & & & & & 0 & 0 \\
 & & & & & \vdots & \vdots \\
 & & & & & 0 & 0 \\
 & & & -1 & 0 & -1 & 0 \\
 & & & & -1 & 0 & 0 \\
0 & \cdots & 0 & 2 & 0 & -1 & -1 \\
0 & \cdots & 0 & 2 & -1 & 0 & -1
\end{pmatrix}
\end{array}
$$

$$
\overset{1.}{\longmapsto}
\begin{array}{c} \\ n{-}1 \\ n \\ n{+}1 \\ n{+}2 \end{array}
\begin{array}{c}
\begin{array}{ccccccc} & & & x_{n-1} & x_n & x_{n+1} & x_{n+2} \end{array} \\
\begin{pmatrix}
 & & & & & 0 & 0 \\
 & & & & & \vdots & \vdots \\
 & & & & & 0 & 0 \\
 & & & -1 & -1 & -1 & 0 \\
 & & & & -1 & 0 & 0 \\
0 & \cdots & 0 & 2 & -1 & -1 & -1 \\
0 & \cdots & 0 & 2 & -1 & 0 & -1
\end{pmatrix}
\end{array}
$$

$$
\overset{2.}{\longmapsto}
\begin{array}{c} \\ n{-}1 \\ n \\ n{+}1 \\ n{+}2 \end{array}
\begin{array}{c}
\begin{array}{ccccccc} & & & x_{n-1} & x_n & x_{n+1} & x_{n+2} \end{array} \\
\begin{pmatrix}
 & & & & & 0 & 0 \\
 & & & & & \vdots & \vdots \\
 & & & & & 0 & 0 \\
 & & & -1 & -1 & -1 & 0 \\
 & & & & -1 & 0 & 0 \\
0 & \cdots & 0 & 0 & 0 & -1 & 0 \\
0 & \cdots & 0 & 2 & -1 & 0 & -1
\end{pmatrix}
\end{array}
$$

$$\overset{3.}{\mapsto} \begin{array}{c} \\ n-1 \\ n \\ n+1 \\ n+2 \end{array} \begin{array}{c} \begin{array}{ccccccc} & & & x_{n-1} & x_n & x_{n+1} & x_{n+2} \end{array} \\ \begin{pmatrix} & & & & & 0 & 0 \\ & & & & & \vdots & \vdots \\ & & & & & 0 & 0 \\ & & & -1 & -1 & 0 & 0 \\ & & & & -1 & 0 & 0 \\ 0 & \cdots & 0 & 0 & 0 & -1 & 0 \\ 0 & \cdots & 0 & 0 & 0 & 0 & -1 \end{pmatrix} \end{array},$$

where we have applied the following elementary matrix operations numbered as follows:

1. $C_n \mapsto C_n + C_{n+1}$.
2. $R_{n+1} \mapsto R_{n+1} - R_{n+2}$.
3. $R_{n-1} \mapsto R_{n-1} - R_{n+1}$ and $C_{n-1} \mapsto C_n - 2C_{n+2}$ and $C_n \mapsto C_n - C_{n+2}$.

C Graphs and Combinatorial Surfaces

We provide more information to gain better understanding of the graph-theoretic approach we took in Remark 5.22 and Lemma 5.23. The graph theory we present is found in [Wil96]. We conclude this section with an explicit construction of the identification graph and its dual in relation to the Klein bottle.

Definition C.1 A graph is the pair $G = (V, E)$, where V is a (finite) set of vertices and E is a set of pairs of vertices we call edges.

Example C.2 Consider the graph $G = (V, E) := (\{1, 2, 3, 4\}, \{12, 13, 14, 34\})$. This means that we have edges between vertices 1&2, 1&3, 1&4, 3&4. This can be drawn in Figure 45 below.

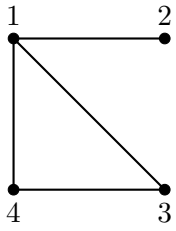

Figure 45: A representation of a graph on four vertices.

This particular graph is connected since there exists a path (a sequence of edges) between any two vertices. We can see that some vertices are contained at the ends of more than just one edge; the number of edges where this occurs we call the degree of a vertex. However, we can clearly see that the graph $G' = (V \cup \{5\}, E)$ is disconnected because there are no edges involving vertex 5, let alone a path between that and any other vertex.

Definition C.3 Let G be a graph. A cycle is a closed path in G containing at least one edge, in other words a non-trivial path which starts and ends at the same vertex.

Definition C.4 Let G be a graph. It is called a tree if it is connected and has no cycles.

Lemma C.5 *A graph on n vertices G is a tree if and only if G has no cycles and $n - 1$ edges.*

Proof: ($\Rightarrow$) If G is a tree, then there are no cycles by Definition C.4. Now, note that removing any edge will disconnect the tree into two subtrees by the assumption that G contains no cycles. Here, we proceed by induction on the number of edges, noting that the number of edges across the two subtrees is one less than the number of vertices. Consequently, there are $n - 1$ edges to begin with.

($\Leftarrow$) Suppose to the contrary that G is not a tree. Then, it must contain (at least) one cycle. Removing an edge from this cycle will not change connectedness but will give us a connected graph on n vertices with $n-2$ edges, which is clearly a contradiction. $\square$

There is a natural way to relate the Euler characteristic to graphs. Suppose $G = (V, E)$ is a graph where $|V| = v$ and $|E| = e$. We can define the Euler characteristic of a graph as

$$\chi(G) = v - e.$$

Remark C.6 A special type of graph is that of a planar graph, meaning it can be embedded in $\mathbb{R}^2$ in such a way that edges do not intersect (they meet only at vertices). For such a graph, we can define a face to be a region which is enclosed by a series of edges. From this, we recover a more familiar form of the Euler characteristic, but if G is planar, we always have that $\chi(G) = v - e + f = 2$, were f is the number of faces, including the unbounded face surrounding the graph. However, there is clearly a restriction here on what types of graph we can assign faces and we have no reason to impose this. As such, we work in the more general setting laid out above.

Proposition C.7 *Let G be a connected graph. Then, $\chi(G) \leq 1$ with equality if and only if G is a tree.*

Proof: Without loss of generality, let G be a graph on v vertices and e edges that contains no vertex of degree one. If this is the case, removing the vertex and corresponding edge will clearly not affect the Euler characteristic, so we can always reduce our graphs ones of this form. Then, either $\deg(x) \geq 2$ for every $x \in V$ or there is only one vertex and no edges.

(i) In the first case, we appeal to the Handshaking Lemma [Wil96, page 12]; this result provides us with the following relationship: $\sum_{x \in V} \deg(x) = 2e$. From here, we can conclude that

$$2v \;=\; \sum_{x \in V} 2 \;\leq\; \sum_{x \in V} \deg(x) \;=\; 2e,$$

which rearranges to $\chi(G) = v - e \leq 0$.

(ii) In the second case, it is immediate that $\chi(G) = 1$.

As such $\chi(G) \leq 1$. In the case that G is a tree, Lemma C.5 implies that it has $v-1$ edges and so $\chi(G) = v - (v-1) = 1$. Conversely, if $\chi(G) = 1$, then removing the degree one vertices in turn from G yields one vertex and no edges as the above working shows; the reverse of this process is to add one edge and one vertex at each stage, which does not introduce any cycles, so our original G must have been a tree. $\square$

Consider a triangulation of some surface Σ. Then, it is possible to draw the identification graph G and the identification dual graph G^* as in Figure 46.

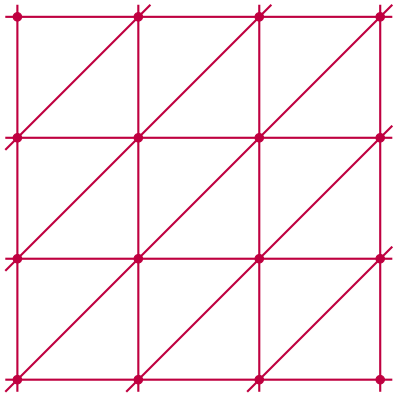

(a) The identification graph.

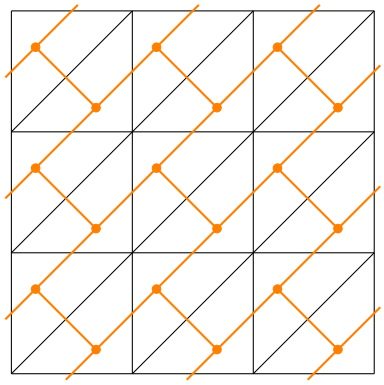

(b) The identification dual graph.

Figure 46: The two graphs that we can relate to surfaces introduced in Remark 5.22.

In the proof of Lemma 5.23, we chose a spanning tree T of G^* and a subgraph H of G formed by omitting the edges of G that intersect those of T. We shall now demonstrate this procedure with the Klein bottle.

Example C.8 We justify why the Klein bottle K^2 is non-orientable using this graph-theoretic technique. Recall we have seen its planar drawing of K^2 in Figure 15, which we can split into 2-simplices, forming a triangulation. On this triangulation, we can construct the graphs G and G^*, as in Figure 47. If we prescribe a circulation on one of the faces and extend this along our tree T, we will see Figure 28 appearing as a subsurface. In fact, a careful look at the failing of our attempted orientation will convince us that $K^2 = M^2 \cup M^2$.

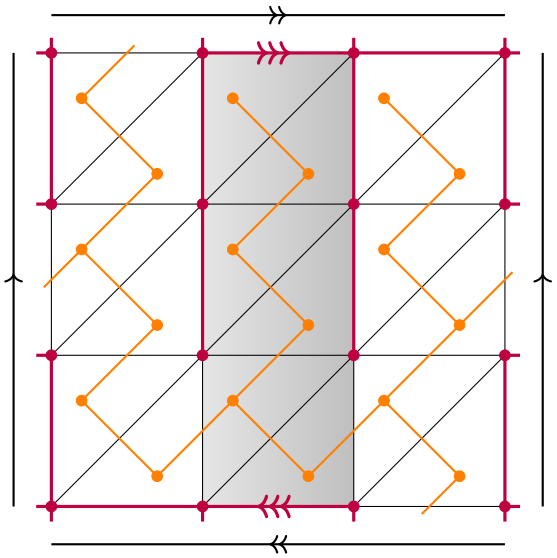

Figure 47: A triangulation of the Klein bottle, with shaded region a Möbius strip.